“Computer Aided Design and Analysis of Swing Jaw Plate of Jaw Crusher”

Thesis Submitted in Partial Fulfillment
of the Requirements for the Award of

Master of Technology
In
Machine Design and Analysis

By

Bharule Ajay Suresh
Roll No: 207ME111

Department of Mechanical Engineering
National Institute of Technology
Rourkela
2009

“Computer Aided Design and Analysis of Swing Jaw Plate of Jaw Crusher”

Thesis Submitted in Partial Fulfillment
of the Requirements for the Award of

Master of Technology
In
Machine Design and Analysis

By

Bharule Ajay Suresh
Roll No: 207ME111

Under the Guidance of

Prof. N. KAVI

Department of Mechanical Engineering
National Institute of Technology
Rourkela
2009

ACKNOWLEDGEMENT

Successful completion of work will never be one man's task. It requires hard work in right direction. There are many who have helped to make my experience as a student a rewarding one.

In particular, I express my gratitude and deep regards to my thesis guide **Prof. N. Kavi** first for his valuable guidance, constant encouragement and kind co-operation throughout period of work which has been instrumental in the success of thesis.

I also express my sincere gratitude to **Prof. R. K. Sahoo**, Head of the Department, Mechanical Engineering, for providing valuable departmental facilities.

I would like to thank my fellow post-graduate students.

Bharule Ajay Suresh
Roll No.207ME111
Dept. of Mechanical Engg.

National Institute Of Technology
Rourkela

CERTIFICATE

This is to certify that the thesis entitled, **"Computer Aided Design and Analysis of Swing Jaw Plate of Jaw Crusher"** submitted by **Mr. Bharule Ajay Suresh** in partial fulfillment of the requirements for the award of Master of Technology Degree in **Mechanical Engineering** with specialization in **"Machine Design and Analysis"** at the National Institute of Technology, Rourkela is an authentic work carried out by him under my supervision and guidance.

To the best of my knowledge, the matter embodied in the thesis has not been submitted to any other University / Institute for the award of any Degree or Diploma.

Date:

Dr. N. Kavi
Professor
Department of Mechanical Engineering
National Institute of Technology
Rourkela-769008

CONTENTS

ABSTRACT

Traditionally, stiffness of swing plates has not been varied with changes in rock strength. Rock strength has only been of interest because of the need to know the maximum force exerted by the toggle for energy considerations. Thus a swing plate, stiff enough to crush taconite with an unconfined compressive strength (q_u) of up to 308 MPa, may be overdesigned (and, most importantly, overweight) for crushing a softer fragmental limestone, amphibolites. Design of lighter weight jaw crushers will require a more precise accounting of the stresses and deflections in the crushing plates than is available with traditional techniques.

Efforts to decrease energy consumed in crushing have lead to consideration of decreasing the weight of the swing plate of jaw crushers for easily crushed material. In the present work the design of the swing jaw plate using point-load deformation failure (PDF) relationships along with interactive failure of rock particles as a model for such a weight reduction. The design of the corrugated swing jaw plate is carried out by using CAD i.e. jaw crusher plate has been solid modeled by using CatiaV5R15. The calculated dimensions are validated with the drawing of reputed manufacturers. Finite Element Analysis of jaw plates are carried out by using ALGOR V19 software. Computerization of the theoretical design calculations of jaw plates of the jaw crusher has been carried out. The computerized program facilitates for quick design of the plates of the jaw crusher.

The different comparisons of corrugated swing jaw plates behavior, calculated with the traditional and the new FEA failure models with stiffeners, shows that some 10-25% savings in plate weight may be possible.

Key Words:

Jaw Crusher, Computer Aided Design (CAD), Point-Load Deformations and Failure (PDF), Finite Element Analysis, Solid Modeling, Corrugated Jaw plate, Stiffened-Jaw Plate.

Nomenclature

a and K	Power law Deformation Descriptors
c	One-half the beam thickness
d	Diameter of Specimen
D	Diametral Deformation
D_f	Deformation at failure
D_{nf}	Normalized Deformation at failure
D_{px}	Deflection of the beam at any rock particle position
D_{rx}	Rock Deformation
E_r	Young's Modulus of Rock
K	Rock stiffness
L	Length of the beam
N_i	Shape Function
P	Maximum Point Load
P_b	Load at any b
P_f	Load at failure
P_{nf}	Normalized failure loads
q_u	Unconfined Compressive Strength
Q	Total Loading Force
R	Radius of Rock Particles
S_t	Tensile Strength of Rock Materials
U_x	Beam movement
T	Toggle Force
ν	Poisson's Ratio
ΔW	Change in energy per cycle
x	Position of consideration
X	Proportionality Factor

List of Figures

List of Tables

CHAPTER-1

INTRODUCTION AND SCOPE FOR STUDY

1. INTRODUCTION AND SCOPE FOR STUDY

1.1 Introduction

Jaw crusher is a machine designed to reduce large solid particles of raw material into smaller particles. Crushers are major size reduction equipment used in mechanical, metallurgical and allied industries. They are available in various sizes and capacities ranging from 0.2 ton/hr to 50 ton/hr. They are classified based on different factors like product size and mechanism used. Based on the mechanism used crushers are of three types namely Cone crusher, Jaw crusher and Impact crusher.

The first stage of size reduction of hard and large lumps of run-of-mine (ROM) ore is to crush and reduce their size. Large scale crushing operations are generally performed by mechanically operated equipment like jaw crushers, gyratory crusher and roll crushers. For very large ore pieces that are too big for receiving hoppers of mechanically driven crushers, percussion rock breakers or similar tools are used to break them down to size. The mechanism of crushing is either by applying impact force, pressure or a combination of both. The jaw crusher is primarily a compression crusher while the others operate primarily by the application of impact.

Crushing is the process of reducing the size of the lump of ore or over size rock into definite smaller sizes. The crusher crushes the feed by some moving units against a stationary unit or against another moving unit by the applied pressure, impact, and shearing or combine action on them. The strain in the feed material due to sufficiently applied pressure, impact forces, or shearing effect when exceeds the elastic limit of the feed material, the fracturing will occur on them. The crushers are very much rugged, massive and heavy in design and contact surfaces have replaceable high tensile manganese or other alloy steel sheet having either flat or corrugated surfaces. To guard against shock and over load the crushers are provided with shearing pins or nest in heavy coiled springs.

Many engineering structures consist of stiffened thin plate elements to improve the strength/weight ratio. The stiffened plates subjected to impact or shock loads are of considerable importance to mechanical and structural engineers. The main object of the

present work is to propose an efficient use of modeling in the connection between the plate and the stiffener, and as part of it the constraint torsion effect in the stiffener.

1.2 Overview of Jaw Crushers

1.2.1 Introduction to Jaw Crusher

The first stage of size reduction of hard and large lumps of run-of-mine (ROM) ore is to crush and reduce their size. Softer ores, like placer deposits of tin, gold, mineral sands etc. do not require such treatment. Large scale crushing operations are generally performed by mechanically operated equipment like jaw crushers, gyratory crusher and roll crushers. For very large ore pieces that are too big for receiving hoppers of mechanically driven crushers, percussion rock breakers or similar tools are used to break them down to size. The mechanism of crushing is either by applying impact force, pressure or a combination of both. The jaw crusher is primarily a compression crusher while the others operate primarily by the application of impact. [6]

Jaw crusher is one of the main types of primary crushers in a mine or ore processing plant. The size of a jaw crusher is designated by the rectangular or square opening at the top of the jaws (feed opening). For instance, a 24 x 36 jaw crusher has a opening of 24" by 36", a 56 x 56 jaw crusher has a opening of 56" square. Primary jaw crushers are typically of the square opening design, and secondary jaw crushers are of the rectangular opening design. However, there are many exceptions to this general rule. Jaw crusher is a primary type of crusher which has two jaws, out of which one is stationary attached rigidly with the crusher frame whereas the other moves between a small throw forward and retarded back successively to crush the ore or rock boulders.

Jaw crushers are typically used as primary crushers, or the first step in the process of reducing rock. They typically crush using compression. The rock is dropped between two rigid pieces of metal, one of which then move inwards towards the rock, and the rock is crushed because it has a lower breaking point than the opposing metal piece. Jaw crusher movement is obtained by using a pivot point located at one end of the “swing jaw”, and an eccentric motion located at the opposite end. [6]

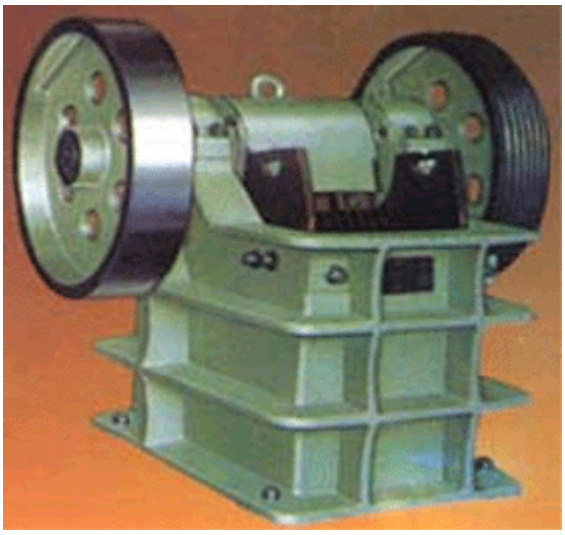

Fig 1.1.Typical Jaw Crusher [36]

1.2.2 Different Types of Jaw Crusher

Jaw crusher can be divided into two according to the amplitude of motion of the moving face. The different types of Jaw Crushers are:

1) Blake Type Jaw Crusher

In this the movable jaw is hinged at the top of the crusher frame so that the maximum amplitude is obtained at the bottom of the crushing jaws. Blake Crushers are operated by toggles and controlled by a pitman. These are commonly used as primary crushers in the mineral industry. The size of the feed opening is referred to as the *gape.* The opening at the discharge end of the jaws is referred to as the *set.* The Blake crushers are single or double toggle drives. The function of the toggle(s) is to move the pivoted jaw. The retrieving action of the jaw from its furthest end of travel is by springs for small crushers or by a pitman for larger crushers. As the reciprocating action removes the moving jaw away from the fixed jaw the broken rock particles slip down, but are again caught at the next movement of the swinging jaw and crushed. This process is repeated until the particle sizes are smaller than the smallest opening between the crusher plates at the bottom of the crusher (the closed set).

For a smooth reciprocating action of the moving jaws, heavy flywheels are used in both types of crushers. Blake type jaw crusher may be divided into two types. [6]

(a) Single toggle type: - In this the number of toggle plate is only one. It is cheaper and has less weight compare to a double toggle type jaw crusher. The function of the toggle(s) is to move the pivoted jaw.

(b) Double toggle type: - Here the number of toggle plate is two. Over the years many mines have used the double-toggle style of crusher because of its ability to crush materials, including mineral bearing ores that were both tough and abrasive. While many aggregate producers have used the overhead eccentric style. There are many factors that should be considered when deciding which style would be best for your application. For larger material crushing, always larger Blake type jaw crushers are selected. The characteristics of this type of crusher are as following

1. Larger, rough, blocky as well as sticky rock or ore lumps can be crushed.
2. Reinforcement of the crusher is possible with the help of high strength crusher frame to crush very hard rock or ore lumps.
3. It is very simple to adjust to prevent much of wear and also very easy to repair,
4. Maintenance o the crusher is very easy.

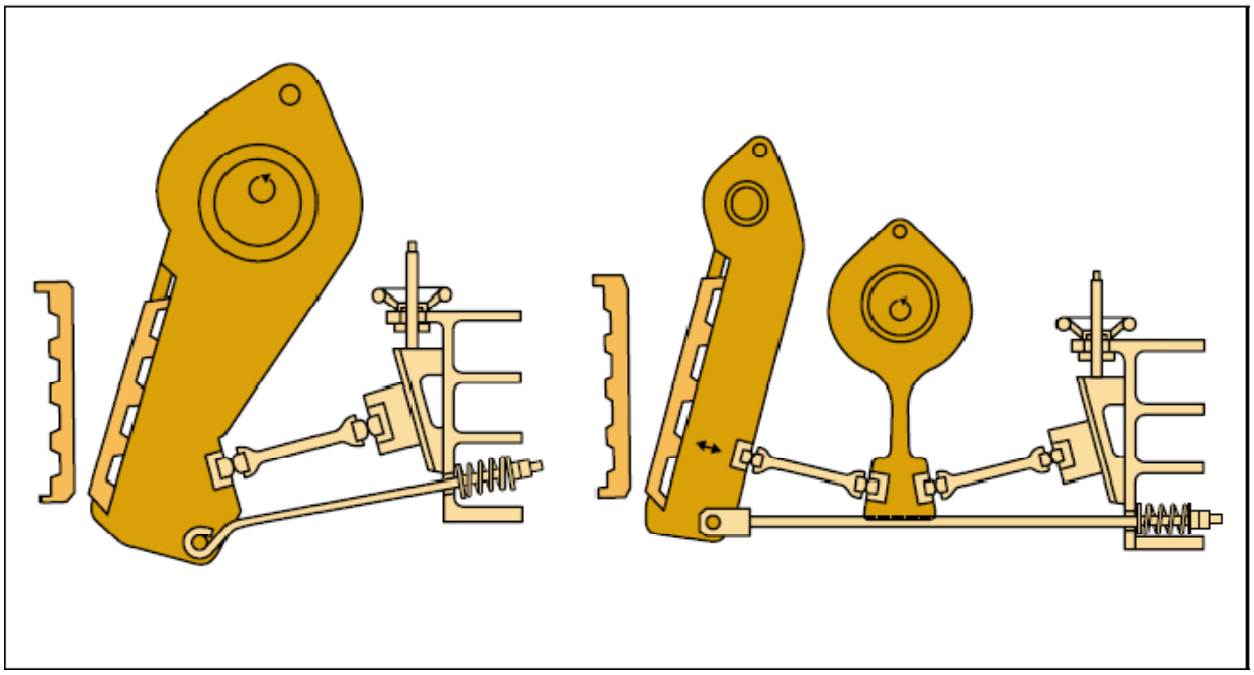

Single-Toggle Jaw Crusher Double-Toggle Jaw Crusher

Fig.1.2. Types of Blake Type Jaw Crusher [43]

2) Dodge Type Jaw Crusher

The moving plate is pivoted at the bottom and connected to an eccentric shaft. In universal crushers the plates are pivoted in the middle so that both the top and the bottom ends can move. The movable jaw is hinged at the bottom of the crusher frame so that the maximum amplitude of motion is obtained at the top of the crushing jaws. They are comparatively lower in capacity than the Blake crushers and are more commonly used in laboratories.

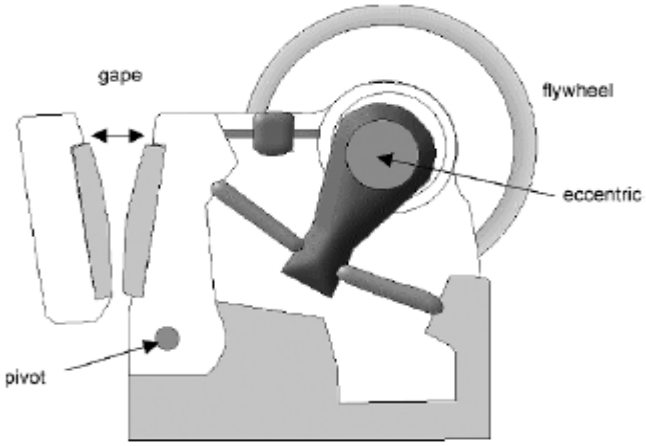

Fig.1.3. Dodge Type Jaw Crusher [6]

1.3 Major Components of a Jaw Crusher

Crusher Frame:

Crusher Frame is made of high welding. As a welding structure, it has been designed with every care so as to ensure that it is capable of resistant to bending stress even when crushing materials of extremely hard.

Jaw Stock:

Jaw Stock is also completely welded and has renewable bushes, Particular importance has been given to jaw Stock of a design resistant to bending stresses. All jaw stocks are provided with a renewable steel Alloy or manganese steel toggle grooves.

Jaw Crusher Pitman:

The pitman is the main moving part in a jaw crusher. It forms the moving side of the jaw, while the stationary or fixed jaw forms the other. It achieves its movement through the

eccentric machining of the flywheel shaft. This gives tremendous force to each stroke. As an interesting aside the term "pitman" means "connecting rod", but in a jaw crusher it really doesn't perform this function, which is it doesn't connect two things. Other mechanisms called pitman such as linkages in car/truck steering systems actually do connect things. Thus it appears this is just the name that was applied to this part. Pitman is made of high quality steel plates and carefully stress relived after welding. The Pitman is fitted with two renewable steel Alloy or manganese steel toggle grooves housings for the bearings are accurately bored and faced to gauge.

Manganese Dies in the Jaw Crusher:

The jaw crusher pitman is covered on the inward facing side with dies made of manganese, an extremely hard metal. These dies often have scalloped faces. The dies are usually symmetrical top to bottom and can be flipped over that way. This is handy as most wear occurs at the bottom (closed side) of the jaw and flipping them over provides another equal period of use before they must be replaced.

Jaw Crusher Fixed Jaw Face:

The fixed jaw face is opposite the pitman face and is statically mounted. It is also covered with a manganese jaw die. Manganese liners which protect the frame from wear; these include the main jaw plates covering the frame opposite the moving jaw, the moving jaw, and the cheek plates which line the sides of the main frame within the crushing chamber.

Eccentric Jaw Crusher Input Shaft:

The pitman is put in motion by the oscillation of an eccentric lobe on a shaft that goes through the pitman's entire length. This movement might total only 1 1/2" but produces substantial force to crush material. This force is also put on the shaft itself so they are constructed with large dimensions and of hardened steel. The main shaft that rotates and has a large flywheel mounted on each end. Its eccentric shape moves the moving jaw in and out. Eccentric Shaft is machined out of Alloy Steel Fitted with anti-friction bearings and is housed in pitman and dust proof housing.

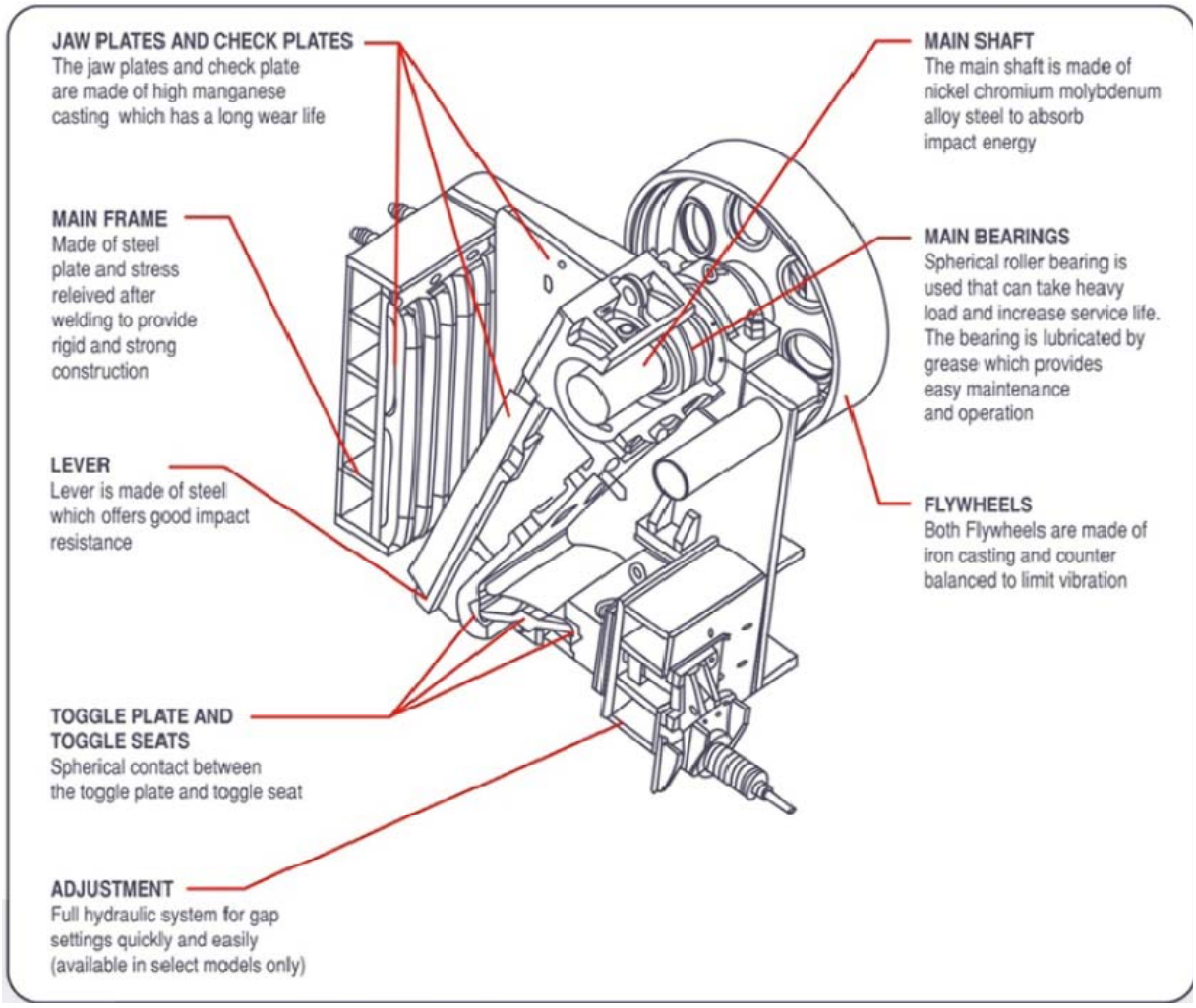

Fig.1.4. Sectional view showing Components of a Jaw Crusher

Jaw Crusher Input Sheave/Flywheel:

Rotational energy is fed into the jaw crusher eccentric shaft by means of a sheave pulley which usually has multiple V-belt grooves. In addition to turning the pitman eccentric shaft it usually has substantial mass to help maintain rotational inertia as the jaw crushes material.

Toggle Plate Protecting the Jaw Crusher:

The bottom of the pitman is supported by a reflex-curved piece of metal called the toggle plate. It serves the purpose of allowing the bottom of the pitman to move up and

down with the motion of the eccentric shaft as well as serve as a safety mechanism for the entire jaw. Should a piece of non-crushable material such as a steel loader tooth (sometimes called "tramp iron") enter the jaw and be larger than the closed side setting it can't be crushed nor pass through the jaw. In this case, the toggle plate will crush and prevent further damage.

Tension Rod Retaining Toggle Plate:

Without the tension rod & spring the bottom of the pitman would just flop around as it isn't connected to the toggle plate, rather just resting against it in the toggle seat. The tension rod system tensions the pitman to the toggle plate. The toggle plate and seats. The toggle plate provides a safety mechanism in case material goes into the crushing chamber that cannot be crusher. It is designed to fail before the jaw frame or shaft is damaged. The seats are the fixed points where the toggle plate contacts the moving jaw and the main frame.

Jaw Crusher Sides Cheek Plates:

The sides of the jaw crusher are logically called cheeks and they are also covered with high-strength manganese steel plates for durability.

Jaw Crusher Eccentric Shaft Bearings:

There are typically four bearings on the eccentric shaft: two on each side of the jaw frame supporting the shaft and two at each end of the pitman. These bearings are typically roller in style and usually have labyrinth seals and some are lubricated with an oil bath system. Bearings that support the main shaft. Normally they are spherical tapered roller bearings on an overhead eccentric jaw crusher.

Anti-Friction Bearings are heavy duty double row self-aligned roller-bearings mounted in the frame and pitmans are properly protected against the ingress of dust and any foreign matter by carefully machined labyrinth seals. Crushing Jaws are castings of austenitic manganese steel conforming to IS 276 grade I & II. The real faces of the crushing jaws are levelled by surface grinding in order to ensure that they fit snugly on the crusher

frame and jaw stock. The crushing jaws are reversible to ensure uniform wear and tear of grooves.

Jaw Crusher Adjustment: Closed Side Opening Shims

Depending on the disposition of the material being crushed by the jaw different maximum sized pieces of material may be required. This is achieved by adjusting the opening at the bottom of the jaw, commonly referred to as the "closed side setting". Shims (sometimes implemented and a more adjustable or hydraulic fashion) allow for this adjustment. [41]

1.4 Materials Used For Different Parts

Body:

Made from high quality steel plates and ribbed heavily in welded steel construction which withstand heavy crushing, any load and least vibration.

Swing Jaw Plates:

Different types of jaw plates are available to suit various applications. Mainly mangenese steel. (Work hardening steel)

Stationary Jaw Plates:

Made of manganese steel (work hardening) having longer crushing life with least ware -n-tare.

Pitman:

Mistry crushers have a light weight pitman having white-metal lining for bearing surface which prevents excessive friction.

Toggle:

Double toggles, for even the smallest size crushers give even distribution of load. Wall designed compression springs provide cushioning to the toggle mechanism which eliminate knocks and reduce the resultant wear.

Flywheel:

Fly wheel cum pulley made of high grade cast iron. This is with low inertia and starts crushing instantly.

Tension Rod:

Pullback rods helps easy movement, reduces pressure on toggles and machine vibration.

Hinge Pin:

Strong hinge pin of special steel in located in correct relation to the crushing zone for crushing without rubbing.

Shaft and Bearings:

Massive rigid eccentric shaft of special steel is carried in self aligned spherical roller bearings of ample capacity which ensures smooth running.

Lubrication:

Automatic, continuous spray lubrication, by positive gear pump for the pitman-toggle mechanism, enables the crusher to run safely.

Diaphgram:

Specially designed will resistant flexible diaphragm seals the opening in the oil chamber and protects the mechanism against dust.[40]

1.5 Jaw Crusher Working Principle

The working principal of Jaw Crusher is based on modern design "CRUCHING WITHOUT RUBBING" The machine consists, two Jaws, one fixed and the other moving. The opening between them is smaller at the bottom and wider at the top. The pitman moving on an eccentric shaft on bearing, swing lever (Moving Jaw) swing on center pin. The Rock held in between two Jaws and crushed by mechanical pressure.

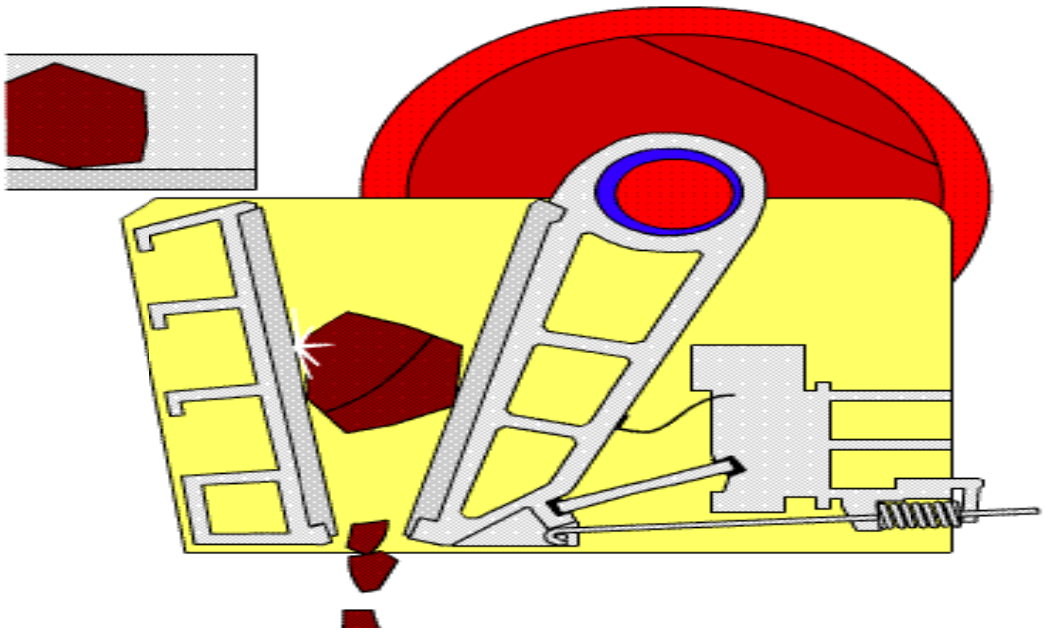

Fig.1.5. Working Principle of Jaw Crusher [42]

The motor drives the belt pulley and the belt pulley drives the eccentric shaft to rotate, and make the moving jaw approach and leave the fixed jaw periodically, to crush, rub and grind the materials repeatedly, thus to make the material slower and slower and gradually fall down and finally discharge from the discharge opening. A fixed jaw mounted in a “V” alignment is the stationary breaking surface while the movable jaw exerts force on the rock by forcing it against the stationary plate. The space at the bottom of the “V” aligned jaw plates is the crusher product size gap or size of the crushed product from the jaw crusher. The remains until it is small enough to pass through the gap at the bottom of the jaws. [42]

The ore or rock is fed to the crusher where the jaws are furtherest apart, i.e. at the maximum opening or gape. When the jaws come together the ore is crushed into smaller sizes and slip down the cavity. In the return stroke, further reduction of size is experienced and the ore moves down further. The process is repeated till particles having size less than the bottom opening or set pass through as product. The function of the toggle(s) is to move the pivoted jaw. The retrieving action of the jaw from its furthest end of travel is by springs for small crushers or by a pitman for larger crushers. For a smooth reciprocating action of the moving jaws, heavy flywheels are used in both types of crushers.

1.6 Crusher Sizes and Power Ratings

The size of a jaw crusher is usually described by the gape and the width, expressed as gape x width. The common crusher types, sizes and their performance is summarized in Table 1.1.Currently, the dimension of the largest Blake-type jaw crusher in use is 1600 mm x 2514 mm with motor ratings of 250-300 kW. Crushers of this size are manufactured by Locomo, Nordberg (Metso) and others. The Metso crusher is the C 200 series having dimensions 1600 x 2000 mm. driven by 400 kW motors. Various sizes of jaw crushers are available, even a crusher size of 160 x 2150 mm (1650 mm is the width of the maximum opening at the top and the jaws are 2150 mm in long) are not uncommon. The maximum diameter of the feed is ranged in 80 to 85% of the width of the maximum opening. Such a heavy crusher (16540x 2150mm) crushes rock, mineral or ore varying from 22.5 cm to 30cm with a capacity ranging from 420 to 630 ton per hour. The motor rpm and power are around 90 and 187.5 kW respectively. The jaw and the sides of the unit are lined with replaceable wear resistant plate liners. [6]

Table 1.1 Jaw Crusher Performances

Crusher Type	**Size mm**				**Reduction Ratio**		**Power, kW**		**Toggle Speed, rpm**	
	Gape, mm		Width, mm		Range	Average	Min	Max	Min	Max
	Min	Max	Min	Max						
Blake double toggle	125	1600	150	2100	4:1/9:1	7:1	2.25	225	100	300
Blake single toggle	125	1600	150	2100	4:1/9:1	7:1	2.25	400	120	300
Dodge Type	100	280	150	28	4:1/9:1	7:1	2.25	11	250	300

1.7 Different Performance Parameters of Jaw Crusher

Crushing of ore, mineral or rock depends upon the characteristics of ore, size of the feed and the discharge openings, speed, throw, nip angle (It is the angle between the jaw faces. Generally it is around 20° to 23° in higher capacity jaw crusher), etc, of the crusher. The capacity of the crushing depends upon the reduction ratio (It is the ratio between the size of the feed and the size of the discharge. Higher the reduction ratio less the capacity of the crusher) nip angle (increase in the angle will decrease of the capacity of crusher), increase in speeds, throw curved shaped jaws, etc. will increase the capacity.

The Jaw Crusher should not be buried by the feeding minerals or ores which will tend to chock the mouth of the crusher and open a power operated hook will be necessary to remove the ore or mineral lumps which jam the crusher unit. Generally average reduction ratio is around 1.8 to 7 with a maximum setting of gap around 2 to 2.4mm. However this reduction ratio may vary depending upon many operating condition. The jaws do not touch each other and have a wide gap at the top. The faces that are flat or flat / convex (convex jaws are better which reduces the frequencies of chocking and also increases the capacity of production).

1.8 Objective of Present Work

The objective of the present work is to strive for a design and analysis of commercially available swing jaw plates (including stiffening elements), that is 0.9 m (36 in.) wide with 304 mm and 51 mm (12 in. and 2 in.) top and bottom openings of jaw crusher. The finite element method is applied to the analysis of the swing jaw plate. Also further study of swing jaw plate with stiffener is done using finite element analysis.The theoretical design calculations of jaw plates have been computerized. The design and modeling jaw plates of crusher is accomplished by using CAD i.e. parametric design package (CATIAP3V5R15). By using this package three dimensional model of jaw plates jaw crusher has been developed. Finite Element Analysis of jaw plates are carried out by using ALGOR V19 programming. This work is extended to improve the strength/weight ratio of swing jaw plate by adding different number of stiffener elements on the jaw plates.

CHAPTER-2

LITERATURE REVIEW

2. LITERATURE REVIEW

Jaw crushers are used to crush material such as ores, coals, stone and slag to particle sizes. Jaw crushers operate slowly applying a large force to the material to be granulated. Generally this is accomplished by pressing it between jaws or rollers that move or turn together with proper alignment and directional force. The jaw crusher squeezes rock between two surfaces, one of which opens and closes like a jaw. Rock enters the jaw crusher from the top. Pieces of rock those are larger than the opening at the bottom of the jaw lodge between the two metal plates of the jaw. The opening and closing action of the movable jaw against the fixed jaw continues to reduce the size of lodged pieces of rock until the pieces are small enough to fall through the opening at the bottom of the jaw. It has a very powerful motion. Reduction in size is generally accomplished in several stages, as there are practical limitations on the ratio of size reduction through a single stage.

The jaw crushers are used commercially to crush material at first in 1616 as cited by Anon [1].It is used to simplify the complex engineering. Problem those were prevailing in Mining and Construction sector. An important experimental contribution was made in1913 when Taggart [2] showed that if the hourly tonnage to be crushed divided by Square of the gape expressed in inches yields a quotient less than 0.115 uses a jaw crusher.

Lindqvist M.and Evertsson C. M. [3] worked on the wear in rock of crushers which causes great costs in the mining and aggregates industry. Change of the geometry of the crusher liners is a major reason for these costs. Being able to predict the geometry of a worn crusher will help designing the crusher liners for improved performance. Tests have been conducted to determine the wear coefficient. Using a small jaw crusher, the wear of the crusher liners has been studied for different settings of the crusher. The experiments have been carried out using quartzite, known for being very abrasive. Crushing forces have been measured, and the motion of the crusher has been tracked along with the wear on the crusher liners. The test results show that the wear mechanisms are different for the fixed and moving liner. If there were no relative sliding distance between rock and liner, would yield no wear. This is not true for rock crushing applications where wear is observed even though there is no macroscopic sliding between the rock material and the liners. For this reason has been modified to account for the wear induced by the local sliding of particles being crushed. The predicted worn geometry is similar to the real crusher. A jaw crusher is a machine

commonly used in the mining and aggregates industry. The objective of this work, where wear was studied in a jaw crusher, is to implement a model to predict the geometry of a worn jaw crusher.

DeDiemar R.B. [4] gives new ideas in primary jaw crusher design and manufacture of Jaw crusher utilizing open feed throat concept, power savings and automation features. Jaw crushers with two jaw openings can be considered to be a completely new design. Jaw crushers are distinguished by reciprocating and complex movement of the moving jaw. Jaw crushers with hydraulic drives produced in France and jaw crushers with complex movement of two-sided jaws produced have advantages as well as a common shortcoming. This is due to the discharge gap being almost vertical or sharply inclined so that a large part of the material is crushed only to a size corresponding to the maximum width of the gap between the jaws at the crusher exit. A new design has a gently sloping gap between the movable and stationary jaws .This causes material to move slowly and be subjected to repeated crushing. In addition the movement of the movable jaw relative to the stationary one is such that its stroke is equal both at the inlet and outlet of the discharge gap. When the eccentric moves in different quadrants. The power consumption of this jaw crusher is low since the work of crushing is distributed between two quadrants. The precrushed material falls under its own weight onto the movable jaws which are lowered by the movement of the eccentric through the third and fourth quadrants. During this movement the material moved down slightly along the gap between the jaws and comes in contact with the movable jaws at approximately the time when they are furthest removed from stationary jaws. The material is again crushed as the eccentric continues to move through the first and second quadrant. The material thus undergoes repeated crushing when it passes through the gap between the jaws. Efforts to intensify the crushing process and to increase throughput capacity of crushers sometimes leads to interesting solutions of kinematic systems. The jaw crusher has six movable and three stationary two-sided jaws with a planetary drive. The high throughput capacity is achieved by a significantly more complicated construction. Analysis of crusher operation leads to the conclusion that development of their design is proceeding both along the path of improved design and development of fundamentally new efficient kinematic systems.

Gupta Ashok and Yan D.S. [6] worked in design of jaw crushers which impart an impact on a rock particle placed between a fixed and a moving plate. The faces of the plates

are made of hardened steel. Both plates could be flat or the fixed plate flat and the moving plate convex. The surfaces of both plates could be plain or corrugated. The moving plate applies the force of impact on the particles held against the stationary plate. Both plates are bolted on to a heavy block. The moving plate is pivoted at the top end or at the bottom end and connected to an eccentric shaft. In universal crushers the plates are pivoted in the middle so that both the top and the bottom ends can move. The Blake crushers are single or double toggle drives. The function of the toggle is to move the pivoted jaw. The retrieving action of the jaw from its furthest end of travel is by springs for small crushers or by a pitman for larger crushers. As the reciprocating action removes the moving jaw away from the fixed jaw the broken rock particles slip down, but are again caught at the next movement of the swinging jaw and crushed. This process is repeated until the particle sizes are smaller than the smallest opening between the crusher plates at the bottom of the crusher (the closed set). For a smooth reciprocating action of the moving jaws, heavy flywheels are used in both types of crushers.

Russell A.R., Wood D. M.[5] helps in failure criterion for brittle materials is applied to a stress field analysis of a perfectly elastic sphere subjected to diametrically opposite normal forces that are uniformly distributed across small areas on the sphere's surface. Expressions are obtained for an intrinsic strength parameter of the material, as well as its unconfined compressive strength. An expression for the unconfined tensile strength is obtained by introducing an additional parameter accounting for the micro structural features of the material. The expressions indicate that failure initiates in the sphere where the ratio between the stress invariant and the first stress invariant is a maximum. Such a criterion does not coincide with the location of maximum tensile stress. The expressions are used to reinterpret published point load test results and predict unconfined compressive strengths. The configuration of the point load test as well as surface roughness and elastic properties of the pointer and samples are taken into account to establish the size of the area on which the point loads act. The predictions are in good agreement with measured values obtained directly using unconfined compressive strength tests. It is concluded that the point load test provides a more reliable estimate of the compressive strength than the tensile strength.

Dowding Charles H. [7] designed jaw plates to reduce efforts to decrease energy consumed in crushing have lead to consideration of decreasing the weight of the swing plate of jaw crushers for easily crushed material. This paper presents the results of an

investigation of the feasibility of using point load-deformation-failure (PDF) relationships along with interactive failure of rock particles as a model for such a weight reduction. PDF relationships were determined by point-loading various sizes of materials: concrete mortar, two types of limestone, amphibolites and taconite. Molling [7], who proposed this hypothetical distribution, was only concerned with the total loading force. The parameter which most controls the design of the swing plate is the load distribution. Instrumentation of toggle arms in has since led to correlation of measured with rock type. Ruhl [7] has presented the most complete consideration of the effect of rock properties on Q and the toggle force. His work is based upon the three-point loading strength of the rock, which he found to be one-sixth to one eleventh the unconfined compressive strength. He calculated hypothetical toggle forces based upon the sum of forces necessary to crush a distribution of regular prisms fractured from an initial cubical rock particle. These approaches involved both maximum resistance and simultaneous failure of all particles and thus neither can lead to an interactive design method for changing stiffness (and weight) of the swing plate. In this study point-loading of cylinders are undertaken to model behavior of irregular rock particles.

Hiramatsu and Oka [8] worked to model irregular particle behavior with that of cylinders by appropriate consideration. From photoelastic studies of plate-loaded spheres and point-loaded cubes, prisms and ellipsoids, they determined that the stresses produced in plate and point-loaded spheres of identical diameter are equal. Thus, the plate idealization may be replaced by the point load. Niles I. L. [14] showed that point-load failure of a sphere was equal to that of a point-loaded ellipsoid. Therefore, ultimate point loads on spheres will be approximately equal to ultimate point loads on cylinders (or discs). For both the ellipsoids and the cylinders, the excess volume outside the spherical dimensions does not change the circular failure surface parallel to the smallest dimensions of the body. This circular failure surface for the sphere and cylinder is shown by the jagged lines on the two shapes. These authors and others also compared disc and irregular particle point-load strengths from tests on dolomite, sandstone and shale and found the point load strength of the disk and irregularly shaped particles to be equal. Thus, the properties determined from point-loading of discs or cylinders are appropriate for the point-loading of irregular particles. Hiramatsu and Oka's [8] photoelastic studies and theoretical calculations reveal that point loads produce tensile stresses across the middle 70% of the axis between the point loads.

However, the volume directly beneath the contact is found to be in a state of compression, which leads to early, local compression failure. Early work by Bergstrom et al. and Stevenson and Bergstrom presented measurements of the deformability of small iron ore pellets and glass beads when crushed between two plates. Their work showed that the load-deformation relationships of both materials displayed deformation hardening in the initial stages of loading as predicted by the Hertzian theory for the behavior of contacting spheres .The more plastic (and weaker) iron ore pellets showed strain softening behavior in the latter stages of deformation, whereas the more brittle glass beads continued to stiffen, up to the point of failure. These observations indicate that the deformation stiffening or Hertzian behavior should be expected for point-loading of brittle rock particles.

Whittles D.N. et al [8] worked to optimize of the efficiency of crushers is desirable in terms of reducing energy consumption, increasing throughput and producing better downstream performance as a result of improved size specification. The mechanism of rock fragmentation within crushers is dominated by compression at high strain rates. Research presented in this paper has investigated the relationship between strain rate, impact energy, the degree of fragmentation and energy efficiencies of fragmentation. For the investigation two laboratory test methods were use to generate compressive failure under different strain rates. The tests were namely a variable speed unconfined compressive strength test, and a laboratory drop weight test. Laboratory testing and computer simulations showed that a greater amount of energy was required for breakage with increasing strain rate and also samples broken at higher strain rates tended to produce a greater degree of fragmentation. It was also observed that not only the impact energy influences the degree of fragmentation but the combination of drop weight/height also has an effect.

King R.P. [9] investigation largely improved our understanding of the mechanism of the particle fracture process. It is found that although the particle is loaded predominantly in compression, substantial tensile stresses are induced within the particle under various loading conditions. It is those tensile stresses that induce a major catastrophic splitting crack to be responsible for the particle breakage. Moreover, around the loading points there is progressive localized crushing caused by the high compressive stress. Therefore, two major failure mechanisms are recognized: catastrophic splitting and progressive crushing. Correspondingly, the particle is broken into two kinds of progenies with two distinct size ranges. Coarse particles are products resulting from the induced tensile failure and fines are

products resulting from compressive or shear failure near the points of loading. On the basis of the simulated results, it is demonstrated that the behavior of particle breakage is strongly dependent on heterogeneous particle material properties, the irregular particle shape and size, and the various loading conditions. The fracture characteristics of the particle such as the peak load, the particle tensile strength and the energy utilization ratio are greatly influenced by the irregular particle shape and size. It seems that their influence on particle stiffness is not so obvious.

Briggs, C.A. and Bearman, R.A. [10] reported that the particle breakage is the fundamental mechanism in all industrial comminution process. In this study, the breakage processes of particles with heterogeneous material property, irregular shape and size under various loading conditions are numerically investigated by the Rock Failure Process Analysis code from a mechanics point of view. The loading conditions include point-to-point loading, multipoint loading, point-to-plane loading, and plane-to-plane loading. The simulated results reproduce the particle breakage process: at the first loading stage, the particle is stressed and energy is stored as elastic strain energy with a few randomly isolated fractures. As the load increases, the isolated fractures are localized to form a macroscopic crack. At the peak load, the isolated fractures unstably propagate in a direction parallel to the loading direction following tortuous paths and with numerous crack branches. Finally, the major crack passes through the particle and several coarse progeny particles are formed. Moreover, in the vicinity of the contacting zone the local crushing is always induced to cause fines. Georg Muir [16] found that the dominant breakage mechanisms are catastrophic splitting and progressive crushing, which correspondingly result in progenies with two distinct size range: coarse particle and fines, respectively. It is pointed out that the particle breakage behavior strongly depends on the heterogeneous material property, the irregular shape and size, and the various loading conditions. Because of heterogeneity, the crack propagates in tortuous path and crack branching becomes a usual phenomenon. Depending on the loading conditions, with the irregular shape and size used in this study, the particle strength increase but the energy utilization ratio decreases, and the particle behavior has shown a brittle–ductile transition in a sequence of point-to-point loading, multipoint loading, point-to-plane loading, and plane-to-plane loading.

Berry P. et al [11] studied the laws of mechanics and constitutive relations concerning rock breakage characteristics. The simulated results are consistent with the general

description and experimental results in the literature on particle breakage. A descriptive and qualitative particle breakage model is summarized as the following: at the first loading stage the particle is stressed and energy is stored as elastic strain energy in the particle. A number of randomly distributed isolated fractures are initiated because of the heterogeneity. Georg Muir [16] showed as load increases, the isolated fractures are localized to form macroscopic crack or cracks and the particle behavior becomes weaken. Around the peak load, the macroscopic cracks propagate unstably in a direction parallel to the loading direction following a tortuous path and with various crack branches. Finally, the major crack passes through the particle and several coarse progeny particles are formed. The number and size of the progeny particles depend on the size and location of the initiating cracks and on the extent of crack branching that occurs. During the loading process, in the vicinity of the contacting zone the compressive failure is always induced to cause the local crushing.

Guangjun FAN, Fusheng MU [12] worked on the certain domain, called the liner domain, of the coupler plane is chosen to discuss the kinetic characteristic of a liner or a crushing interface in the domain. Based on the computation and the analysis of the practical kinetic characteristic of the points along a liner paralleling to the direction of coupler line, some kinematics arguments are determined in order to build some kinetic characteristic arguments for the computing, analyzing and designing. Weiss N.L. [13] work is helpful for a design of new prototype of this kind of machine on optimizing a frame, designing a chamber and recognizing a crushing character. A liner of jaw crusher is an interface for analyzing the crushing force, on which the crushing force occurs, in other words, the directly contact and the interaction between the material and the liner occur there. So the interface has great effect on the crushing feature of jaw crusher. The liner is one of the curves in the cross-section of the couple plane, which is also given a definition as one of the coupler curves in a four bar crank-rocker model. Qin Zhiyu [20] studied different positions of liners in the coupler plane have different moving features, the motion of points along the liners in the computing domain is quite different from that of them in the straight-line coupler of the simple four bar crank-rocker model. Therefore, it is necessary to consider motion differences caused by different liner positions and their motion features to select a coupler curve as the swing liner with good crushing character.

Georget Jean-Pirre and Lambrecht Roger [15] invented jaw crushers comprising a frame, a stationary jaw carried by the frame a mobile jaw associated with the stationary jaw

and defining a crushing gap therewith; an eccentric shaft supporting one end of the frame and a connecting rod or toggle supporting the other mobile jaw end on the crossbeam. The position of the crossbeam in relation to the frame is adjustable to change the distance between the jaws i.e. the size of crushing gap. A safety system permits the mobile jaw to recoil when the pressure it exerts on the connecting rod exceeds a predetermined value, for example because an unbreakable piece is in the crushing gap. In the illustrated jaw crusher, the crossbeam is pivotally mounted on the frame for pivoting about an axis parallel to the shaft and the safety system acts; on the crossbeam to prevent it from pivoting when the force applied by the mobile jaw to the crossbeam remains below a predetermined value. Pollitz H.C.[17] presents invention concerns an improved design of stationary and movable jaw plates for jaw type crusher which minimizes warping of the jaws and increases their life more particularly the present invention concerns an improved structure for mounting the stationary jaw plate to the crusher frame and for increasing the rigidity and life of both plates. Zhiyu Qin, Ximin Xu [18] indicated that the relationship between the increasing rate of holdup and the material-feeding rate were examined. From the results, the maximum crushing capacity was defined as the maximum feed rate where holdup did not change with time and remained at a constant value.

FishmanYu.A. [19] work of evolutionary algorithms for finding applications in engineering design tasks which uses evolutionary algorithms to optimize the performance of a comminution circuit for iron ore processing. In work reported earlier, a simple evolution strategy algorithm was used to solve this problem. We have restated the details of the problem description here for completeness. The performance of a processing plant has a large impact on the profitability of a mining operation, and yet plant design decisions are often guided more by engineering intuition and previous experience than by analysis. This is because plants are extremely complex to model, so engineers often must rely on simulation tools to evaluate and compare alternative hand-crafted designs. This is a time-consuming process and the lack of an analytical model means that there is little theoretical guidance to narrow the search for better solutions. Evolutionary algorithms can be of great benefit here, providing a means to search large design spaces and present the engineer with superior designs optimized for different operating scenarios. Cao Jinxi [20] found the combinations of design variables (including geometric shapes and machine settings) to maximize the capacity of a simple comminution circuit, whilst also minimizing the size of the product.

Earlier work in showed the effectiveness of a single-objective evolution strategy algorithm for this task. However, the multi-objective approach described in this paper offers clear advantages over the single-objective algorithm. We begin the paper with a description of the problem, including a brief background on crushers and comminution circuits. Finally, we discuss future enhancements to the system and plan to extend the work to include greater complexity in the simulation model, including circuits. Yashima et al. [21] found that the amount of strain energy required for fragmentation increased with strain rate, indicating higher strain rates are less efficient in producing fractures. The fracture characteristics of particles within a roller mill have been studied by Tavares. In his study he found that as the energy input was increased the extent of the damage induced in the material also increased. This indicated that there is an optimum level of strain rate and energy to produce the desired degree of fragmentation and that the fragmentation process is less energy efficient at high strain rates. Tavares also investigated the energy absorbed in breakage of single rock particles in modified drop weight testing. This worker calculated the energy absorbed in particle breakage and again concluded that the energy required producing rock fragmentation decreased with strain rate. Lytwynyshyn G. R [22] reported that the slow compression test was the most efficient method of particle fragmentation with impact loading being approximately 50% efficient, whilst the ball mill was considered to be approximately 15% as efficient as the slow compression test. Krogh undertook drop weight tests on small samples of quartz with the impact speed in the range 0.64-1.9 m/s, but with constant impact energy. It was found that the probability of breakage of each individual particle was not influenced by impact speed nor was the size distribution of the fragments produced.

Jaw plates used in modern crushing operations are fabricated almost exclusively from what is generally known as Hadfield manganese steel [26], steel whose manganese content is very high and which possesses austenitic properties. Such jaw plates are not only extremely tough but are also quite ductile and work-harden with use. Under the impact of crushing loads “flow” of the metal at the working surface of the plate occurs in all directions. This “flow” occurs chiefly in the central area of the plate, particularly the lower central area, because the lower portion of the plate does very substantially more work than the upper portion. This is particularly true in case of the stationary jaw, which, as well known receives the greater wear in operation. If the “flow” is not compensated for, the jaw

will distort or warp, particularly in its more central area, so that it will no longer contact its seat. Thus crushing loads will cause it to flex with consequent decrease in crushing efficiency and increase in wear both of the jaw itself and particularly its seat.

Gabor M. Voros [23] presents the development of a new plate stiffener element and the subsequent application in determine impact loads of different stiffened plates. In structural modeling, the plate and the stiffener are treated as separate finite elements where the displacement compatibility transformation takes into account the torsion – flexural coupling in the stiffener and the eccentricity of internal forces between the beam – plate parts. The model becomes considerably more flexible due to this coupling technique. The development of the stiffener is based on a general beam theory, which includes the constraint torsional warping effect and the second order terms of finite rotations. Numerical tests are presented to demonstrate the importance of torsion warping constraints. As part of the validation of the results, complete shell finite element analyses were made for stiffened plates.

Kadid Abdelkrim [24] carried out investigation to examine the behavior of stiffened plates subjected to impact loading. He worked to determine the response of the plates with different stiffener configurations and consider the effect of mesh dependency, loading duration, and strain-rate sensitivity. Numerical solutions are obtained by using the finite element method and the central difference method for the time integration of the non-linear equations of motion. Special emphasis is focused on the evolution of mid-point displacements, and plastic strain energy. The results obtained allow an insight into the effect of stiffener configurations and of the above parameters on the response of the plates under uniform blast loading and indicate that stiffener configurations and time duration can affect their overall behavior.

CHAPTER-3

THEORETICAL ANALYSIS
AND
DATA COLLECTION

3. THEORETICAL ANALYSIS AND DATA COLLECTION

3.1 Introduction to Design of Jaw Plates

Recently, concern for energy consumption in crushing has led to the consideration of decreasing the weight (and consequently the stiffness) of the swing plate of jaw crushers to match the strength of the rock being crushed. An investigation of the energy saving of plate rock interaction when point load deformability and failure relationships of the rock are employed to calculate plate stresses. Non simultaneous failure of the rock particles is incorporated into a beam model of the swing plate to allow stress calculation at various plate positions during one cycle of crushing. In order to conduct this investigation, essentially two studies were required. First, point load-deformation relationships have to be determined for differing sizes of a variety of rock types. Even though much has been written about the ultimate strength of rock under point loads, very little has been published about the pre and post-failure point load-deformation properties. Therefore, some 72 point, line and unconfined compression tests were conducted to determine typical point load-deformation relationships for a variety of rock types. Secondly, a numerical model of the swing plate A as shown in Fig.3.2 has been developed.

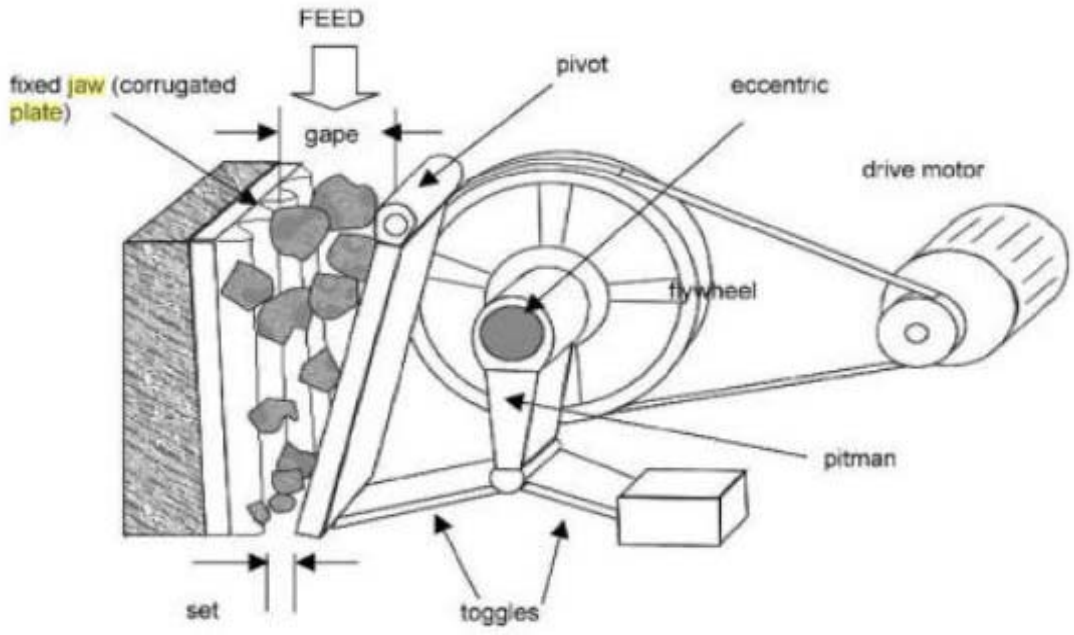

Fig.3.1 Elevation View of Jaw Crusher [6]

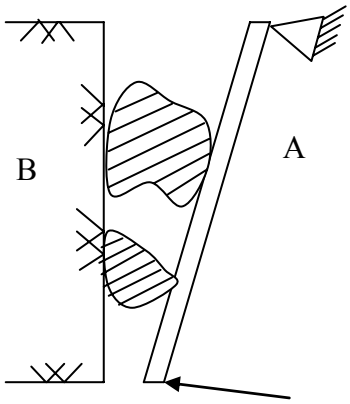

Fig.3.2 Idealization of particles within jaw crusher.

The swing plate A is idealized as shown in Fig.3.3 (a) as a unit width beam loaded at a number of points by different sized particles. Each row of uniformly sized particles in Fig. 3.3 (b) is idealized as one point load on the unit width model of the swing plate. Because of the interactive nature of this model, the failure of any row of particles permits redistribution of stresses within the beam.

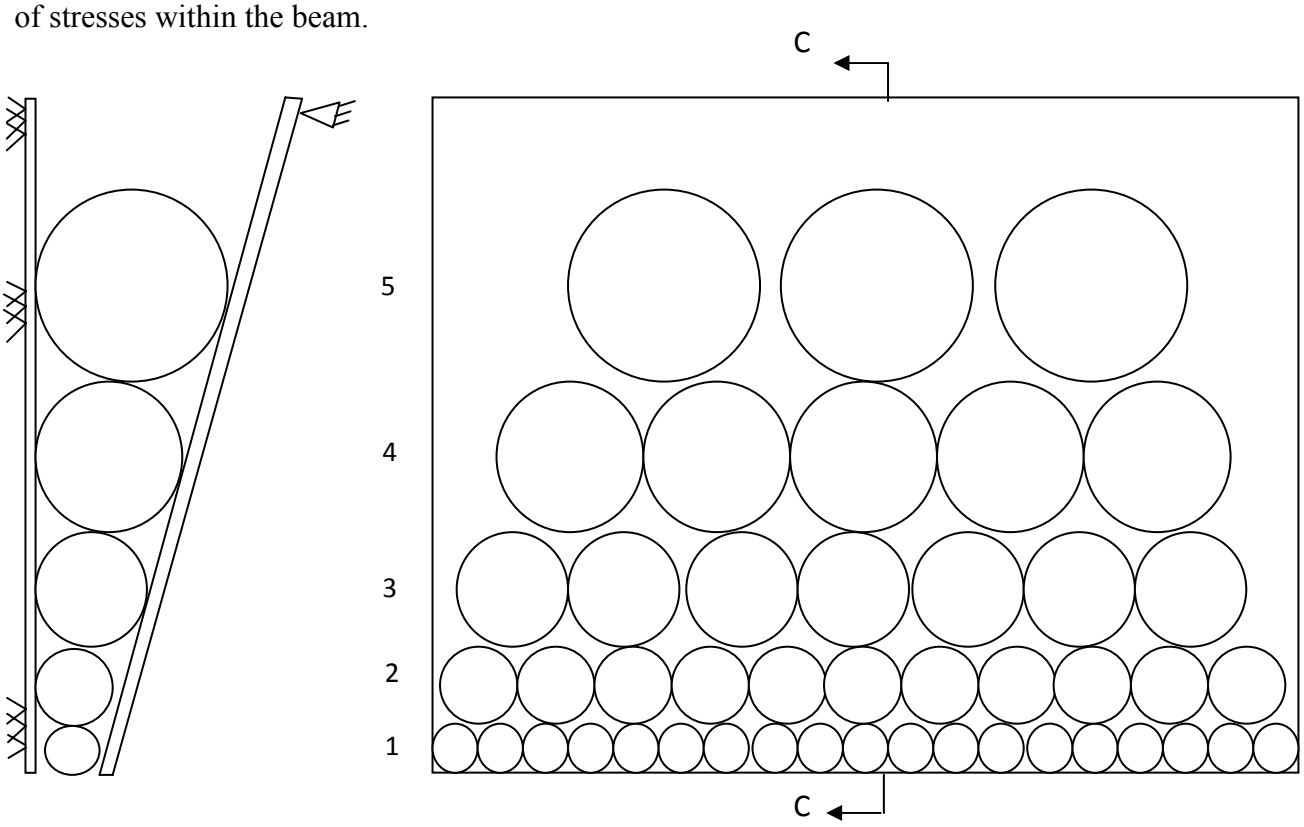

(a) Cross section CC (b) Plan View of Plate A

Fig.3.3 Modeling of particles within jaw crusher.

3.1.1 The load distribution along the swing plate

The parameter which most controls the design of the swing plate is the load distribution, shown in Fig.3.4.This hypothetical distribution, was only concerned with the total loading force (Q). Instrumentation of toggle arms in Germany has since led to correlation of measured Q with rock type. The most complete consideration of the effect of rock properties on Q and the toggle force (T). His work is based upon the three-point loading strength of the rock, which he found to be one-sixth to one eleventh the unconfined compressive strength (q_u). The hypothetical toggle forces based upon the sum of forces necessary to crush a distribution of regular prisms fractured from an initial cubical rock particle. These approaches involved both maximum resistance and simultaneous failure of all particles and thus neither can lead to an interactive design method for changing stiffness (and weight) of the swing plate.

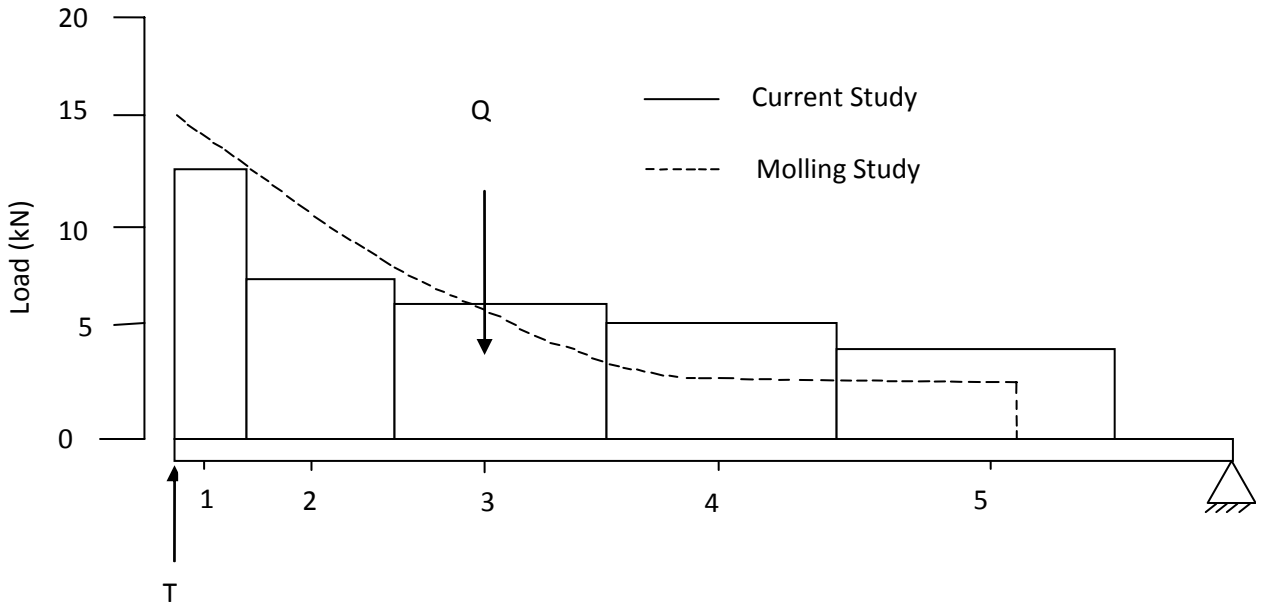

Fig.3.4 Load distribution along plate A only.

Normally, the stiffness and dimensions of swing plates are not changed with rock type and all plates are capable of crushing rock such as taconite with an unconfined compressive strength (q_u) of up to 308 MPa. Only the facing of the swing plate is changed with rock type, to account for changes in abrasiveness or particle shape. For instance, ridged plates are employed with prismatic particles both to stabilize the particles and to ensure the point-loading conditions. Communications with manufacturers of jaw crushers have revealed that

no consideration is currently given to force displacement characteristics of the crushed rocks in the design of swing plates.

Consideration of the two particles between the crusher plates in Fig.3.2 reveals the importance of the point-load failure mechanism. As a rock tumbles into position it will catch on a comer of a larger diameter and thus will be loaded at two 'points' of contact. Throughout the paper, 'point' describes contact over a small and limited region of the circumference of the particle. Should flat-sided contact occur, the ribbed face plates of most crushers will apply point loads to the particle. The particle will then fail either by two or three point loading. Thus, any design based upon both deformation and strength must begin with a point-load idealization.

3.1.2 Modeling irregular particle behavior with that of cylinders

In this study point-loading of cylinders (or discs) are undertaken to model behavior of irregular rock particles. Modeling irregular particle behavior with that of cylinders can be shown to be appropriate by consideration of work presented by Hiramatsu and Oka .From photoelastic studies of plate-loaded spheres and point-loaded cubes, prisms and ellipsoids, they determined that the stresses produced in plate and point-loaded spheres of identical diameter are equal. Thus, the plate idealization may be replaced by the point load shown in Fig.3.5.

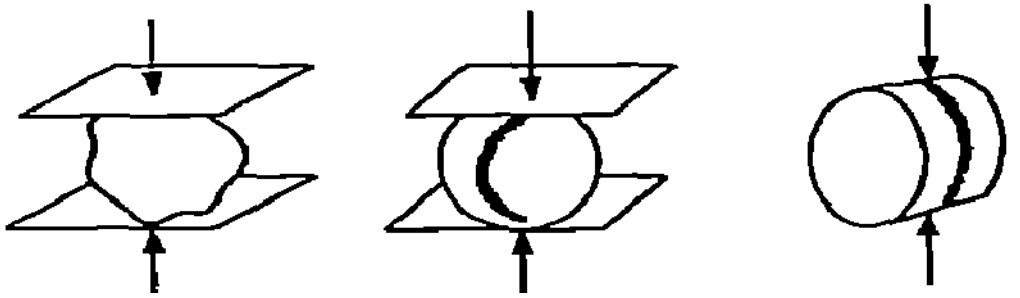

Irregular Particle Sphere Particle Cylinder Particle

Fig.3.5 Comparison of plate and point-loaded particles.

They also showed that point-load failure of a sphere was equal to that of a point-loaded ellipsoid. Therefore, ultimate point loads on spheres will be approximately equal to ultimate point loads on cylinders (or discs). For both the ellipsoids and the cylinders, the excess volume outside the spherical dimensions does not change the circular failure surface parallel

to the smallest dimensions of the body. This circular failure surface for the sphere and cylinder is shown by the jagged lines on the two shapes in Fig.3.5. These results compared with disc and irregular particle point-load strengths from tests on andecite, dolomite, sandstone and shale and found the point load strength of the disk and irregularly shaped particles to be equal. Thus, the properties determined from point-loading of discs or cylinders are appropriate for the point-loading of irregular particles. The photo elastic studies and theoretical calculations reveal that point loads produce tensile stresses across the middle 70% of the axis between the point loads. However, the volume directly beneath the contact is found to be in a state of compression, which leads to early, local compression failure. Thus, any deformation measured between the two points of contact will have two components:

(1) Elastic over the middle 70% of the particle and

(2) Plastic (as a result of local crushing) immediately beneath the point of load application.

As has been shown by numerous workers [7], the maximum point load, P, is related to the tensile strength (S_t) as shown in eqn. (1).

$$P=\frac{S_t d^2}{X} \quad \text{----------(3.1)}$$

where d is diameter of specimen and X is a proportionality factor. The proportionality factor X has been reported by the above investigators to range between 0.96 and 0.79.In this study 0.79 will be employed for cylinders (discs) and 0.96 for spheres.

The measurements of the deformability of small iron ore pellets and glass beads when crushed between two plates. The load-deformation relationships of both materials displayed deformation hardening in the initial stages of loading as predicted by the Hertzian theory for the behavior of contacting spheres. The more plastic (and weaker) iron ore pellets showed strain softening behavior in the latter stages of deformation, whereas the more brittle glass beads continued to stiffen, up to the point of failure. These observations indicate that the deformation stiffening or Hertzian behavior should be expected for point-loading of brittle rock particles.[6] According to the Hertzian theory, the total diametrial deformation (D) of a sphere loaded by two plates (spheres of infinite radius) is given by:

$$D=2\left[\frac{9}{16}.\frac{P^2\left(1-\nu^2\right)}{RE_r^2}\right]^{1/3} \quad \text{----------(3.2)}$$

Where P is the point load, R is the radius of rock particles, E, is Young's modulus of rock, and ν is Poisson's ratio. For ν between 0.25and 0.33, eqn. (2) reduces to

$$D=1.6\frac{P^{2/3}}{R^{1/3}E_r^{2/3}} \text{----------(3.3)}$$

Therefore any given sphere will deform according to a deformation hardening power law:

$$D=KP^{a} \text{----------(3.4)}$$

where *a* for completely elastic behavior is 2/3.

3.2 Experimental Data Collection

3.2.1 Point load deformability testing apparatus

The deformability of point-loaded specimens is determined with the loading method suggested by Reichmuth. As shown in Fig.3.6, cores were compressed with 19 mm diameter steel rods (oriented transversely to the long axis) by a universal testing machine. Diametral displacements were recorded with the two dial gages shown in the figure to eliminate any effects of tilting of the upper platen. Force-displacement data were recorded at equal load intervals throughout compression, and the loading rate was set so that the total time to failure was ten minutes or less. Failure was defined by a sudden loss of load capacity or the appearance of a fracture. When sudden brittle failure occurred, displacements at failure were extrapolated from the previously recorded values according to the maximum compressive load. No post-failure data were recorded.

Two other tests were performed to characterize the rocks Line loading was performed between two plates according to ASTM standards except that wooden strips were not placed between the specimen and plates to ensure that the specimen's diametral deformation was equal to platen convergence. Unconfined compression (q_u), tests were also performed according to ASTM standards to measure Young's modulus.

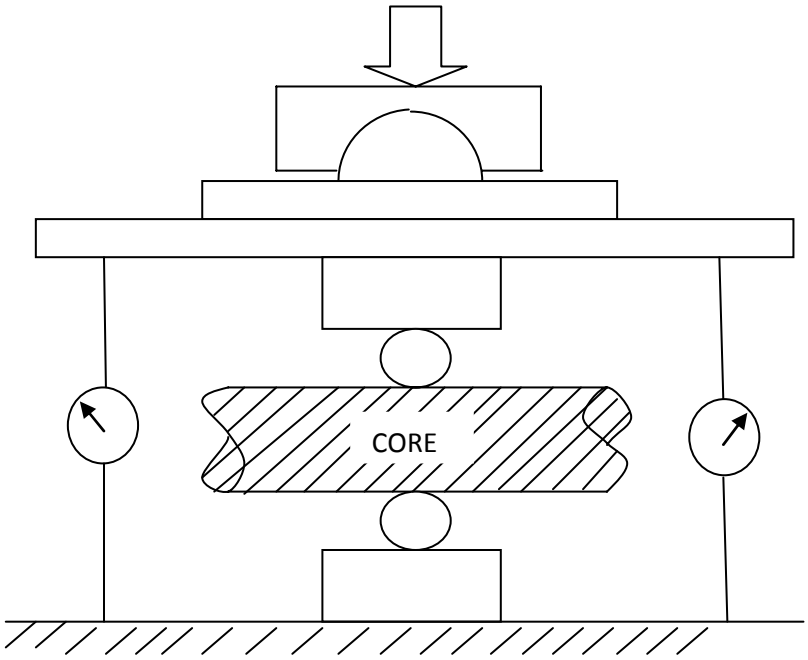

Fig.3.6 Point-Load Testing Apparatus.

3.2.2 Point load deformation and failure (PDF) data for materials

Point load deformation and failure (PDF) data were obtained for the five materials: sand-cement mortar, fragmental limestone, dolomitic limestone, taconite and amphibolites (closely banded gneiss) have shown in Table 3.1 with their major properties.

Table 3.1 Materials tested [7]

Material	E (MPa)	q_u (Mpa)	Location	Mineralogy, Texture
Mortar	9.7	20.7	Made in laboratory Chicago Lyons, IL Northern Minnesota Massachusetts	Sand and cement mixture fragmental, porous Dolomitic siliceous, finely grained crystalline.
Fragmental limestone	30.3	54.5		
Dolomitic limestone	48.3	151.7		
Taconite	41.4	234.4		
Amphibolites	33.6	124.1		

3.2.3 Effects of size on both strength and deformability

Cylinders ranging in size from 25 mm (1 in) to 150 mm (6 in) in diameter were point-loaded to investigate the effects of size on PDF properties (both strength and deformability). Knowledge of this size effect is necessary to model accurately the crushing behavior of the range of particle sizes found in jaw crushers Table 3.2 summarizes the results of the 30 point-load tests to determine the PDF relationships. To compare PDF data for a variety of diameters, the force and displacement at failure, P_f and D_f, were normalized. The normalized failure load (P_d) is the tensile strength given by eqn.1 (X = 0.79) and is relatively independent of size. Deformation at failure (D_f) was normalized through division by the original diameter to obtain (D_{nf}). The power law deformation descriptors, K and a in Table 3.2, were found by plotting non-normalized PDF data on log-log paper. Average values of the normalized failure loads and deformation and K and a are given in Table 3.3.

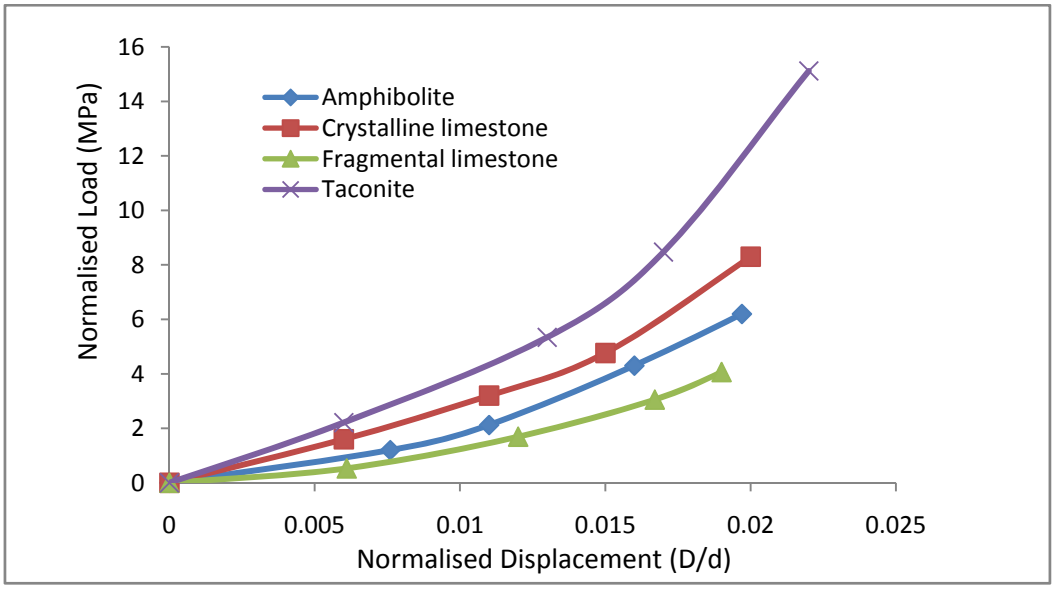

Fig.3.7. Typical point load-deformability relationships.

The point load-deformation and failure (PDF) relationships display definite Hertzian behavior. This upward curvature is evident in the comparison of typical rock PDF behavior

in Fig. 3.7. These typical relationships are based upon the 28 mm specimens of taconite, amphibolites and dolomitic limestone and the 56-mm specimens of fragmental limestone.

Table 3.2 Summary or point-load strengths and deformability [7]

Type of material	Diameter		P_f	P_{nf}	D_f	D_{nf}	K	Q
	(mm)	(in.)	(kN)	(MPa)	(mm)	(D_f /d)	(m/kN) (X l0-5)	
Dolomitic limestone	28.6	(1)	7.6	7.4	0.37	0.0131	32.5	0.74
	28.6	(1)	11.1	10.7	0.43	0.0150	23.4	0.77
	28.6	(1)	12.5	12.1	0.45	0.0158	22.8	0.76
	50.8	(2)	38.3	11.7	0.81	0.0158	20.0	0.76
	50.8	(2)	46.3	14.3	0.95	0.0196	67.3	0.61
	50.8	(2)	33.7	10.3	0.70	0.0146	16.0	0.80
Fragmental limestone	55.9	(2)	10.7	2.7	0.79	0.0141	61.6	0.71
	55.9	(2)	6.7	1.7	0.51	0.0092	6.8	1.0
	55.9	(2)	7.9	2.0	0.86	0.0156	9.7	1.04
Taconite	28.6	(1)	20.8	20.1	0.58	0.0170	26.8	0.75
	28.6	(1)	15.6	15.1	0.53	0.0210	23.4	0.75
	28.6	(1)	19.8	19.2	0.58	0.0210	18.2	0.80
Amphibolite	28.6	(1)	8.7	8.5	0.35	0.0160	28.5	0.75
	26.6	(1)	8.9	8.6	0.35	0.0122	22.8	0.76
	28.6	(1)	10.6	10.3	0.47	0.0133	10.8	0.98
	53.9	(2)	26.8	7.3	0.76	0.0140	35.3	0.71
	53.9	(2)	23.8	6.5	0.60	0.0112	16.5	0.79
	53.9	(2)	24.0	6.5	0.61	0.0114	22.8	0.75
	152.4	(6)	115.7	3.9	1.4	0.0092	5.4	0.87
	152.4	(6)	111.2	3.8	1.09	0.0070	5.4	0.81
	162.4	(6)	122.6	4.2	1.33	0.0087	10.3	0.77
	152.4	(6)	121.4	4.1	0.70	0.0046	23.9	0.63

The values in Table 3.3 are larger than the 0.67 predicted by the theory of elasticity for spherical contact. The weaker rocks (fragmental limestone and mortar) display the larger

a's or have the more linear PDF relations. These rocks are more susceptible to local compression failure at the points of contact. The specimen size does not appear to affect the shape of the PDF curve. However, as can be seen in the comparison of average curves for amphibolites, Fig. 3.8, size does affect Pnf and Dnf, The larger specimens fail at lower normalized loads or tensile stresses.

Table 3.3 Effect of size on average point-load strength and deformability [7]

Diameter	29mm					51.56mm				
Type of material	P_f (kN)	P_{nf} (MPa)	D_{nf} (D/d)	K (m/kN) ($\times 10^{-6}$)	a	P_f (kN)	P_{nf} (MPa)	D_{nf} (D/d)	K (m/kN) ($\times 10^{-6}$)	a
Mortar	7.6	7.4	0.0124	18.5	0.84	8.6	2.6	0.0181	22.8	0.94
Amphibolite	9.4	9.1	0.0138	20.7	0.83	24.9	6.8	0.0122	24.9	0.75
Crystalline limestone	10.4	10.1	0.0146	20.2	0.76	39.4	7.3	0.0107	34.4	0.72
Fragmental limestone	10.7	8.3	0.0165	21.4	0.74	18.4	5.4	0.0130	26.0	0.92
Taconite	18.7	18.1	0.0197	22.8	0.77	33.4	11.3	0.0143	28.2	0.95

Diameter	107mm					152mm				
Type of material	P_f (kN)	P_{nf} (MPa)	D_{nf} (D/d)	K (m/kN) ($\times 10^{-6}$)	a	P_f (kN)	P_{nf} (MPa)	D_{nf} (D/d)	K (m/kN) ($\times 10^{-6}$)	a
Mortar	15.3	1.32	0.011	12.3	0.76	23.3	0.71	0.014	9.7	0.72
Amphibolite	64.3	6.36	0.019	29.1	0.71	117.7	4.21	0.074	11.4	0.77
Crystalline limestone	58.4	4.52	0.017	45.2	0.70	104.4	2.34	0.096	54.2	0.70
Fragmental limestone	23.7	2.53	0.015	32.3	0.78	76. 6	1.47	0.013	35.6	0.75
Taconite	48.5	3.65	0.012	33.4	0.88	108.3	2.12	0.010	38.7	0.76

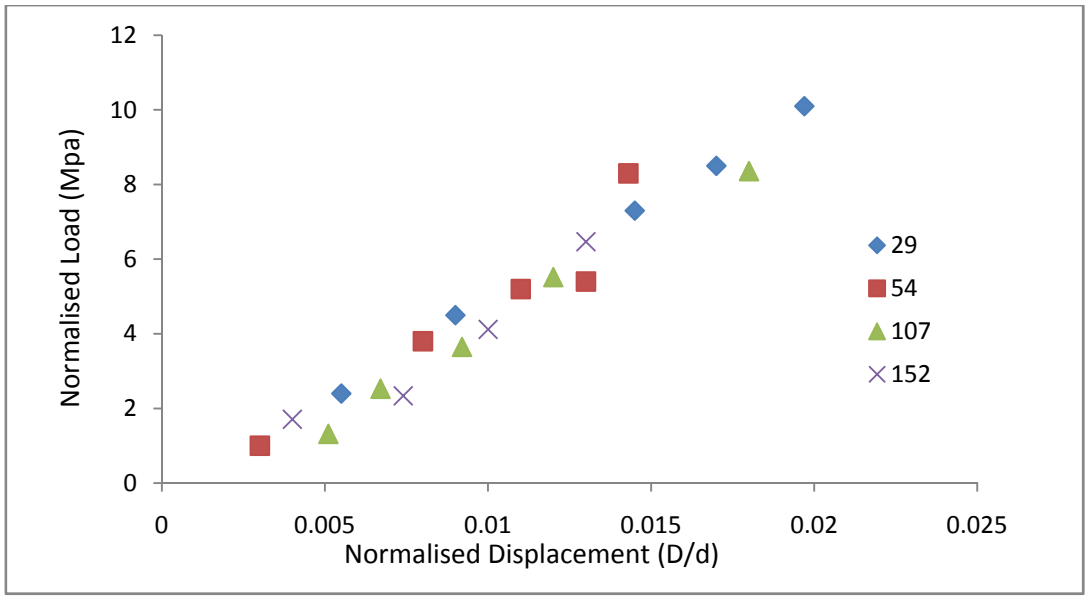

Fig.3.8. Effect of specimen size on ultimate strength and deformability.

This size dependency has been shown by Brochand Franklin, whose results are compared with those of this study in Fig. 3.9. Furthermore, the larger specimens tend to fail at smaller normalized deformations as shown in Fig. 3.10. Both of these size effects are included in the rock-plate interaction model.

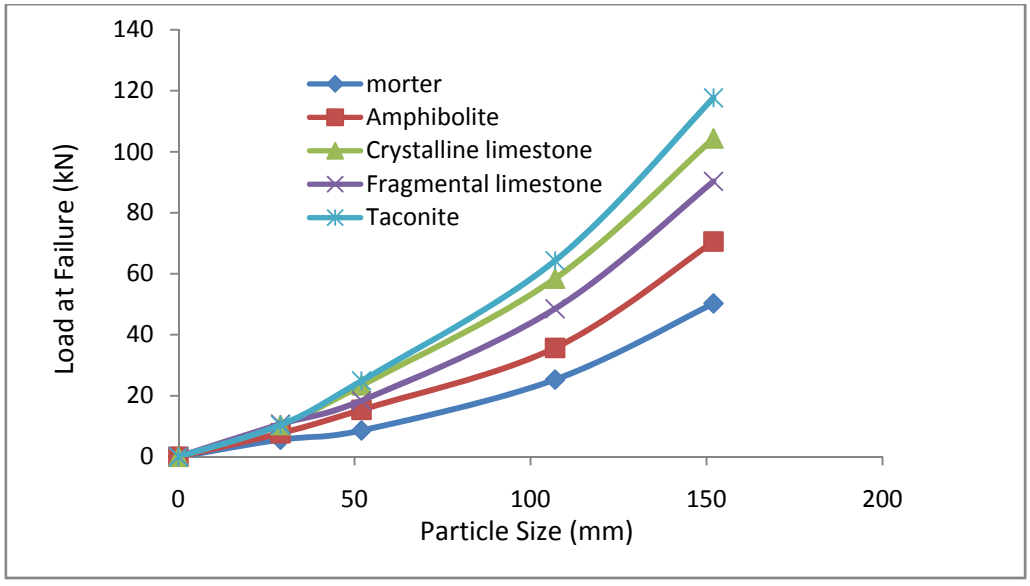

Fig.3.9. Comparison of the effect of size on point load at failure.

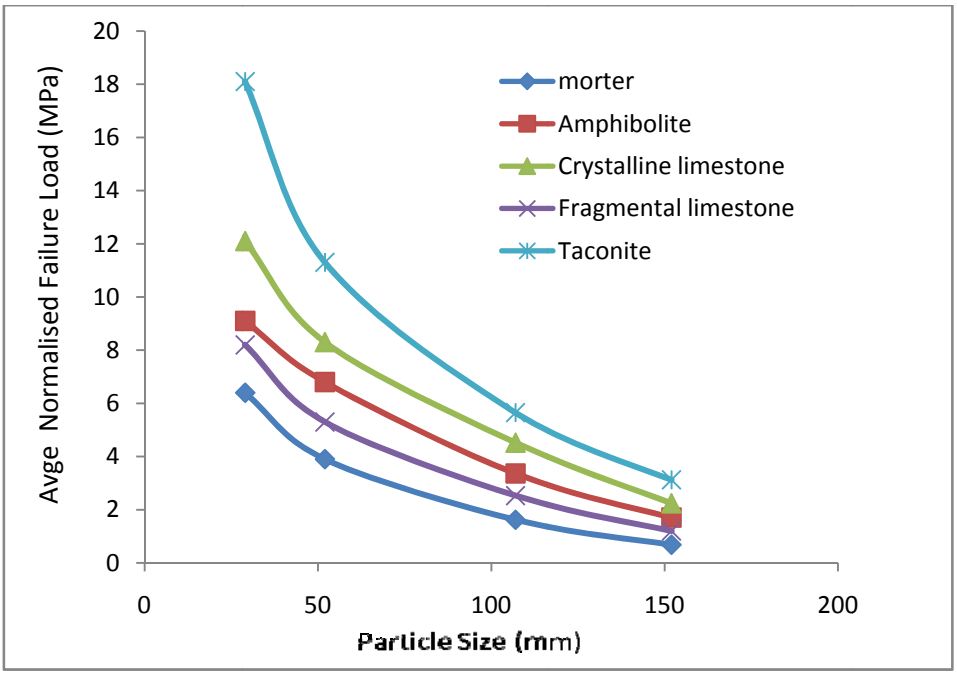

Fig.3.10. Effect of size on deformation at failure.

3.3 Rock - Plate Interaction Model

3.3.1 Simple Interactive Beam Model

Traditionally, stiffness of swing plates has not been varied with changes in rock strength. Rock strength has only been of interest because of the need to know the maximum force exerted by the toggle for energy considerations. Thus a swing plate, stiff enough to crush taconite, may be overdesigned (and, most importantly, overweight) for crushing a softer fragmental limestone. Design of lighter weight jaw crushers will require a more precise accounting of the stresses and deflections in the crushing plates than is available with traditional techniques.

The already presented PDF relations, when combined with a simple interactive beam model, permit simultaneous consideration of the rock and swing plate stiffness. Swing plate A is idealized as a beam loaded by different sized particles which are presented by the springs in Fig.3.11. Each row of particles in Fig.3.11 is represented by one spring or point load. The rows of particles fail at different plate movements during one crushing cycle, and after failure the stresses are redistributed in the beam. The moment of inertia (I), and Young's modulus (E), of beam A is set equal to that of a commercially available swing plate

(including stiffening elements), that is 0.9 m (36 in.) wide with 304 mm and 51 mm (12 in. and 2 in.) top and bottom openings. The stationary plate B is modeled as a rigid base for simplicity.

Each row of rock particles in Fig. 3.3(a) is represented by a spring in Fig. 3.11 with stiffness *K*. As shown in Fig.3.11 and eqn. (5), rock deformation (D_{rx}) is the beam movement (U_x), if the rock were not in place, minus the deformation of the beam due to the rock (D_{px})**:**

$$D_{rx} = U_x - D_{px} \text{ ----------(3.5)}$$

An equivalent PDF linear spring stiffness K can be found by solving eqn. (4) for P:

$$P = (D_{rx}/K)^{1/a} \text{ ----------(3.6)}$$

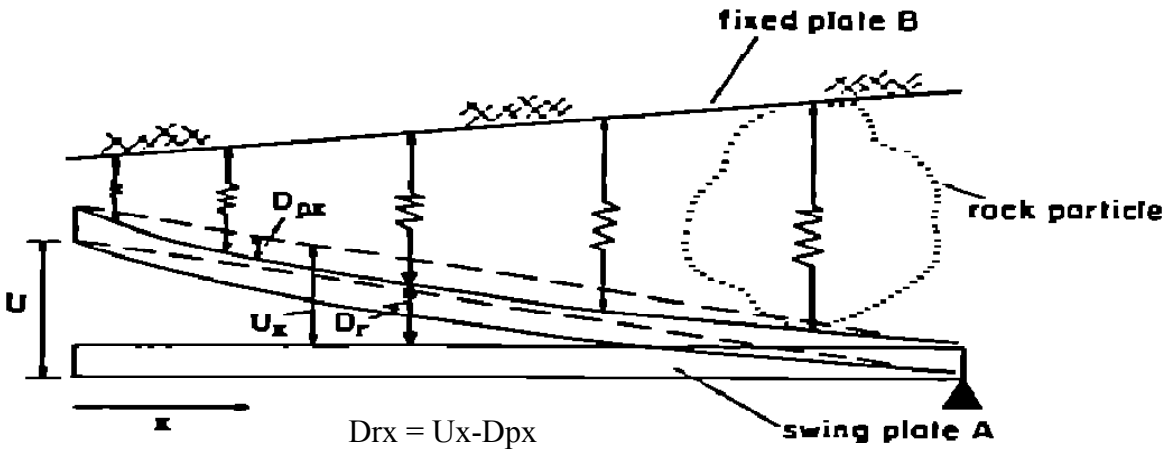

Fig.3.11. Deflection terminology and plate beam model.

And equating the result to the linear spring relationship

$$P=kD_{rx} \text{ ----------(3.7)}$$

To eliminate P as shown below.

$$k=D_{rx}^{(1/a-1)}/K^{1/a} \text{ ----------(3.8)}$$

The spring constant K is thus the secant modulus to any D, point on the PDF curve and changes as the rock load and deformation, (D_{rx}) increases. Deflection of the beam at any rock particle position, (D_{px}), is given by the sum of the deflections at that position caused by all rock loads. Each deflection, (D_{px}) is given by the influence equation for a simply supported beam as

$$Dpx = \left[P_b x(L^2 - b^2 - x^2) \right]/(6EI)\text{----------(3.9)}$$

where (P_b), is the load at any b, x is the position of consideration, and L the length of the beam. Thus (D_{px}), at the position of the smallest particle in Fig. 3.3 (a) is (D_{px}), calculated with P_b's for all five particles.

For each increment of overall beam movement, U, the forces in all the particles are corrected to account for the deflected shape of the beam, the deformation of the rock particle and the occurrence of failure in any row of particles. The allowable failure loads for the larger particles are obtained by extrapolation of the PDF data in Fig.3.9. At failure (Drx = Df), the rock particle force at that position is reduced to 50% of the maximum point load (Pf). This reduction is arbitrary but is reasonable as the load will not become zero upon failure if the particle is kept in position by nearby particles during one cycle of plate convergence. This ability to model non-simultaneous failure is the most important aspect of the interactive approach.

3.3.2 Calculations for Moments and Stresses

The calculated deformation of the beam is employed to obtain the moments (M) beneath the particles through a series of simple point load moment equations for each row. The equation for row 2, for example, is

$$M_2 = P_i(3) - P_1(2.5)\text{----------(3.10)}$$

where Pi is toggle force, P, is rock particle force at position 1, M is moment beneath particle 2, and 3 and 2.5 are distances from Pi and P, to position 2. After the moments are calculated, the tensile stresses a, in the beam model can also be calculated from simple beam theory as

$$\sigma_t = Mc/I\text{----------(3.11)}$$

where c is one-half the beam thickness. The calculated deformation and tensile stresses are employed to evaluate the importance of interaction in design.

Calculations with the interactive model involve matrix algebra and are solved by a simple computer program. In addition to the matrix algebra, the program handles the changing rock stiffness (k) and load reduction upon failure.

3.4 Design Swing Jaw Plates

The factors of importance in designing the size of jaw crusher's plate are:

Height of jaw plate (H) $\approx 4.0 \times$ Gape
Width of jaw plate (W) $> 1.3 \times$ Gape
$< 3.0 \times$ Gape
Throw (T) $= 0.0502(\text{Gape})^{0.85}$
where the crusher gape is in meters [6].

These dimensions vary as individual manufacturers have their own specifications and design of individual makes. In this case, we have top opening i.e. gape 304 mm (12 in.) and bottom opening 51mm (2 in)

Height of jaw plate (L) = 1200 mm
Width of jaw (W) = 900 mm
Throw (T) = 50 mm

Table 3.4 Dimensional Chart for Jaw Crusher [6]

Model	A	B	C	D	E	F	Weight(Ton)
300X400	400	300	1050	1180	1300	700	2.8
300X600	600	300	1750	1680	1680	950	6.5
300X750	750	300	2050	1930	1850	1150	12
300X900	900	300	1850	2490	2350	1500	17.5

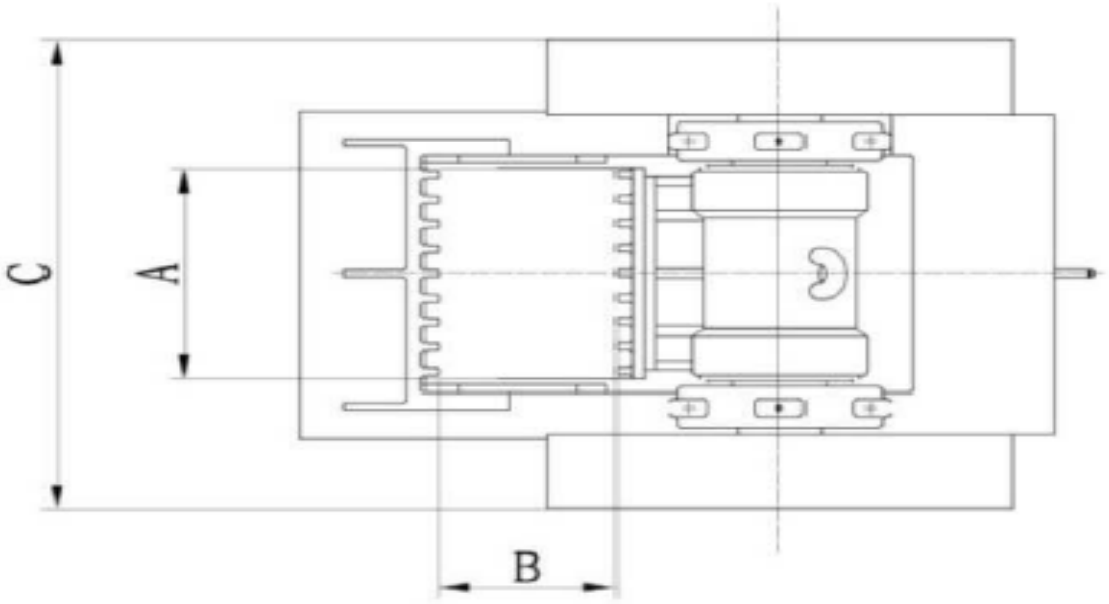

(a) Top View

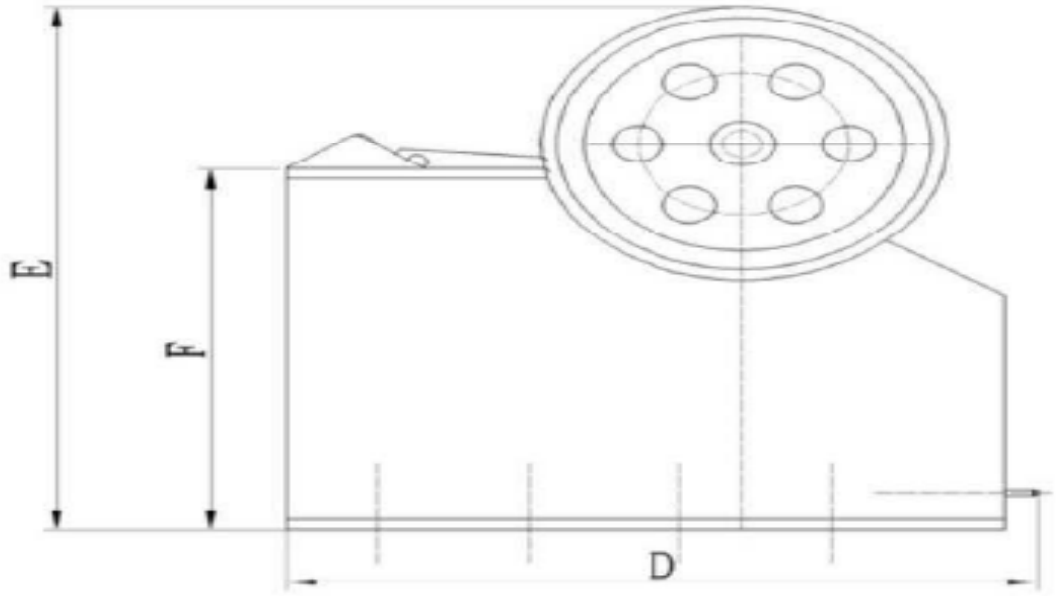

(b) Side View

Fig.3.12 Overall Dimensions of Typical Jaw Crusher [40]

3.5 Finite Element Analysis

3.5.1 Introduction to Finite Element Method

The Finite Element Method is essentially a product of electronic digital computer age. Though the approach shares many features common to the numerical approximations, it possesses some advantages with the special facilities offered by the high speed computers. In particular, the method can be systematically programmed to accommodate such complex and difficult problems as non homogeneous materials, non linear stress-strain behavior and complicated boundary conditions. It is difficult to accommodate these difficulties in the least square method or Ritz method and etc. an advantage of Finite Element Method is the variety of levels at which we may develop an understanding of technique. The Finite Element Method is applicable to wide range of boundary value problems in engineering. In a boundary value problem, a solution is sought in the region of body, while the boundaries (or edges) of the region the values of the dependant variables (or their derivatives) are prescribed.

Basic ideas of the Finite Element Method were originated from advances in aircraft structural analysis. In 1941 Hrenikoff introduced the so called frame work method, in which a plane elastic medium was represented as collection of bars and beams. The use of piecewise-continuous functions defined over a sub domain to approximate an unknown function can be found in the work of Courant (1943), who used an assemblage of triangular elements and the principle of minimum total potential energy to study the Saint Venant torsion problem. Although certain key features of the Finite Element Method can be found in the work of Hrenikoff (1941) and Courant (1943), its formal presentation was attributed to Argyris and Kelsey (1960) and Turner, Clough, Martin and Topp (1956). The term "Finite Element method" was first used by Clough in 1960.

In early 1960's, engineers used the method for approximate solution of problems in stress analysis, fluid flow, heat transfer and other areas. A textbook by Argyris in 1955 on Energy Theorems and matrix methods laid a foundation laid a foundation for the development in Finite Element studies. The first book on Finite Element methods by Zienkiewicz and Chung was published in 1967. In the late 1960's and early 1970's, Finite Element Analysis (FEA) was applied to non-linear problems and large deformations. Oden's book on non-linear continua appeared in 1972. [30]

3.5.2 Basic Concept of Finite Element Method

The most distinctive feature of the finite element method that separate it from others is the division of a given domain into a set of simple sub domains, called 'Finite Elements'. Any geometric shape that allows the computation of the solution or its approximation, or provides necessary relations among the values of the solution at selected points called nodes of the sub domain, qualifies as a finite element. Other features of the method include, seeking continuous often polynomial approximations of the solution over each element in terms of solution and balance of inter element forces. Exact method provides exact solution to the problem, but the limitation of this method is that all practical problems cannot be solved and even if they can be solved, they may have complex solution.

The design procedure does not cease after accomplishing a solid model. With analysis and optimization, design of a component may further be improved. Real life components are quite intricate in shape for the purpose of stress and displacement analysis using classical theories. An example is the analysis of the wing of an aircraft.

Approximations like treating it as a cantilever with distributed loads can yield inaccurate results. We then seek a numerical procedure like the finite element analysis to find the solution of a complicated problem by replacing it with a simpler one. Since the actual problem is simplified in finding the solution, it is possible to determine only an approximate solution rather than the exact one. However, the order of approximation can be improved or refined by employing more computational effort. In the finite element method (FEM), the solution region is regarded to be composed of many small, interconnected sub regions called the finite elements. Within each element, a feasible displacement interpolation function is assumed. Strain and stress computations at any point in that element are then performed following which the stiffness properties of the element are derived using elasticity theories. Element stiffnesses are then assembled to represent the stiffness of the entire solution region. Between solid modeling and the finite element analysis lays an important intermediate step of mesh generation. Mesh generation as a preprocessing step to FEM involves discretization of a solid model into a set of points called nodes on which the numerical solution is to be based. Finite elements are then formed by combining the nodes in a predetermined topology (linear, triangular, quadrilateral, tetrahedral or hexahedral).

Discretization is an essential step to help the finite element method solve the governing differential equations by approximating the solution within each finite element. The process is purely based on the geometry of the component and usually does not require the knowledge of the differential equations for which the solution is sought. The accuracy of an FEM solution depends on the fineness of discretization in that for a finer mesh, the solution accuracy will be better, that is, for the average finite element size approaching zero, the finite element solution approaches the classical (or analytical) solution, if it exists. We would always desire to seek the 'near to classical' solution. However, the extent of computational effort involved poses a limit on the number of finite elements (and thus their average size) to be employed. A relatively small number of finite elements in a coarse mesh would yield a solution at a much faster rate, though it will be less accurate compared to that obtained using a large number of elements in a fine mesh. [31]

3.6 Finite Element Method Applied To Swing Jaw Plate

There are three basic approaches to FEA: the h, p and h-p methods. With the h method, the element order (p) is kept constant, but the mesh is refined infinitely by making the element size (h) smaller. With the p method, the element size (h) is kept constant and the element order (p) is increased. With the h-p method, the h is made smaller as the p is increased to create higher order h elements. Either reducing the element size or increasing the element order will reduce the error in the FEA approximation. FEA software exists for all three methods. Before examining which may be superior, one must first determine which element type results in greater model, and therefore analysis, accuracy.[45]

The objective of finite element analysis of real world models is to simulate destructive testing using a minimum amount of computer memory, computation time and modeling time. The concept of FEA is simple and well-understood. The design is turned into a mesh of finite elements. FEA then tests each finite element for how it responds to such phenomena as stress, heat, fluid flow or electrostatics. FEA has been key in transferring design and analysis from drafting boards.

A designer can select from a variety of element types when building an FEA model. The principal issue in selecting a finite element type is accuracy. Until recently, the engineer would build the solid mesh manually, attempting to make an accurate representation of the part design.

3.6.1 Modeling using Eight-Node "Brick" Element

The swing jaw plate is type rectangular plate. Solution obtained by the application of classical theory of plate flexure is limited to simple types of plates with simple loading and boundary conditions. With the advent of the finite element method, the plate bending problems have received considerable attention. As a result of which, a large number of different plate bending element formulation have been made.

Element types include eight-node hexahedrons, four-node tetrahedrons and ten-node tetrahedrons, but eight-node hexahedrons, which part and die designers call “bricks,” lead to more reliable FEA solutions. There are many reasons why the eight-node hexahedral

element produces more accurate results than other elements in the finite element analysis of real world models. The eight-node hexahedral element is linear (p = 1), with a linear strain variation displacement mode. Tetrahedral elements are also linear, but can have more discretization error because they have a constant strain.

This element is a three dimensional element of the quadrilateral. It is observed that the sides can be considered as straight but its corner nodes take some arbitrary shape in space. As a result, the edges can be warped and hence the shape functions are trilinear.A widely used 3-D element, 8-node hexahedron is the subject of example that goes with this jaw plate analysis. The element is the analogue of the eight-node hexahedral "brick" element along with coordinate system and node numbering as shown in fig.3.13.[34]

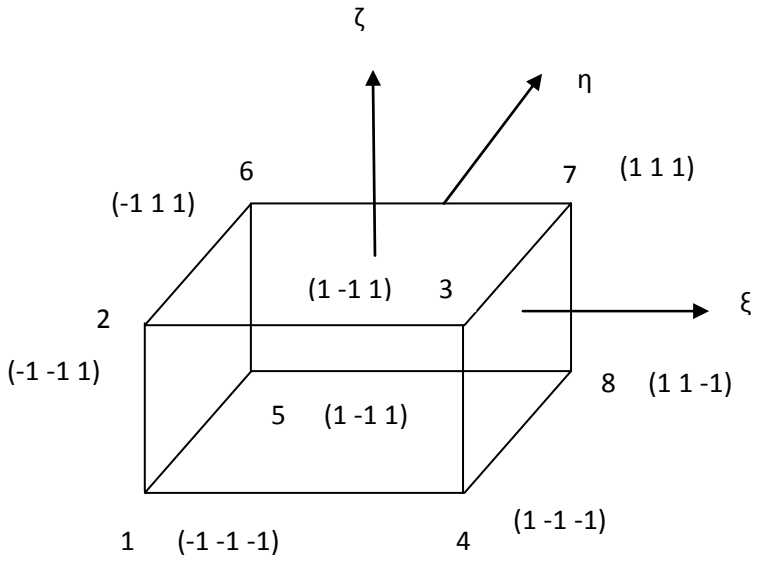

Fig.3.13 Eight-Node Hexahedral "Brick" Element

We have three local coordinates ξ , η and ζ vary from -1 one face to +1 on the opposite face as indicated in figure 3.13.Hence a typical shape function is given by

$$N_i = \frac{1}{8}(1+\xi_i\ \xi)\ (1+\eta_i\ \eta)\ (1+\zeta_i\ \zeta) \text{----------(3.13)}$$

Therefore, shape functions of eight-node brick element for different nodes are given by following eqns.

$$N_1 = \frac{1}{8}(1-\xi)\,(1-\eta)\,(1-\zeta) \quad \text{(3.14)}$$

$$N_2 = \frac{1}{8}(1-\xi)\,(1-\eta)\,(1+\zeta) \quad \text{(3.15)}$$

$$N_3 = \frac{1}{8}(1+\xi)\,(1-\eta)\,(1+\zeta) \quad \text{(3.16)}$$

$$N_4 = \frac{1}{8}(1+\xi)\,(1-\eta)\,(1-\zeta) \quad \text{(3.17)}$$

$$N_5 = \frac{1}{8}(1-\xi)\,(1+\eta)\,(1-\zeta) \quad \text{(3.18)}$$

$$N_6 = \frac{1}{8}(1-\xi)\,(1+\eta)\,(1+\zeta) \quad \text{(3.19)}$$

$$N_7 = \frac{1}{8}(1+\xi)\,(1+\eta)\,(1+\zeta) \quad \text{(3.20)}$$

$$N_8 = \frac{1}{8}(1+\xi)\,(1+\eta)\,(1-\zeta) \quad \text{(3.21)}$$

Besides being more accurate, the hexahedral element presents other advantages in FEA model building. Meshes comprised of hexahedrons are easier to visualize than meshes comprised of tetrahedrons. In addition, the reaction of hexahedral elements to the application of body loads more precisely corresponds to loads under real world conditions. The eight-node hexahedral elements are therefore superior to tetrahedral elements for finite element analysis.

The question remains as to whether eight-node "brick" linear hexahedrons are superior to higher-order elements ($p > 1$), be they p elements (p method) or higher-order h elements (h-p method; see Figure 3) for building the solid mesh model of the part or die. Proponents of higher order elements (which require more nodes per element) claim that using a smaller number of larger-size elements results in less computational time and achieves the same accuracy as lower order h elements. The basis for this claim of less computational time is that higher order elements have less discretization error, even for a coarse mesh.

There is a major logical flaw in this claim: Most parts and products have complex geometries which require fine meshing to accurately resolve the geometry as a solid mesh. The mesh size is so small that the discretization error does not exceed what is required for engineering accuracy. Use of p elements and higher order h elements with mid-side nodes therefore offers no practical engineering benefit over use of eight-node hexahedrons. [45]

The physical system describing the design of a typical part or die often has a complex geometry, and building the software model is therefore an intricate process. A number of software programs now exist which automatically or semi-automatically build the mesh, in some cases, directly from the CAD design. Because the engineer typically goes through many design and analysis cycles before determining the optimal design, automatic mesh generators such as Algor's Hypergen and Hexagen have become popular. All other variables being equal, an automatic mesh generator is by definition more accurate, since it minimizes the element of human error in the transformation of a design to a solid finite element mesh.

When determining which mesh generation software to use, the engineer must evaluate the type of finite element that will be the basis of the FEA model. Elements differ in many ways, but for analysis, the most significant items are the shape of the element and its "order of interpolation," which refers to the degree of the complete polynomial appearing in the element shape functions. There will be an order of polynomial for the element, termed the p. There is also a size for the element, termed the h. Size h is usually the diameter of the smallest circle (smallest sphere for a three-dimensional element) that encloses the element. Every element has a size h and an order p.

FEA, therefore, provides approximate answers to a physical system. If u is the exact solution for the PDE, FEA will produce an approximation uh. The approximation uh will converge to the exact solution u of the mathematical model under certain conditions: when the mesh size (h) decreases to zero or when the element order (p) is increased to infinity.

One cannot really compare the discretization error of a single eight-node hexahedral element and a single four-node tetrahedral element, since the solution cost is directly proportional to the number of nodes. A more appropriate comparison is between an eight-node hexahedron comprised of five tetrahedrons and a single eight-node hexahedron, which

was generated using Hypergen, Algor's automatic tetrahedral mesh generator. The five tetrahedrons will together have more discretization error than the eight-node "brick" because the five tetrahedrons cannot assume all the displacement fields handled by the eight-node element.[45]

The p method suffers from its own accuracy problems, related to the fact that the larger the elements, the greater the effect of each element on the entire FEA result. The error in an element typically stems from a geometric or load singularity present in the solution over that element. This error can "pollute," that is, permeate adjacent elements. The "pollution" problem can seriously impact the accuracy of results because it affects stresses and fluxes. Since geometric and load singularities are common in most designed parts or products, p elements and higher order h elements have to be refined in size to cope with large gradients and discontinuities in the solution near the points of singularities. Refinement of these elements defeats the very purpose of using p or higher order h elements for FEA because the refinements take time to make.

Eight-node hexahedrons capture the singularities of the model at much less cost because they consume much less computer time and memory than the processing of p and higher order h elements. For a mesh of p or higher order h elements, the bandwidth minimizer consumes more disk space and CPU time, and also produces much wider bandwidths. A larger bandwidth increases solution time, since the solution time is proportional to the square of the bandwidth. Finally, eight-node brick hexahedral elements can be easily degenerated to lower order elements (transition and degenerative elements) maintaining spatial isotropy; the same cannot be said for higher order elements.[45]

In conclusion, while there may be perceived theoretical advantages to the p or h-p methods, the eight-node hexahedral "brick" element using the h method is superior to other element formulations for the practical purpose of accurate and fast finite element analysis of real world part and products. A more accurate FEA model leads to more accurate analysis, which in turn results in manufactured products that perform to specification.

3.6.2 Modeling of Swing Jaw Plate and Stiffener

The stiffened plate is assumed to consist of two parts; plate and stiffener. This stiffener is usually treated as a beam element. In case of stiffened plates, both the plate and stiffener undergo bending deformation. The stiffened plate for such cases is analysed as a plate bending problem.

It is convenient to consider the plate middle surface as reference axis. Though the load acts normal to the middle of the plate, the plate as such will be subjected to inplane and bending deformations when the stiffener is placed eccentric to it. The stiffener is considered as eccentric to and integral with the plate. As such it is assumed to be placed along the nodal line parallel to the x axis. Due to the requirement of conformity of displacements between the plate and stiffener, the following displacement functions for the stiffener are assumed.[28]

$$\begin{Bmatrix} u \\ w \\ \Phi \end{Bmatrix} = \begin{bmatrix} 1 & x & 0 & 0 & 0 & 0 & 0 & 0 \\ 0 & 0 & 1 & x & x^2 & x^3 & 0 & 0 \\ 0 & 0 & 0 & 0 & 0 & 0 & 1 & x \end{bmatrix} \begin{Bmatrix} \alpha_1' \\ \alpha_2' \\ . \\ . \\ \alpha_8' \end{Bmatrix} \text{----------(3.22)}$$

or

$$\{f_s\} = [C]\{\alpha\} \text{----------(3.23)}$$

where Φ the angle twist.

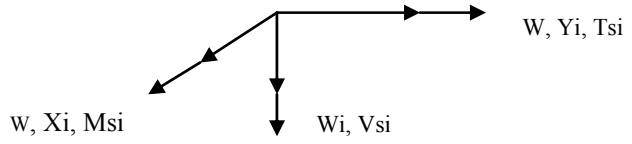

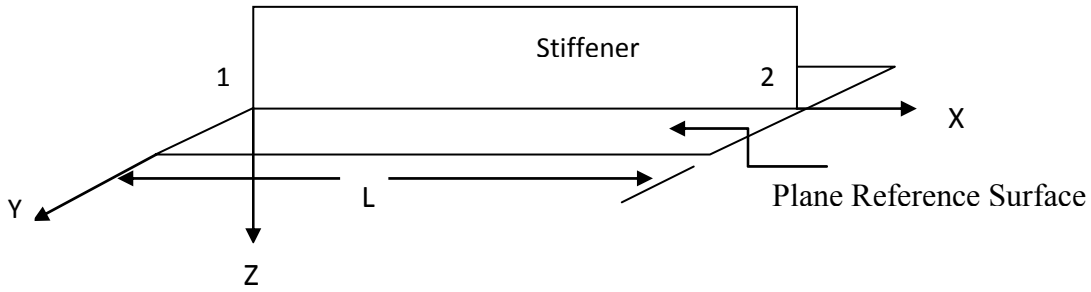

Fig.3.14 Plate with Stiffener Element

The stiffener displacements are along with u and w, Φ the angle of twist. The stiffener indicates four generalized displacements u, w, θy and θx. Substituting nodal values in eqn. (36)

$$\begin{Bmatrix} \alpha_1' \\ \alpha_2' \\ \alpha_3' \\ \alpha_4' \\ \alpha_5' \\ \alpha_6' \\ \alpha_7' \\ \alpha_8' \end{Bmatrix} = \begin{bmatrix} 1 & 0 & 0 & 0 & 0 & 0 & 0 & 0 \\ -1/L & 0 & 0 & 0 & 1/L & 0 & 0 & 0 \\ 0 & 1 & 0 & 0 & 0 & 0 & 0 & 0 \\ 0 & 0 & 1 & 0 & 0 & 0 & 0 & 0 \\ 0 & -3/L^2 & -2/L^2 & 0 & 0 & 3/L^2 & -1/L & 0 \\ 0 & 2/L^2 & 1/L^2 & 0 & 0 & -2/L^2 & 1/L^2 & 0 \\ 0 & 0 & 0 & 1 & 0 & 0 & 0 & 0 \\ 0 & 0 & 0 & -1/L & 0 & 0 & 0 & 1/L \end{bmatrix} = \begin{Bmatrix} u_1 \\ w_1 \\ w, x_1 \\ w, y_1 \\ u_2 \\ w_2 \\ w, x_2 \\ w, y_2 \end{Bmatrix} ---(3.24)$$

Or

$$\{\alpha\} = [Q]\{X_s\}_e \text{ ----------(3.25)}$$

where the subscript s refers to stiffener.

Combing eqns.(36) and (38)

$$\{f_s\} = [N_s]\{X_s\}_e \text{ ----------(3.26)}$$

where [Ns] =[C][Q] whose explicit values are given below by eqn.(40)

$$[N_s]^T = \begin{bmatrix} 1-\frac{x}{l} \\ 1-\frac{3x^2}{l^2}+\frac{2x^3}{L^3} \\ x-\frac{2x^2}{L}+\frac{x^3}{L^2} \\ 1-\frac{x}{L} \\ \frac{x}{L} \\ \frac{3x^2}{L^2}-\frac{2x^3}{L^3} \\ -\frac{x^2}{L}+\frac{x^3}{L^2} \\ \frac{x}{L} \end{bmatrix} \text{----------(3.27)}$$

The strain components for the stiffener are

$$\{\varepsilon_s\} = \begin{Bmatrix} \frac{\partial u}{\partial x} \\ -\frac{\partial^2 w}{\partial x^2} \\ \frac{\partial \Phi}{\partial x} \end{Bmatrix} \text{----------(3.28)}$$

Using eqn.(36),eqn.(41) can be written as

$$\{\varepsilon_s\} = \begin{bmatrix} 0 & 1 & 0 & 0 & 0 & 0 & 0 & 0 \\ 0 & 0 & 0 & 0 & 0 & -2 & -6x & 0 \\ 0 & 0 & 0 & 0 & 0 & 0 & 0 & 1 \end{bmatrix} [Q]\{X_s\}_e \text{----------(3.29)}$$

or

$$\{\varepsilon_s\} = [B_s]\{X_s\}_e \text{----------(3.30)}$$

The stress-strain relation is given by

$$\begin{Bmatrix} N_s \\ M_s \\ T_s \end{Bmatrix} = \begin{bmatrix} EA_s & ES_x & 0 \\ ES_x & EI_x & 0 \\ 0 & 0 & GJ_x \end{bmatrix} \begin{Bmatrix} \dfrac{\partial u}{\partial x} \\ -\dfrac{\partial^2 w}{\partial x^2} \\ \dfrac{\partial \Phi}{\partial x} \end{Bmatrix} \text{----------} (3.31)$$

or

$$\{\sigma_s\} = [D_s]\{\varepsilon_s\} \text{----------} (3.32)$$

Here Ax=the cross-sectional area of the x directional stiffener

Sx=first moment of area of the x directional stiffener with respect to the middle surface of the plate

Ix=the moment of inertia of the x directional stiffener with respect to the reference surface

Jx= the polar moment of inertia of the x directional stiffener

Combining eqns.(43) and (45) we get

$$\{\sigma_s\} = [D_s][B_s]\{X_s\}_e \text{----------} (3.33)$$

It can be shown that the stiffness matrix of the stiffener is given by

$$[K_s]_e = \int_0^L [B_s]^T [D_s][B_s] dx \text{----------} (3.34)$$

$[K_s]_e$ has been evaluated explicitly and is given by eqn.(48)

$$[K_s]_e = \begin{bmatrix} \frac{EA_x}{L} & 0 & -\frac{ES_x}{L} & 0 & -\frac{EA_x}{L} & 0 & \frac{ES_x}{L} & 0 \\ 0 & \frac{2EI_x}{L^3} & \frac{6EI_x}{L^2} & 0 & 0 & -\frac{12EI_x}{L^3} & \frac{6EI_x}{L^2} & 0 \\ -\frac{ES_x}{L} & \frac{6EI_x}{L^2} & \frac{4EI_x}{L} & 0 & \frac{ES_x}{L} & -\frac{6EI_x}{L^2} & \frac{2EL_x}{L} & 0 \\ 0 & 0 & 0 & \frac{GJ_x}{L} & 0 & 0 & 0 & -\frac{GJ_x}{L} \\ -\frac{EA_x}{L} & 0 & \frac{ES_x}{L} & 0 & \frac{EA_x}{L} & 0 & -\frac{ES_x}{L} & 0 \\ 0 & -\frac{12EI_x}{L^3} & -\frac{6EI_x}{L^2} & 0 & 0 & \frac{12EI_x}{L^3} & -\frac{6EI_x}{L^2} & 0 \\ \frac{ES_x}{L} & \frac{6EI_x}{L^2} & \frac{2EL_x}{L} & 0 & -\frac{ES_x}{L} & -\frac{6EI_x}{L^2} & \frac{4EI_x}{L} & 0 \\ 0 & 0 & 0 & -\frac{GJ_x}{L} & 0 & 0 & 0 & \frac{GJ_x}{L} \end{bmatrix} \text{------(3.35)}$$

In the latter, by using the above eqns. the solution time taken will be more. Thus, there is a trade off involved between the average element size and solution time taken which a designer should keep in mind when performing mesh generation which, by itself, is a very vast and active field of research. Most methods may be extended for use in three dimensions. We may realize at this stage that discrete representation of solids is another approach in solid modeling wherein a solid's volume may be regarded as the sum total of the volumes of constituting tetrahedral or hexahedral elements. To create a discrete representation using mesh generation would, however, require information of the solid. With the development of high speed digital computers, the application of the finite element method also progressed at a very impressive rate. This study is done in computational work in next chapter.

CHAPTER-4

COMPUTATIONAL STUDY

4. COMPUTATIONAL STUDY

4.1 An introduction to Computer Aided Design (CAD)

Developing a CAD software is an arduous and challenging task. However, it is the back end wherein the core of Computer Aided Design rests. The concepts emerge as an amalgamation of geometry, mathematics and engineering that renders the software the capability of free-form or generic design of a product, its analysis, obtaining its optimized form, if desired, and eventually its manufacture. By late 1960s, the term Computer Aided Design (CAD) was coined in literature. By 1980s and 1990s, CAD/CAM had penetrated virtually every industry including Aerospace, Automotive, Construction, Consumer products, Textiles and others. Software has been developed over the past two decades for interactive drawing and drafting, analysis, visualization and animation. A few widely used products in Computer Aided Design and drafting are Pro-Engineer, AutoCAD, CATIA, IDEAS, and in analysis are NASTRAN, ABAQUS, ANSYS and ALGOR. Many of these softwares are being planned to be upgraded for potential integration of design, analysis, optimization and manufacture.

The range of computer applications in engineering design covers procedures from preliminary conceptual design to the production of manufacturing drawings and specifications. Most computer applications intended for production use can be classified into five or more major categories: analysis, computer-aided drafting and design, geometric modeling, data base management systems, and artificial intelligence. Traditional software for design optimization may be categorized as analytical applications, based on rational principles of mathematics and linear programming. Emerging computer-based tools for design optimization are an offshoot of research in artificial intelligence, capable of processing a variety of algorithmic, symbolic, deterministic, probabilistic, and fuzzy knowledge.

The CAD packages are the tools used to automate the drafting/designing/engineering processes in almost all industries & technical operations. The CAD program was one of the first tools to be used to automate the technical offices of any organization. Such CAD packages have been in use (commercially) for over 20 years in consulting firms, industrial plants, refineries, petrochemical plants, utilities and other sectors of the industry. They produce drawings of every type: electrical, mechanical, civil, architecture, process,

instrumentation, etc. Depending on the user field of interest, the CAD system can tie in with other automating/analysis/production packages, for example CAM (computer aided manufacturing) and GIS (Geographic information systems). Over the recent few years a lot of development took place with respect to CAD systems. The interface between the user and software is becoming easier & similar to other off the shelf general software packages. The drawings can be checked against specified standards. The drawings can be sent over the internet for viewing or marking & checking. The attributes (fields) of the drawn objects (entities) can be accessed via other non CAD software packages. The drawing can be fed into another program for analysis or displaying detailed information. [34]

4.2 Computer Aided Aspects of Design

Computers can be efficiently in several aspects of the design process. the capabilities of the computers in terms of storing vast amount of data, the astonishing speed with which it can retrieve the required information buried in its knowledge base ,and also the speed with which it can perform routine and repetitive computations with accuracy for the required analysis and optimization of the design ,the graphics capabilities which enables visual representation of the design at every stage in design, convenience with which design information can be transmitted to the production shop in the form of computer drafted drawings or directly to CNC machines, industrial robots etc make it very useful tool for the designer. Design is an activity that facilitates the realization of new products and processes through which technology satisfies the needs and aspirations of the society. Engineering design of a product may be conceived and evolved in four steps:

1. Problem definition: Extracting a coherent appreciation of need or function of an engineering part from a fuzzy mix of facts and myths that result from an initial ill-posed problem. The data collection can be done via observation and/or a detailed survey.

2. Creative process: Synthesizing form, a design solution to satisfy the need. Multiple solutions may result (and are sought) as the creative thought process is aided by the designers' vast experience and knowledge base. Brainstorming is usually done in groups to arrive at various forms which are then evaluated and selected into a set of a few workable solutions.

3. Analytical process: Sizing the components of the designed forms. Requisite functionality, strength and reliability analysis, feasible manufacturing, cost determination

and environmental impact may be some design goals that could be improved optimally by altering the components' dimensions and/or material. This is an iterative process requiring design changes if the analysis shows inadequacy, or scope for further improvement of a particular design. Multiple solutions may be evaluated simultaneously or separately and the best design satisfying most or all functional needs may be chosen.

4. Prototype development and testing: Providing the ultimate check through physical evaluation under, say, an actual loading condition before the design goes for production. Design changes are needed in the step above in case the prototype fails to satisfy a set of needs in step 1. This stage forms an interface between design and manufacture. Many groups encourage prototype failure as many times as possible to quickly arrive at a successful design. [35]

4.2.1 Solid Modeling of Swing Jaw Plates

Engineering components can be of various forms (sizes and shapes) in three-dimensions. A Solid can be thought of as composed of a simple closed connected surface that encloses a finite volume. The closed surface may be conceived as an interweaved arrangement of constituent surface patches, which in turn, can be individually considered as composed of a group of curves. It then behooves to discuss the generic design of curves, surfaces and solids in that order. Even before, it may be essential to understand how three-dimensional objects or geometrical entities are represented on a two-dimensional display screen, and how such entities can be positioned with respect to each other for assembly purposes or construction operations. Engineers have converged to numerous standard ways of perceiving a three-dimensional component by way of engineering drawings depicted on a two-dimensional plane (conventionally blue prints, but for CAD's purpose, a display screen).

Solids represent a large variety of objects we see and handle. Curves and surfaces are intended to form the basis for solid or volumetric modeling. Solid modeling techniques have been developed since early 1970's using wireframe, surface models, boundary representation (b-rep), constructive solid geometry (CSG), spatial occupancy and enumeration. A solid model not only requires surface and boundary geometry definition, but it also requires topological information such as, interior, connectivity, holes and pockets. Wire-frame and surface models cannot describe these properties adequately. Further, in

design, one needs to combine and connect solids to create composite models for which spatial addressability of every point on and in the solid is required. This needs to be done in a manner that it does not become computationally intractable. Manufacturing and Rapid Prototyping (RP) both require computationally efficient and robust solid modelers. Other usage of solid modelers is in Finite Element Analyses (as pre- and post processing), mass property calculations, computer aided process planning (CAPP), interference analysis for robotics and automation, tool path generation for NC machine tools, shading and rendering for realism and many others.[33]

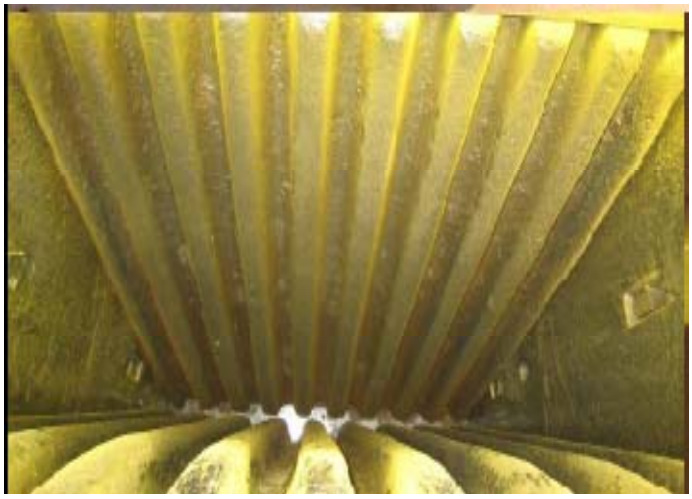

Fig.4.1 Picture Showing Corrugated Cast Steel Jaw Plates [36]

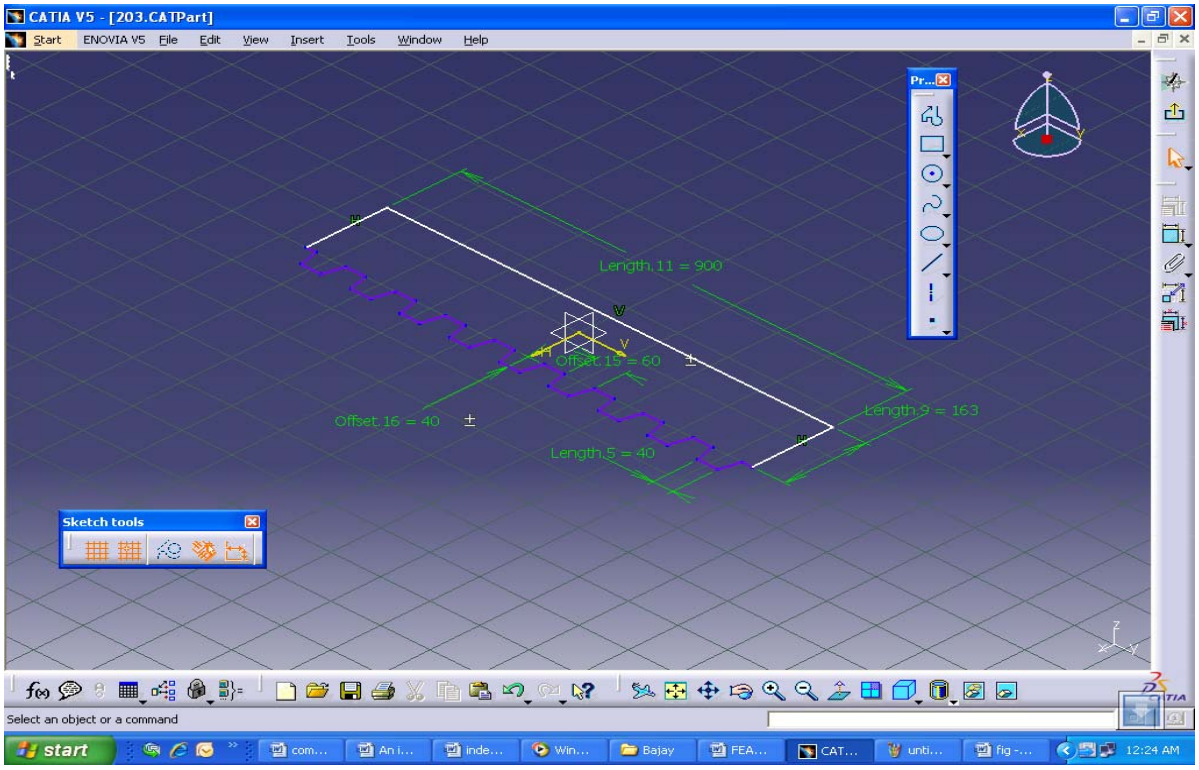

Fig.4.2 Sketch of Swing Jaw Plates Base Feature

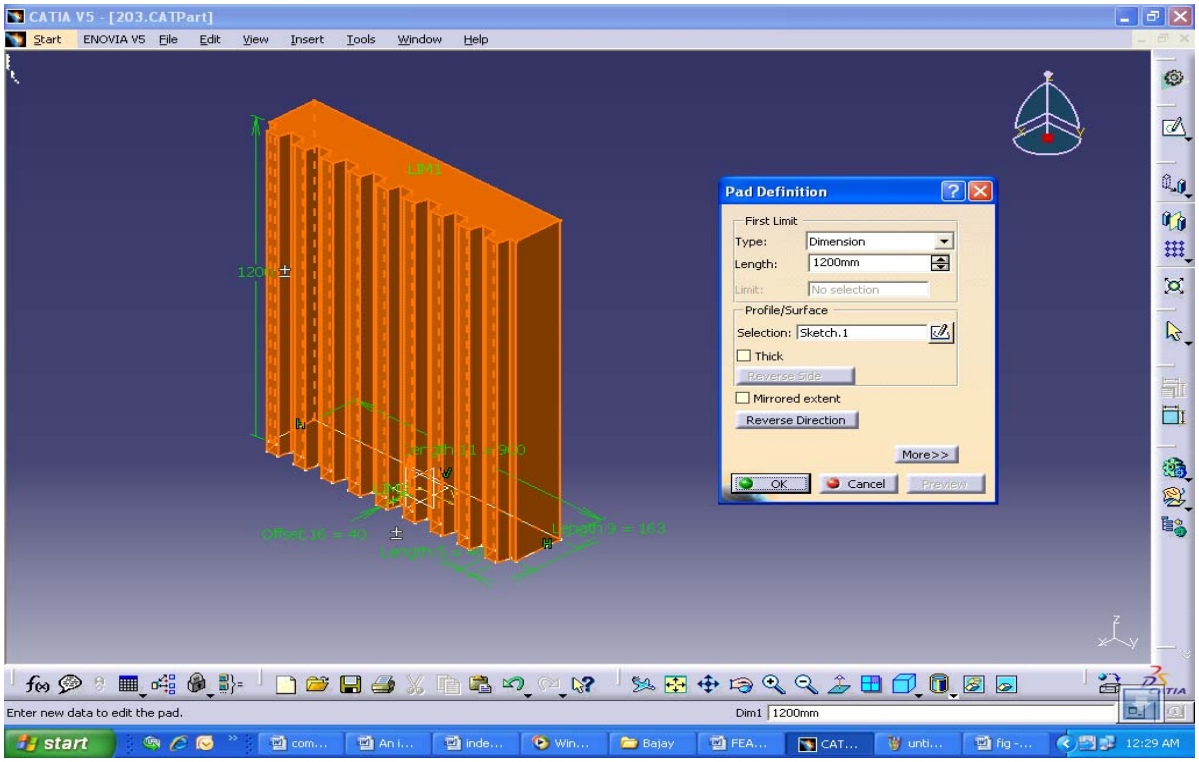

Fig.4.3 Extruding Sketch of Swing Jaw Plates Using Pad Tool

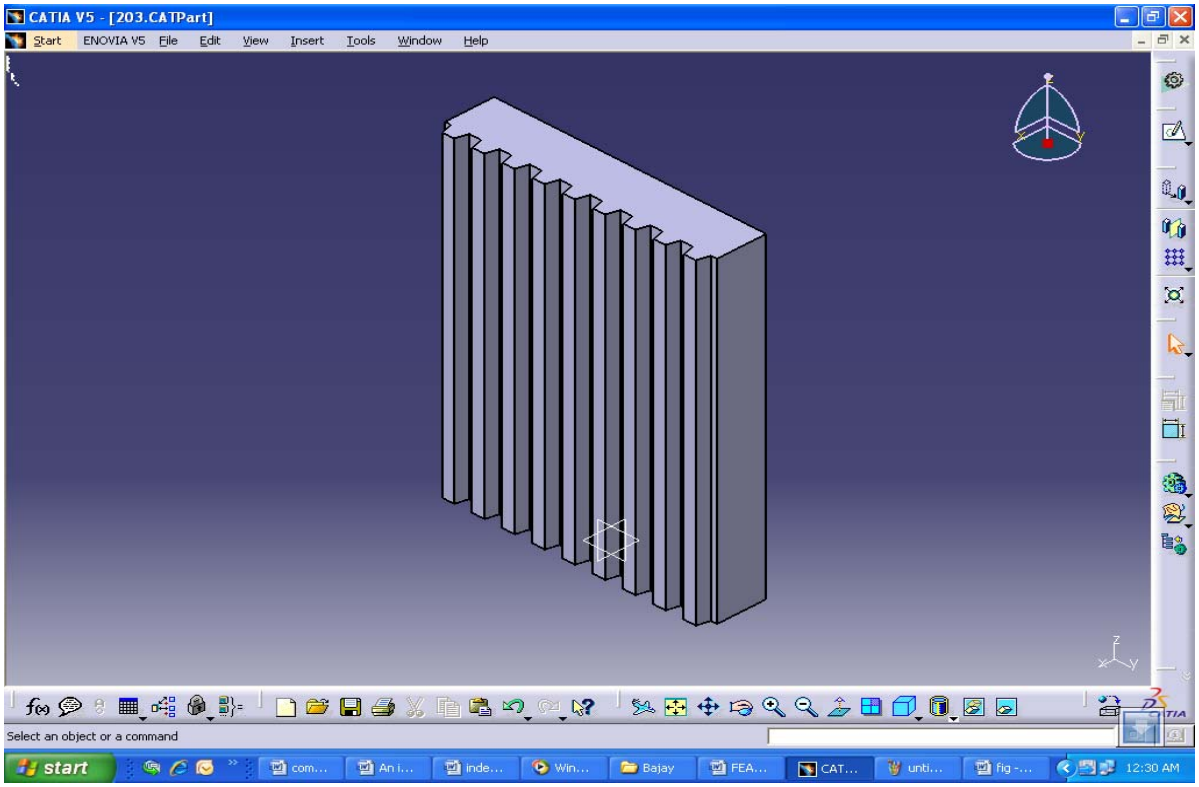

Fig.4.4 Solid Model of Corrugated Swing Jaw Plate

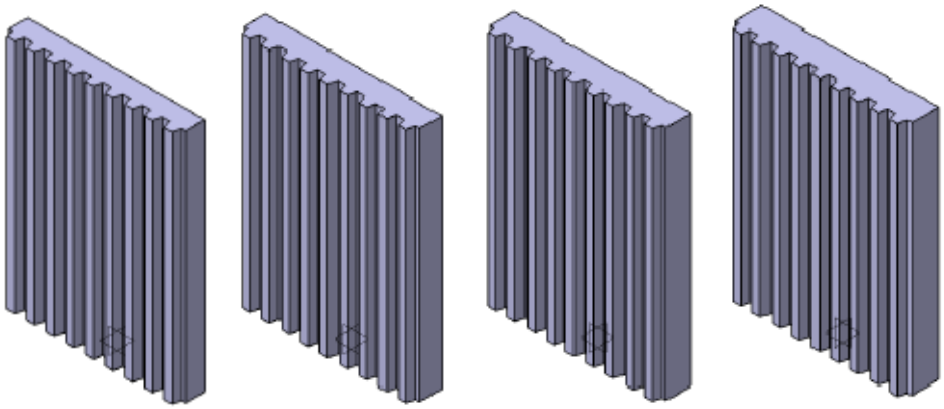

L=1200	L=1200	L=1200	L=1200
W=900	W=9000	W=900	W= 900
T=140	T=152	T=165	T=178

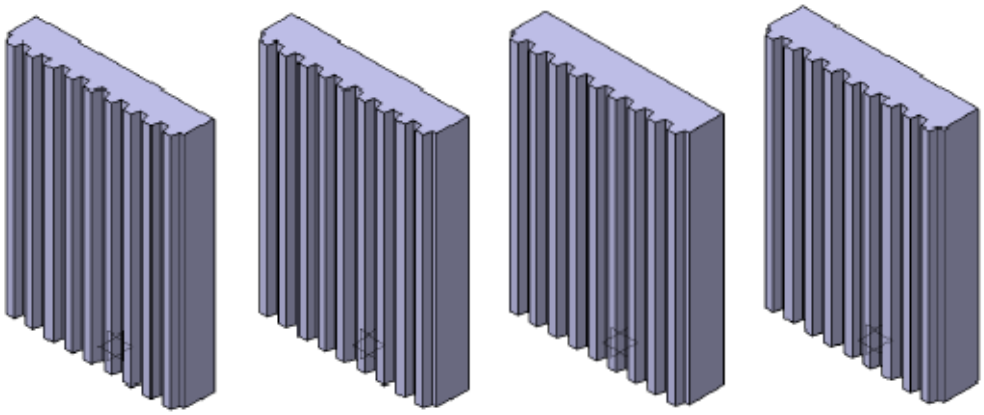

L= 1200	L= 1200	L= 1200	L= 1200
W=900	W= 900	W= 900	W= 900
T=191	T=203	T=216	T=224

Fig.4.5 Corrugated Swing Jaw Plate Models having Dimensions in mm

4.3 Computer Aided Analysis

Machine elements are required to operate in environmental conditions where they may be subjected to forces, extreme thermal conditions, and unfavorable weather conditions and so on. The element must be designed to withstand the harmful effects of the environment and to operate satisfactorily. Hence, the designer must formulate a mathematical model for the element, represent the behavior or the response of the element using differential equations, and analyze for the response when subjected to environmental conditions. The stresses developed in the element due to the external forces under other unfavorable conditions must be obtained and compared with the maximum stresses that the element can withstand safely.

The mathematical model for the element as well as mathematical model for the external forces must be formulated by the designer. There are several methods available to solve the resulting differential equations describing the behavior of the element or the system, of which the element is a part. The past experience in solving similar equations using all the available techniques may be store in an expert system which can suggest the best analysis method for the design problem. Alternatively; the designer can make a choice of the analytical method from the past experience in solving similar problems. Finite difference methods, transfer matrix methods, finite element methods are some of typical methods that can be used for the mathematical representation of the system and direct

numerical integration or modal analysis techniques are some possible analysis techniques to obtain the system response when subjected to environmental excitations.

When the element being designed is quite complex or when the element behavior can be understood only by analyzing the complete system, of which the element is apart, then calculations done manually will be unmanageable and prone to errors. Computers can be very efficiently used for the routine and repetitive computations involved in all these analysis methods. [34]

4.3.1 Features of ALGOR as FEA Tool

1) CAE/CAD Interoperability

Algor's InCADPlus family of products provides a new level of seamless CAD/CAE interoperability with popular CAD solid modelers such as SolidWorks, Mechanical Desktop, Pro/ENGINEER and Solid Edge. InCADPlus captures the exact assembly or part geometry utilizing the CAD solid modeler's application programming interface, thus eliminating data translation problems. When Algor and the CAD solid modeler reside on separate computers, Algor's Direct Memory Image Transfer (DMIT) technology can achieve the same level of interoperability. Algor's CAD/CAE interoperability products connect to every modeling, FEA and MES product offered by Algor. Algor also supports CAD standard neutral (universal) files, including IGES, ACIS, Parasolid and STL.

2) Finite Element Modelling

Superdraw III, Algor's precision finite element model-building tool, offers many design scenarios and mesh enhancement capabilities. Algor enables several design classes, including 2- and 3-D surface and solid models, beam or truss and plate/shell. Algor also enables engineers to build compound models having mixed element types. Superdraw III provides access to Merlin Meshing Technology for automatic surface mesh enhancement or enables engineers to work directly on an FEA model surface for manual mesh enhancement. Engineers can choose tetrahedral, brick or hybrid (bricks outside and tetrahedra inside) solid FEA meshes.

Algor's linear static and dynamic stress analysis capabilities determine stresses, displacements and natural frequencies as well as predict dynamic response to static and dynamic loading. These capabilities are highlighted throughout this brochure. Algor's FEA, Mechanical Event Simulation, modelingand CAD/CAE interoperability tools are designed to

help engineers develop products that are more reliable and less costly to produce with faster times-to-market. To provide the best cost/benefit solution for each customer, Algor's High Technology Core Packages and Extenders can be purchased at special combination pricing or separately to best fit individual needs while allowing for future growth and change.

3) Linear static stress analysis

Linear static stress analysis is the most common type of FEA used today. Industrial products, manufacturing, consumer products, civil engineering, medical research, power transmission and electronic design are just a few of the areas in which linear static stress analysis is often performed. Linear static stress analysis, included in all of Algor's High Technology Core Packages, enables the study of stress, strain, displacement and shear and axial forces that result from static loading. This analysis type is often sufficient for situations in which loads are known and the time of peak stress is evident. When performing a linear static stress analysis, engineers apply static loads, such as forces or pressures, or known "imposed" displacements to a finite element model. Then they add elastic material data, boundary conditions and other information such as the direction of gravity. Static forces are assumed to be constant for an infinite period of time while resulting strain, movement and deformation are small. Engineers assume that the material will not deform beyond its elastic limit and any resulting dynamic effects from the loading are insignificant. [27]

4.4 Swing Jaw Plates Static Stress Analysis Using ALGOR

4.4.1. Assumptions

To simulate the stress behavior of corrugated jaw plate some assumptions and approximations are required. Here analysis was undertaken based on the assumption that the point load strength of the disk and irregularly shaped particles to be equal and tensile point loads of different particle sizes are acting normal to the plate.

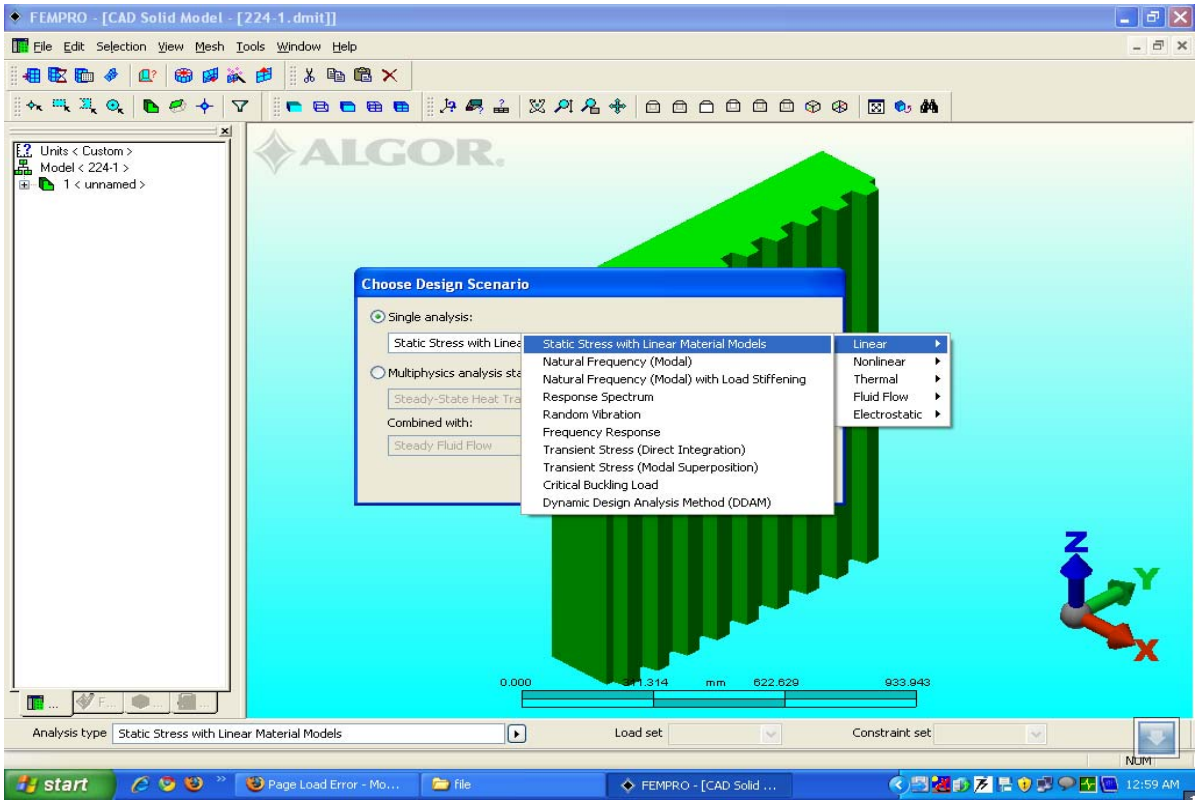

Fig.4.6 Swing Jaw Plate Model Ready for Static Stress Analysis

4.4.2 Meshing and Element Type

Here, eight-noded brick elements are used for discretization of jaw plates

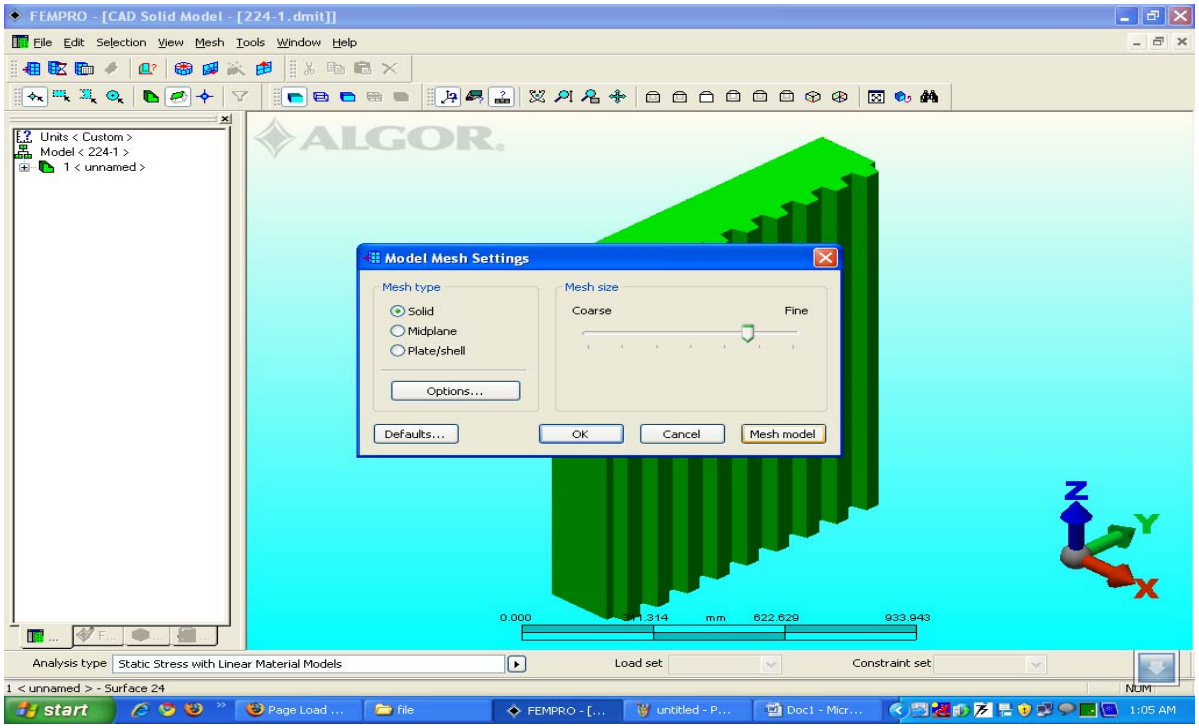

Fig.4.7 Swing Jaw Plate Model Ready for Meshing (Discretization)

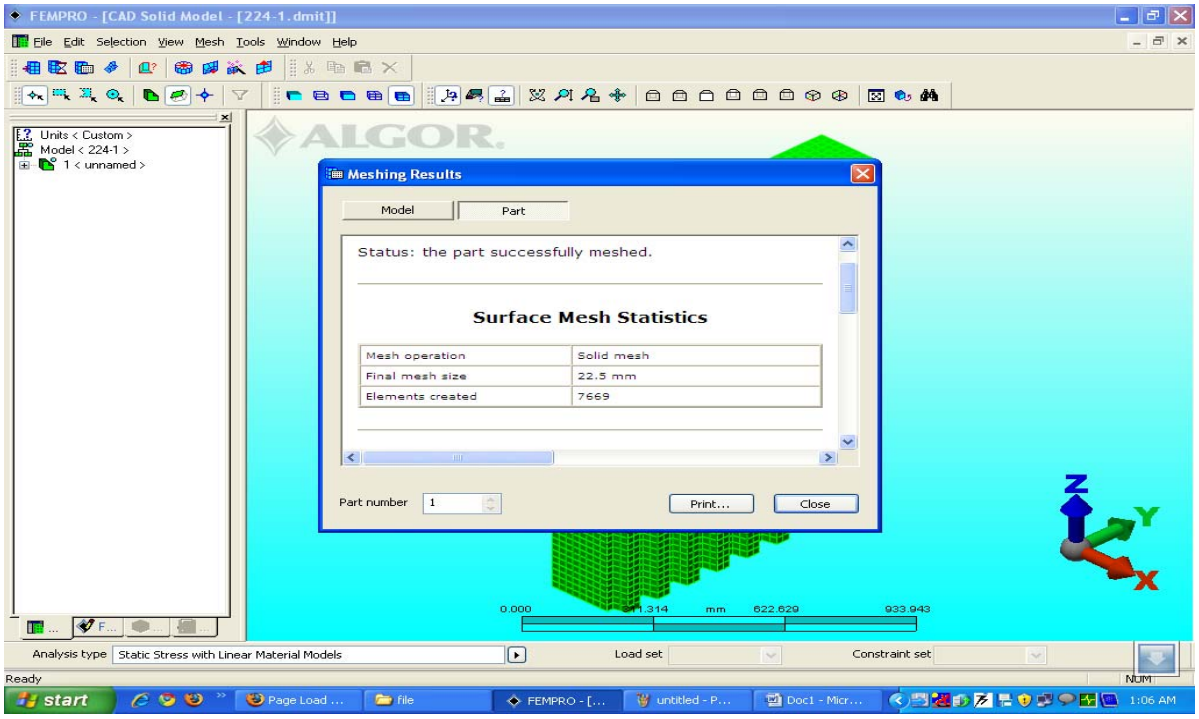

Fig.4.8 Showing Swing Jaw Plate Model Meshing Results

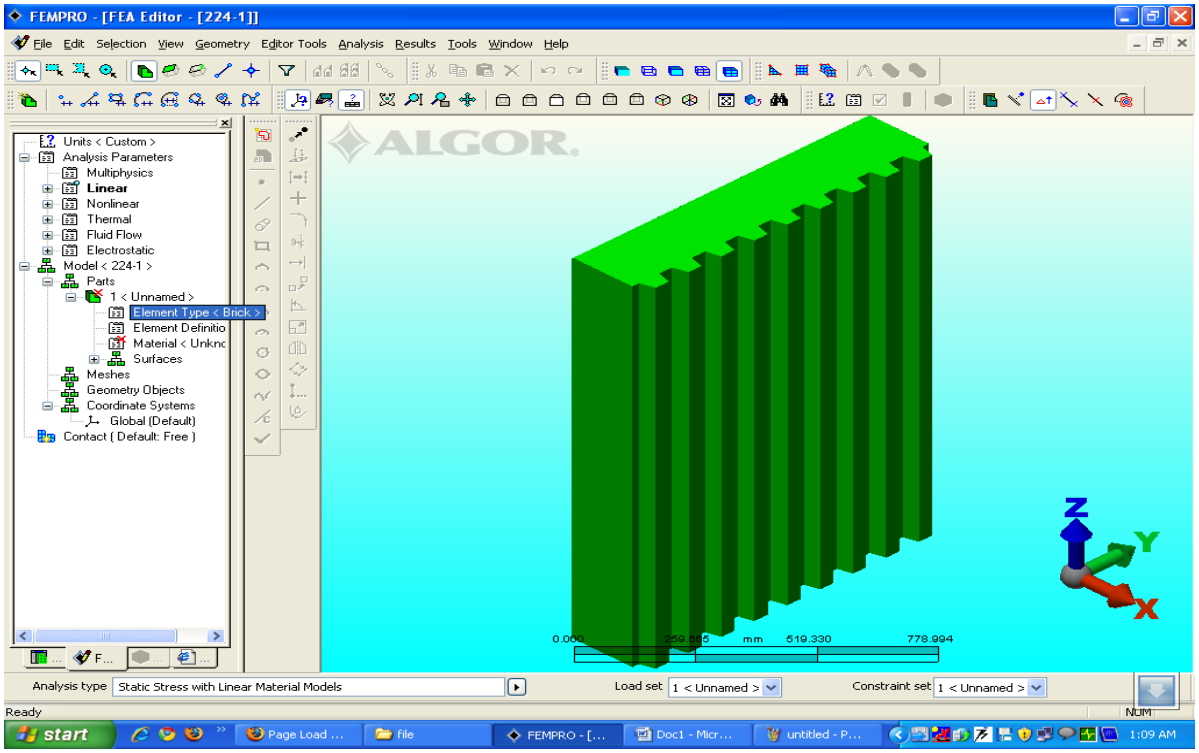

Fig.4.9 Swing Jaw Plate Model Ready for Selection of Element Type

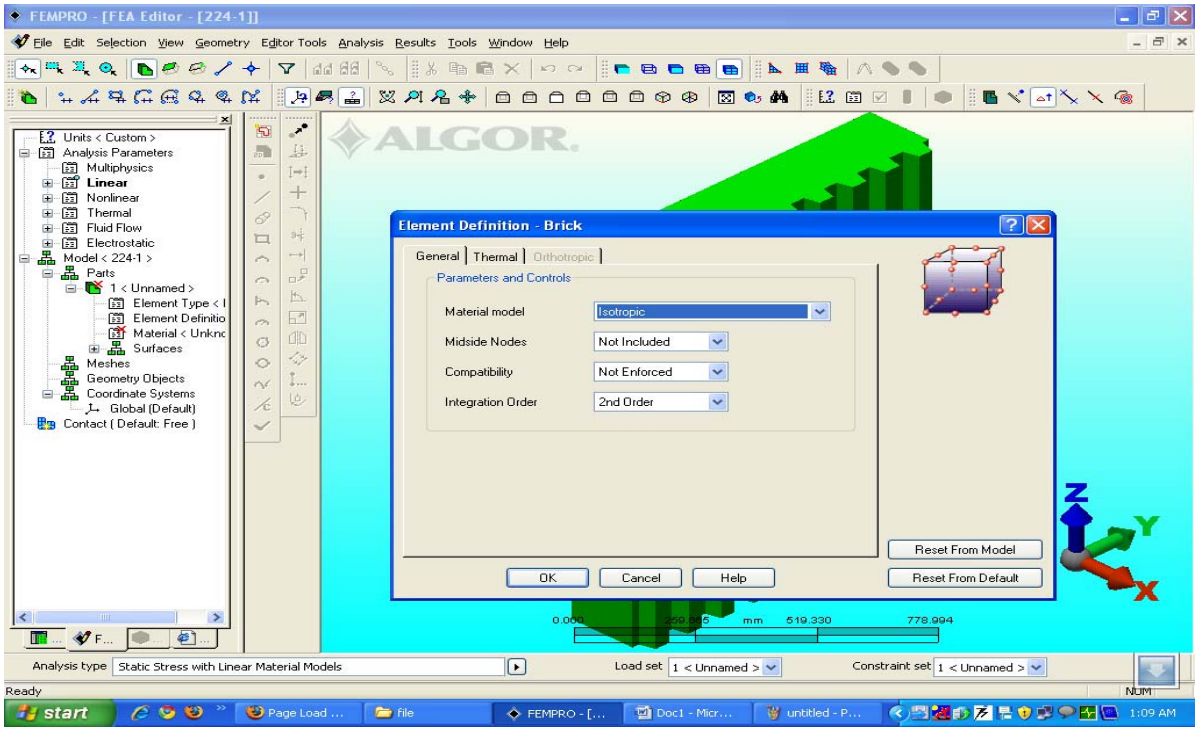

Fig.4.10Showing Swing Jaw Plate Model Element Type for Meshing

4.4.3 Applying Material Properties

Austenitic Manganese Steel is only when the manganese content exceeds about 0.08% that the steel may be classed as an alloy steel. When manganese content exceeds about 10%, the steel will be austenitic after slow cooling. One particular type of steel, known as Hadfield manganese steel, usually contains 12% manganese. Austenitic Manganese Steel-Standard and Specifications (ASTM 128 A/ 128M) .This specification covers Hadfield austenitic manganese steel castings and alloy modifications. Cast cross-section size precludes the use of all grades, and the buyer should consult us, as to grades practically obtainable for a particular design required. Final selection is to be based on consensus between the buyer and Acme Alloys.

The wear resistant cast steel is generally, referred to as Hadfield manganese steel. Although the above mentioned ten grades of austenitic steels have chemical composition to the Hadfield's original composition, its primary reason for existence is the assurance it provides the user from unexpected failure in demanding applications where downtime cannot be accepted. Manganese steel is a low-strength, high-ductility material. But properly controlled heat treating by austenizing and followed by water quenching or controlled air

cooling, the 12% manganese steel, ASTM 128 A, consists of a meta-stable austenitic phase having a face centered cubic (FCC) lattice with strengthening from interstitial carbon and substitutional manganese atoms.

Another property of great significance is its ability to work-harden from an initial hardness of 240 BHN (23 Rc) to well over 500 BHN (51 Rc). The face centered cubic (FCC) lattice has 12 equivalent slip systems and deformations that result in conversion of some austenite to martensite. As this work-hardening deformation process continues, it increases hardness of the affected metal and eventually results in increasing abrasion resistance.Thus, manganese steels perform most efficiently when external conditions cause extensive work hardening of the wear component's surface. If cracking of the work hardened layer occurs, the crack propagation would quickly be checked and prevented by the tougher un-worked hardened core. Hence, in demanding applications such as primary rock crushing austenitic manganese steels are widely used. Mineral and mining equipment, grinding and crushing machinery, power shovel buckets, railway track work, cement plants-kiln and mill liners, stone crushers- jaw and gyratory crushers and ore processing. [26]

Austenitic manganese steel material customer defined using isotropic material properties. Elastic Modulus (E) = 210 GPa, Mass Density (ρ) = 7838 kg/m3,
Poisons ratio (ν) = 0.3, Shear Modulus (Φ) =80.76 GPa, Yield Strength (Ys) =550MPa

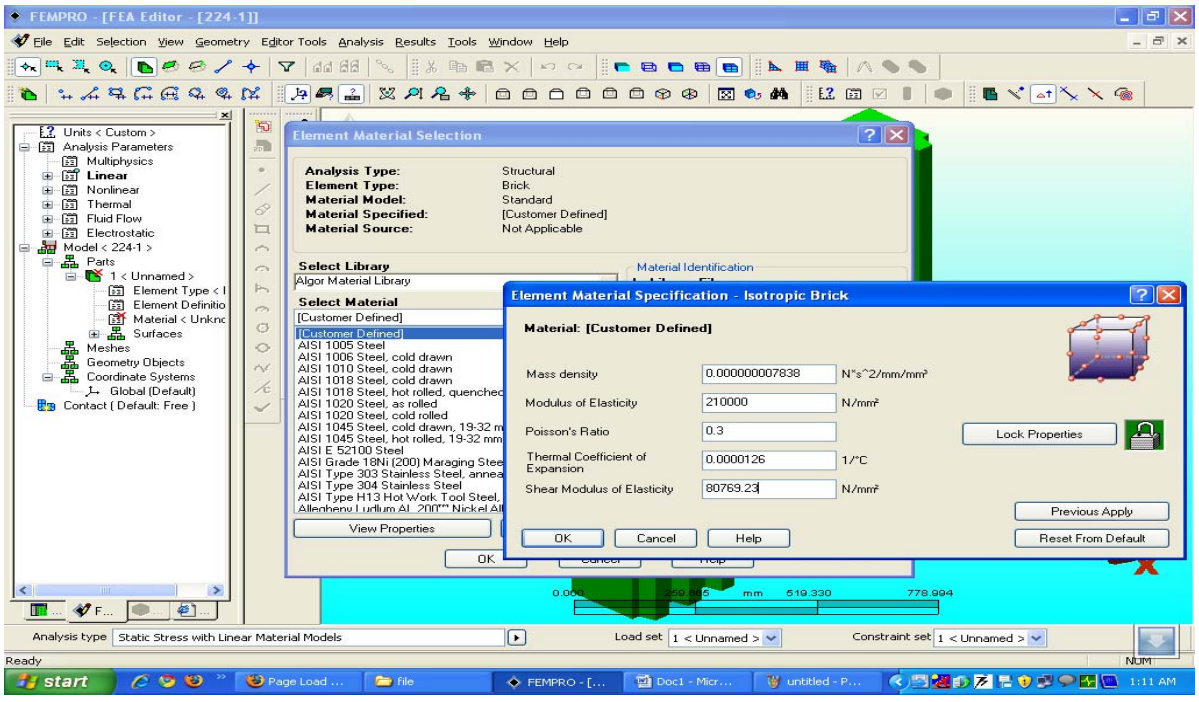

Fig.4.11Showing Swing Jaw Plate Model for Material Selection

4.4.4 Apply Boundary Conditions

Boundary condition for Swing jaw plate is simply supported i.e. the support at bearing location hinge support and at the free end toggle force acting

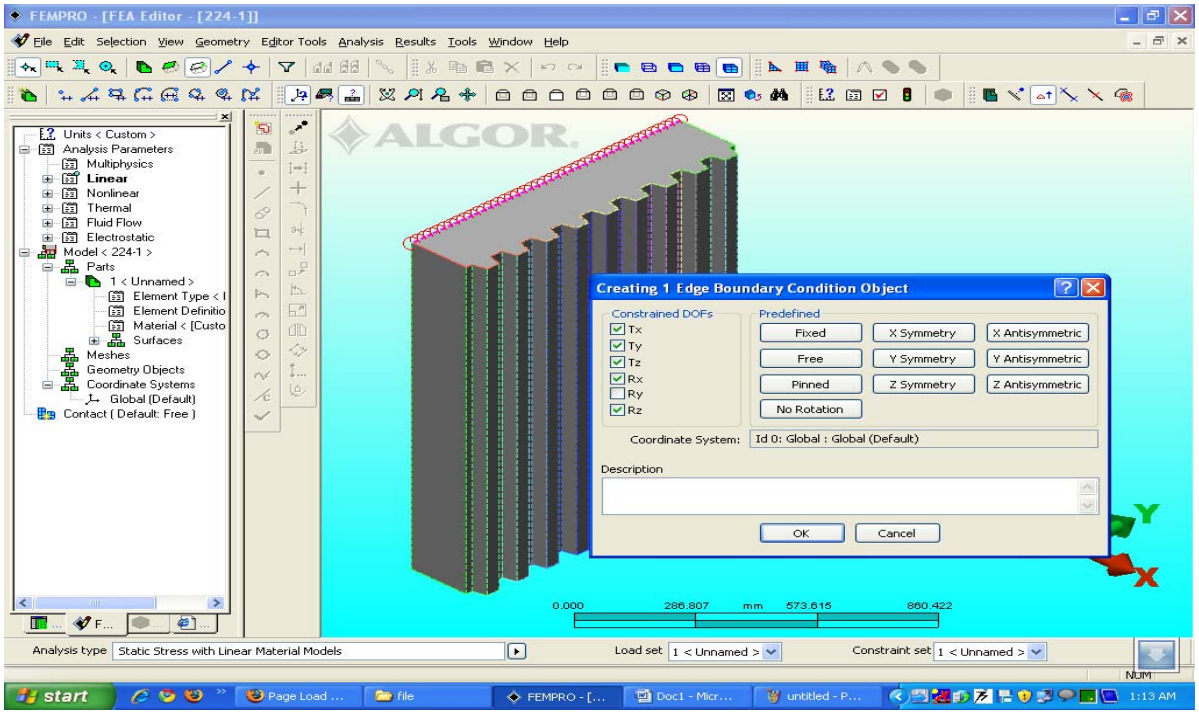

Fig.4.12 Showing Swing Jaw Plate Model Boundary Condition (Support)

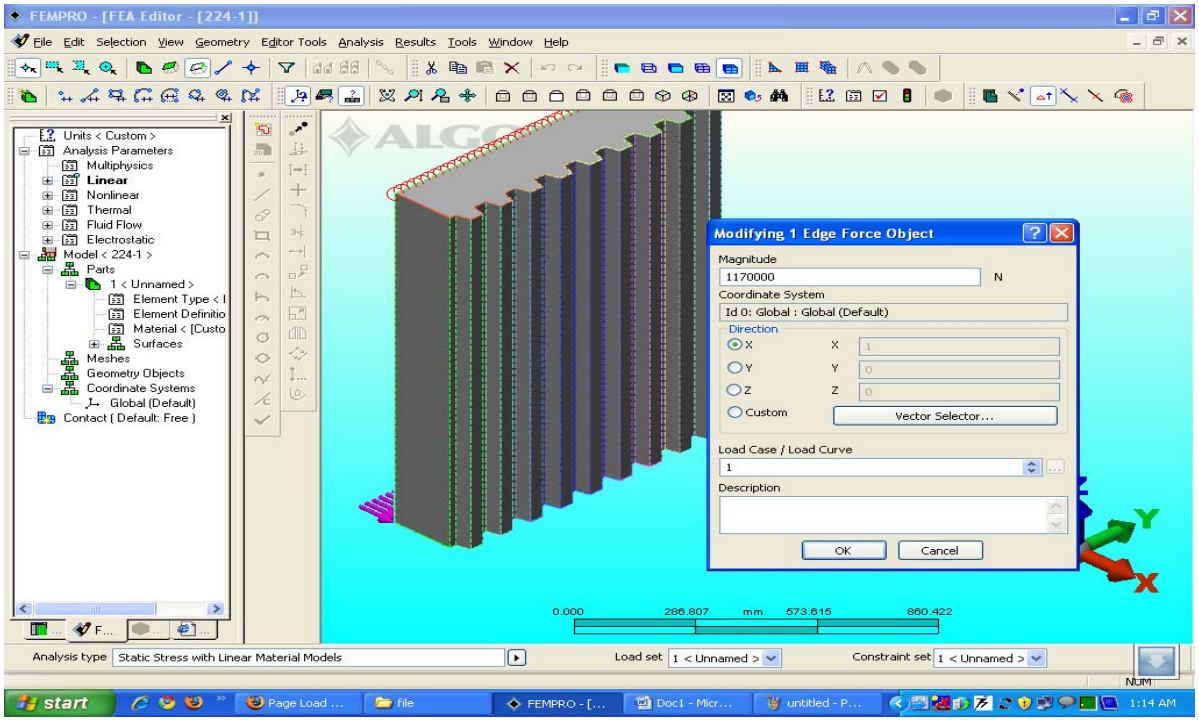

Fig.4.13 Showing Swing Jaw Plate Model Boundary Condition (Toggle Force)

4.4.4 Applying Loads

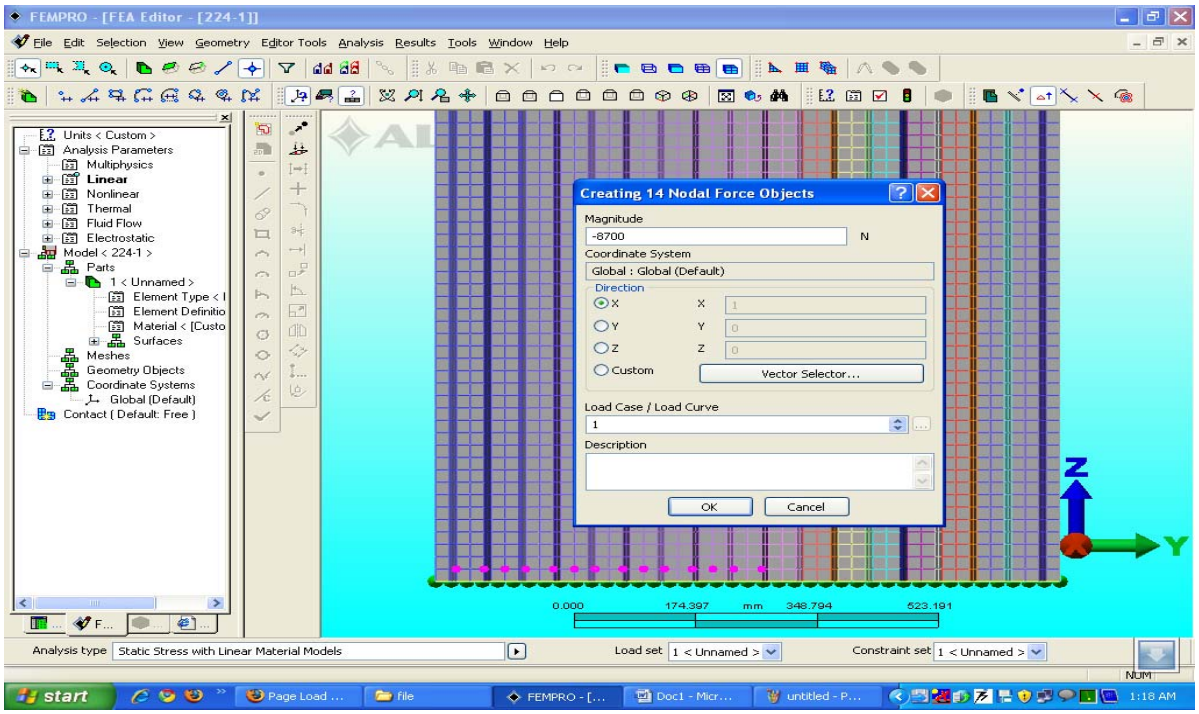

Fig.4.14 Showing Swing Jaw Plate Model Applying Point Loads

4.4.5 Linear Static Stress Analysis

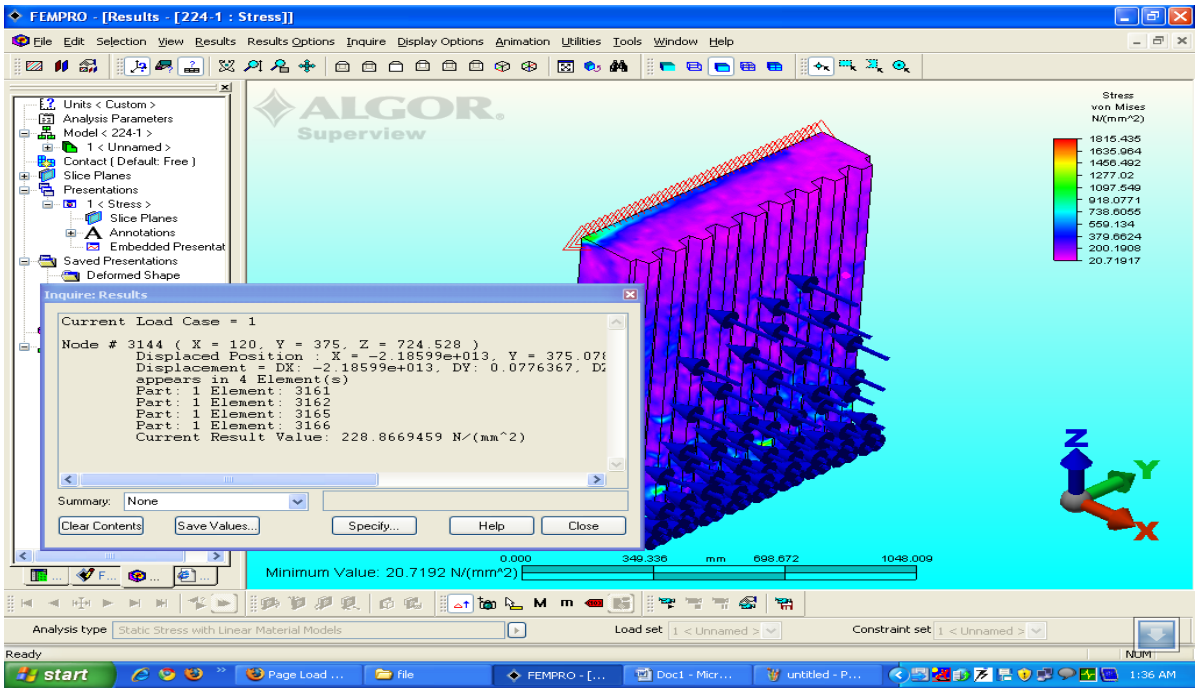

Fig.4.15 Showing Swing Jaw Plate Stress Analysis

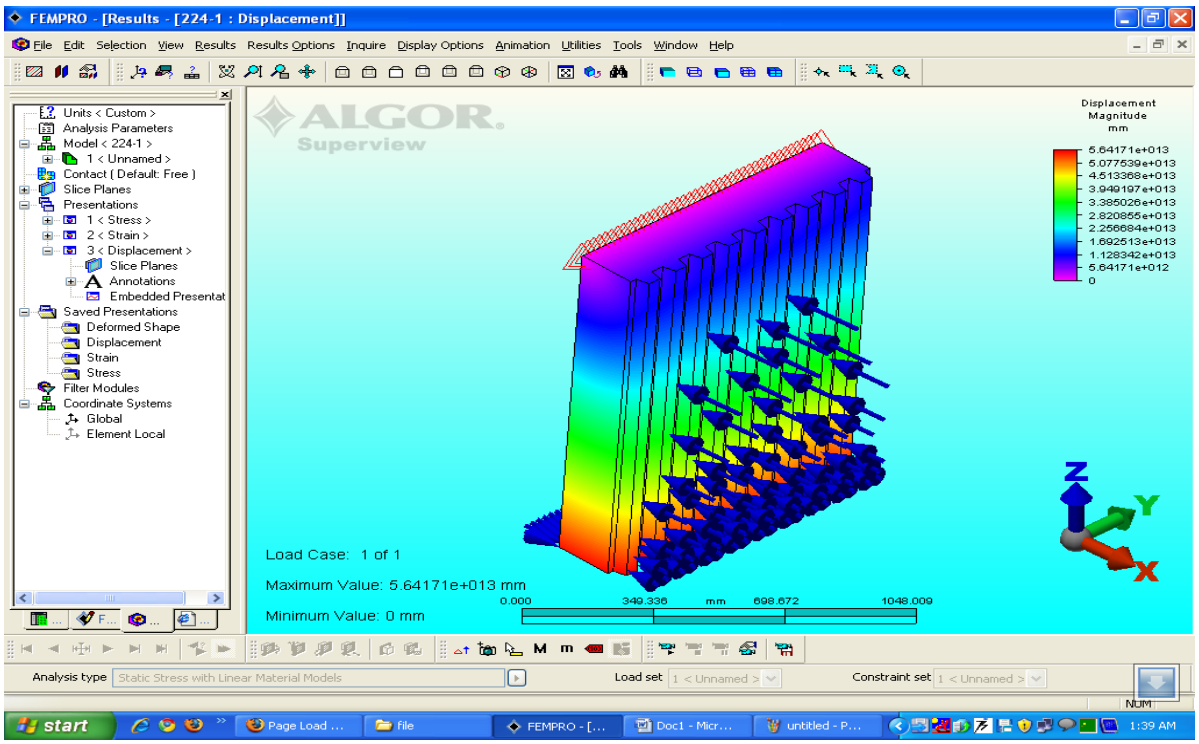

Fig.4.16 Showing Swing Jaw Plate Displacement

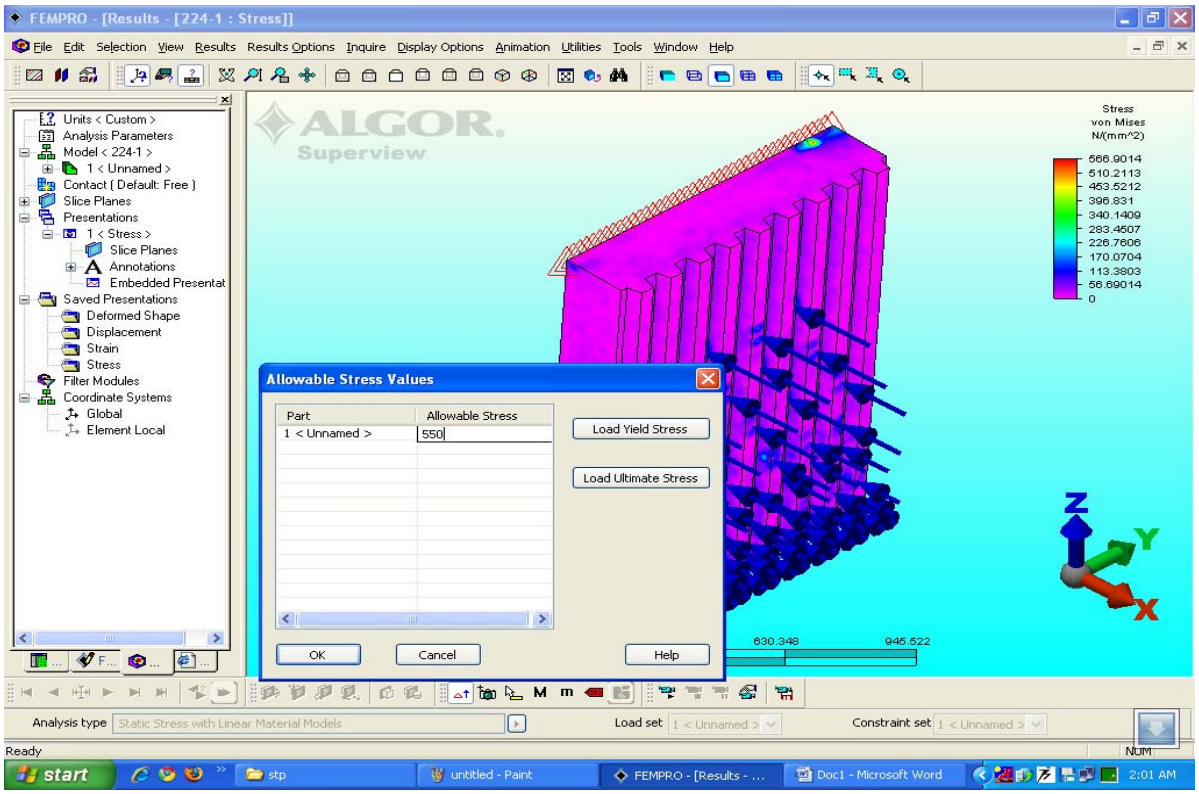

Fig.4.17 Showing Swing Jaw Plate Allowable Stress Value

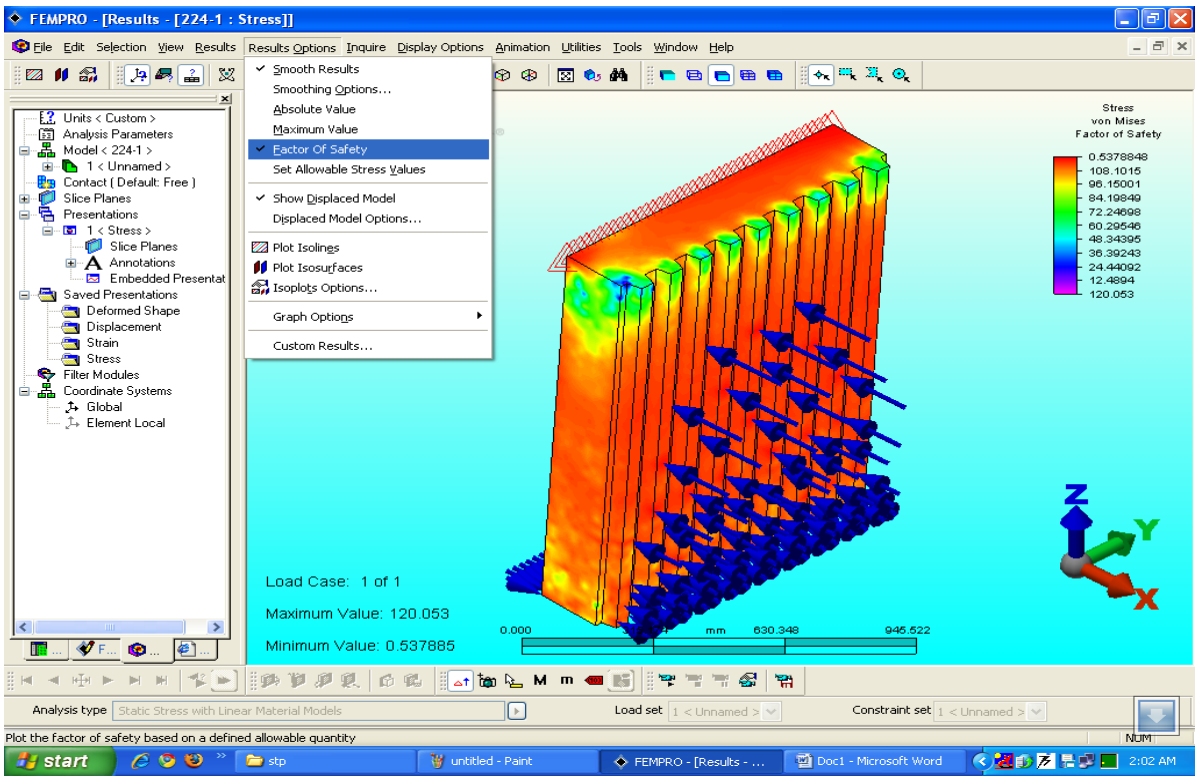

Fig.4.18 Showing Swing Jaw Plate Factor of Safety Tool

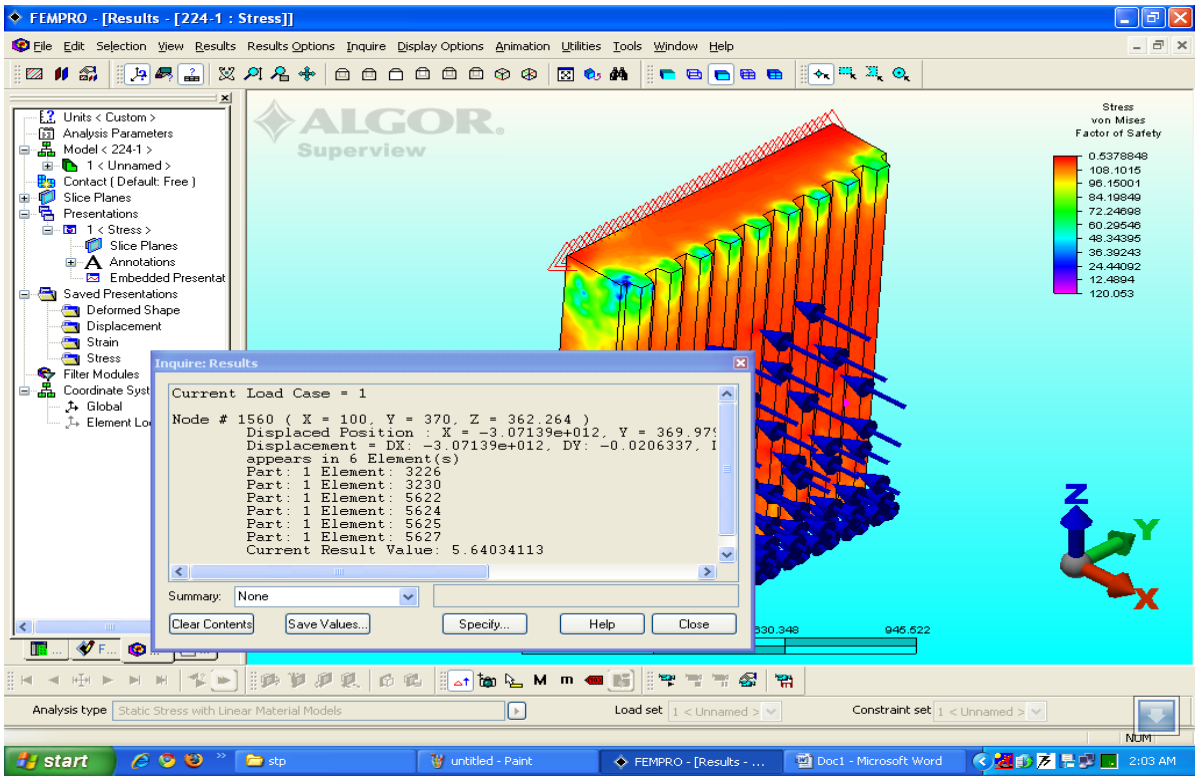

Fig.4.19 Showing Swing Jaw Plate Factor of Safety Values

4.5 Swing Jaw Plates with Stiffeners

4.5.1 Solid Modeling of Swing Jaw Plates with Stiffeners

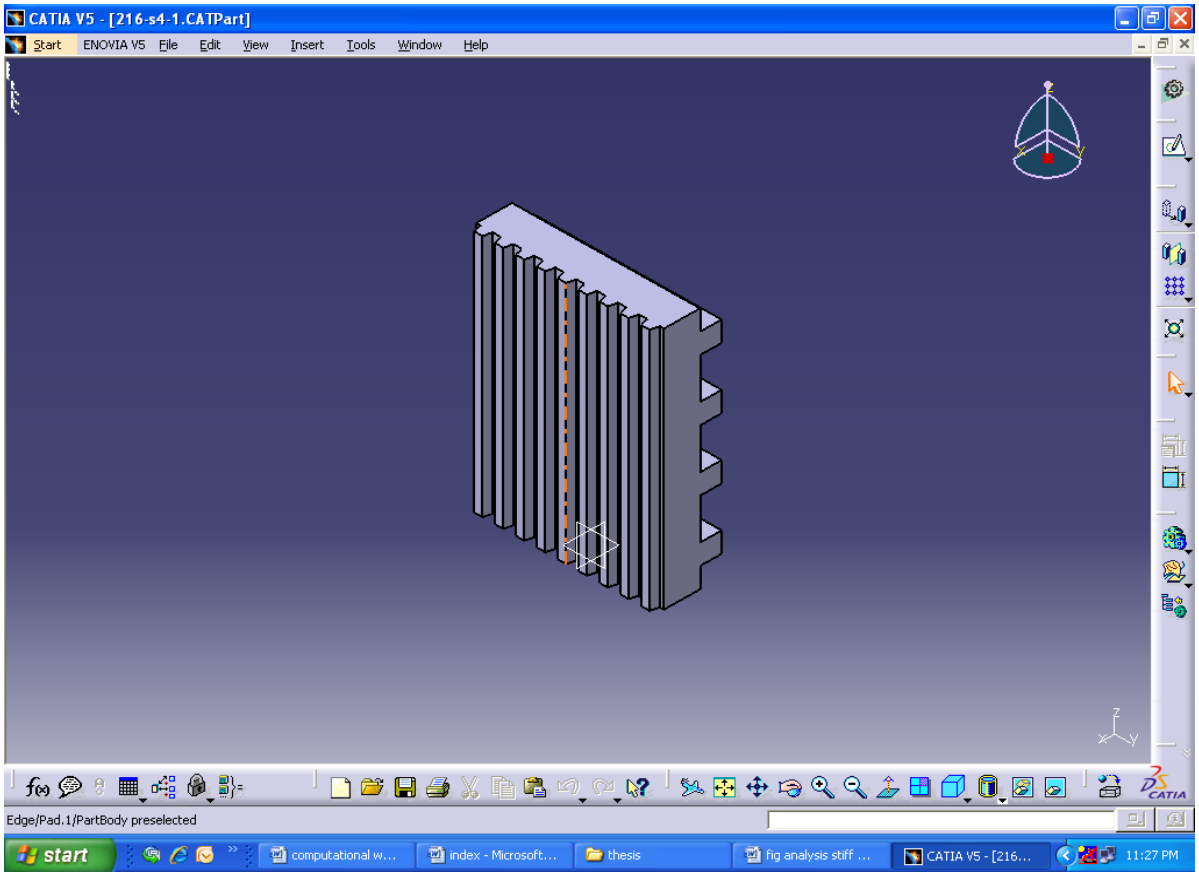

Fig.4.20 Solid Model of Corrugated Swing Jaw Plate with Stiffeners

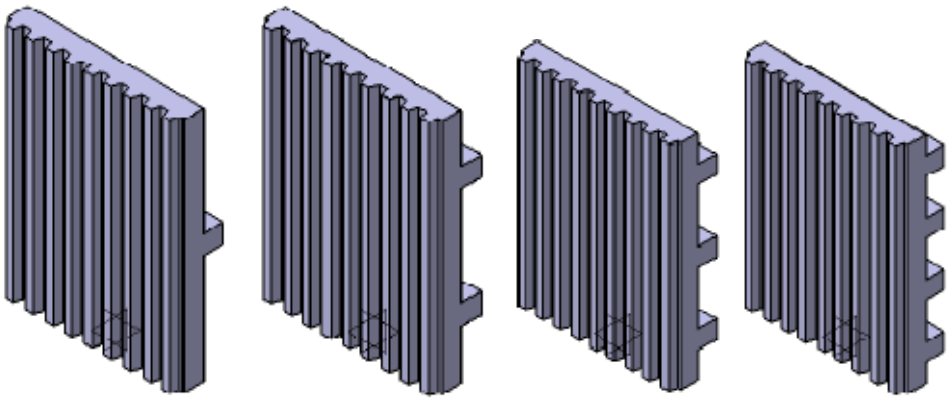

Fig.4.21 Swing Jaw Plates (1200X900X140) with Stiffeners

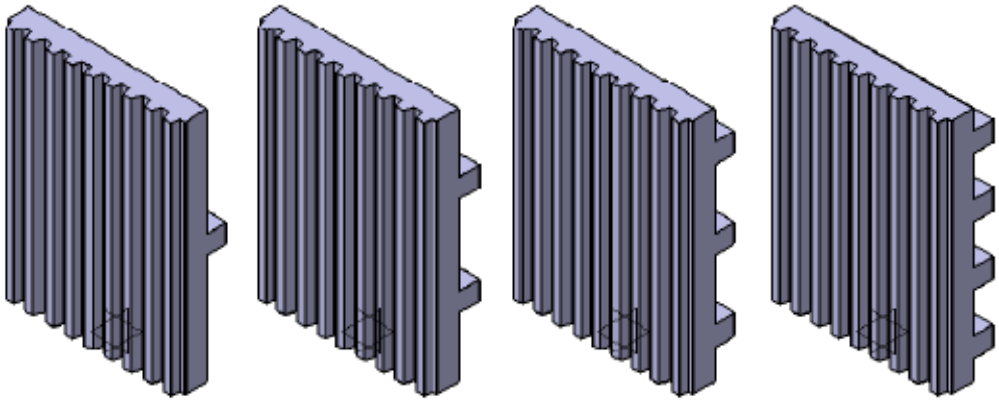

Fig.4.22 Swing Jaw Plates (1200X900X152) with Stiffeners

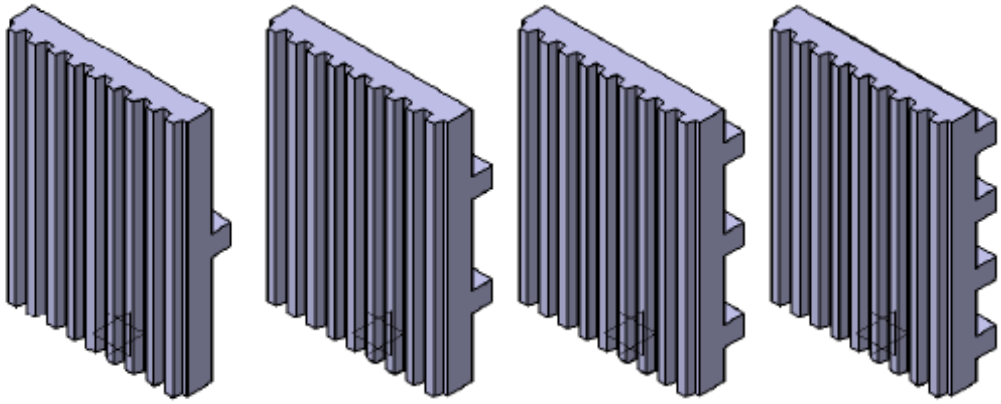

Fig.4.23 Swing Jaw Plates (1200X900X165) with Stiffeners

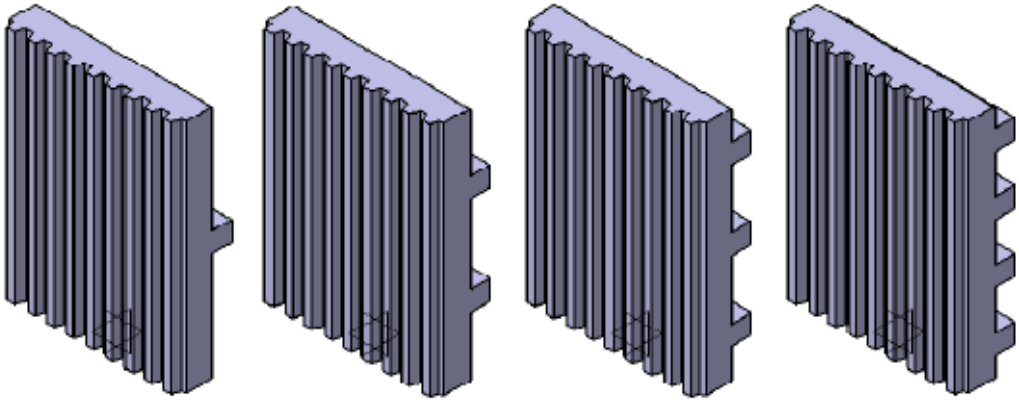

Fig.4.24 Swing Jaw Plates (1200X900X178) with Stiffeners

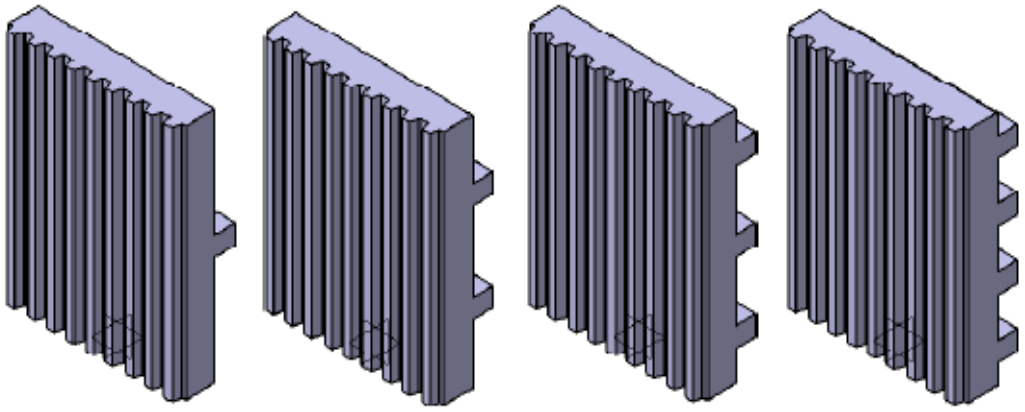

Fig.4.25 Swing Jaw Plates (1200X900X191) with Stiffeners

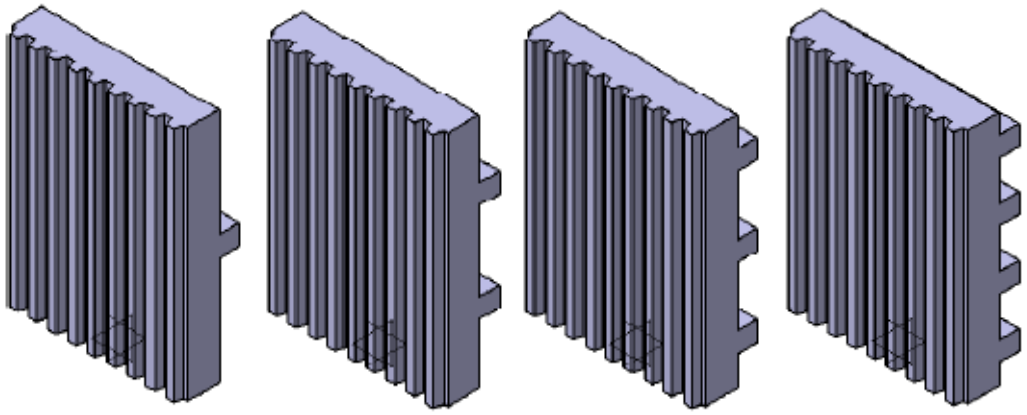

Fig.4.26 Swing Jaw Plates (1200X900X203) with Stiffeners

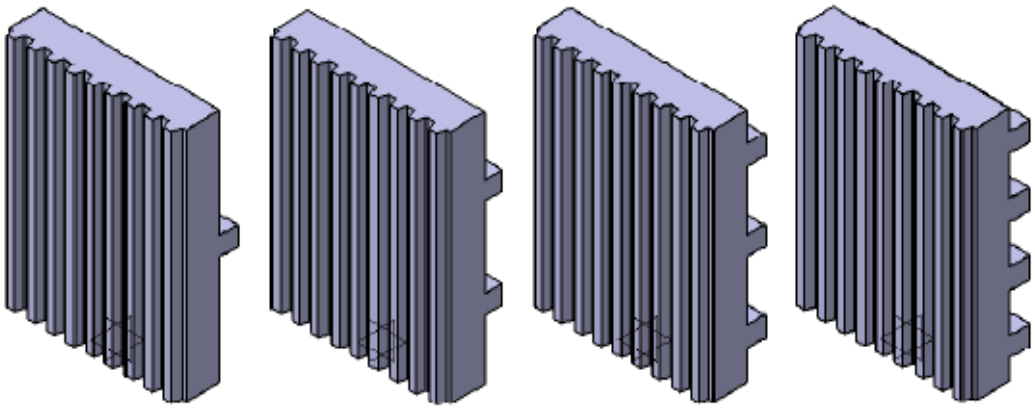

Fig.4.27 Swing Jaw Plates (1200X900X216) with Stiffeners

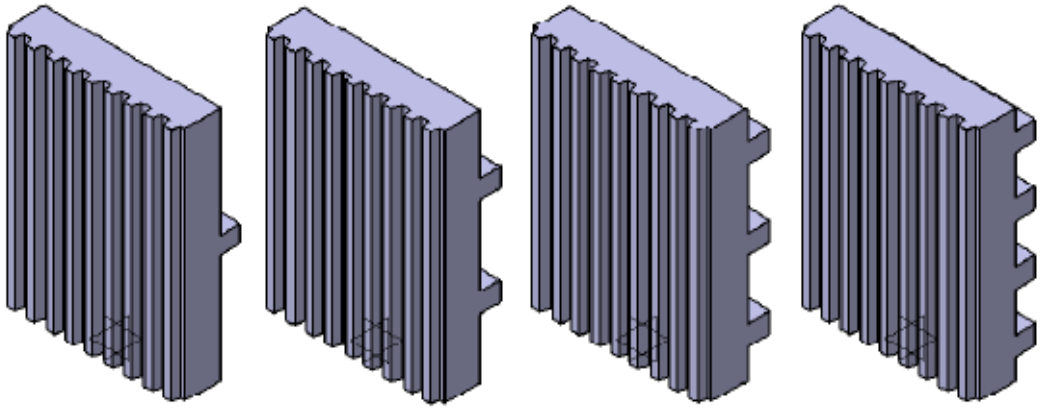

Fig.4.28 Swing Jaw Plates (1200X900X224) with Stiffeners

4.6 Swing Jaw Plates Static Stress Analysis with Stiffeners

Below is a finite element representation of the stiffened plate shown above. The plate is thick, therefore thick plate theory applies. Square beam stiffeners are mounted as shown. The structure is simply supported and point loads at different nodes are applied to the surface of the plate. Because the centroidal axes of the stiffeners coincide with the mid-plane of the plate, need not to define the element properties for the stiffeners.

4.6.1Meshing and Element Type

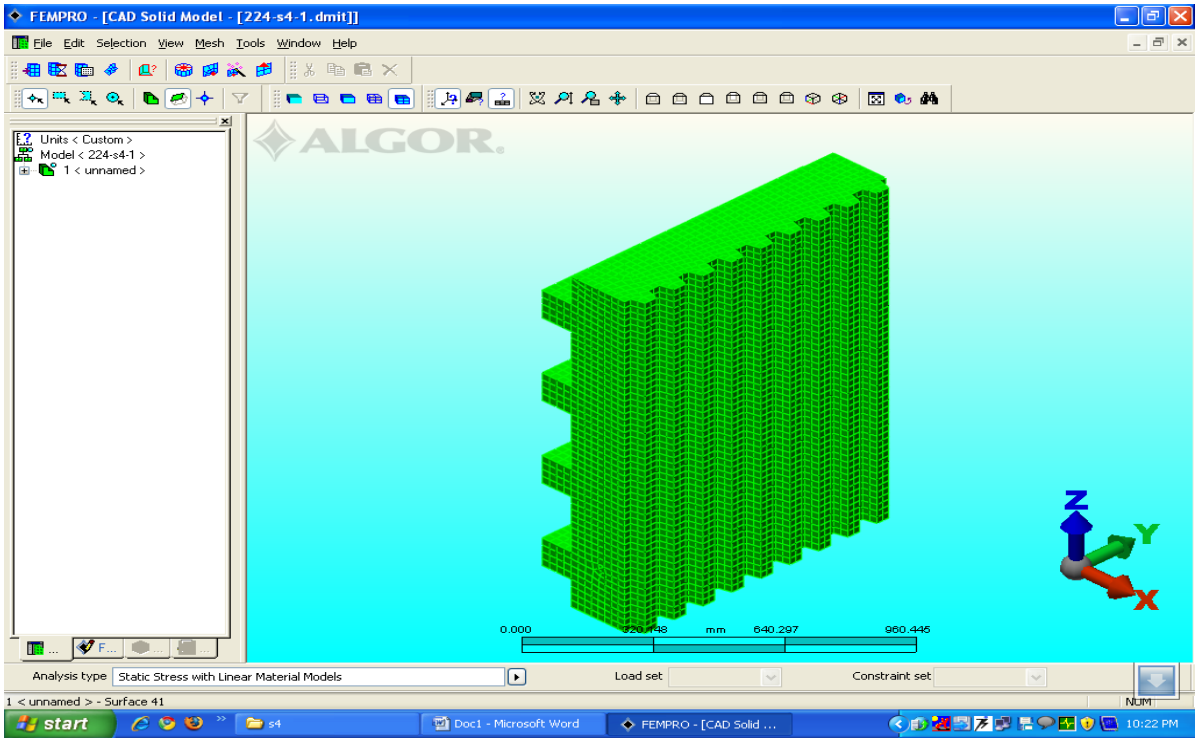

Fig.4.29 Stiffened Swing Jaw Plate Model Ready for Meshing (Discretization)

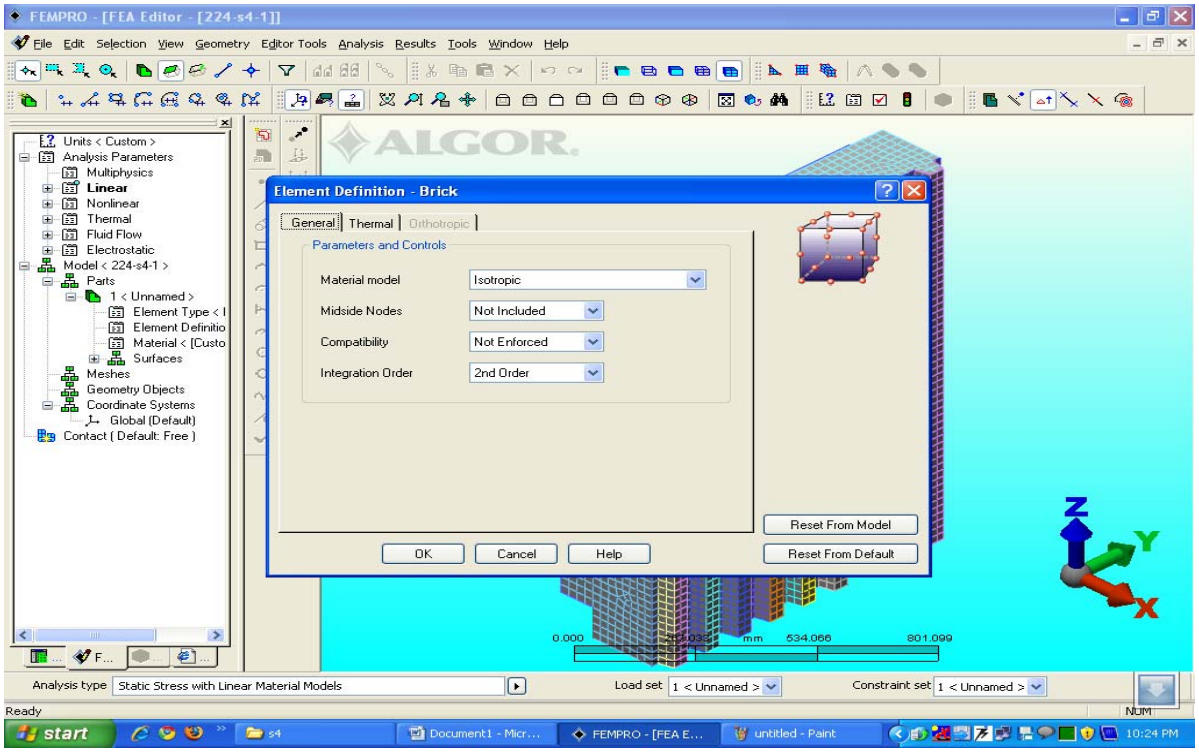

Fig.4.30 Stiffened Swing Jaw Plate Model Ready for Selection of Element Type

4.6.2Applying Material Properties

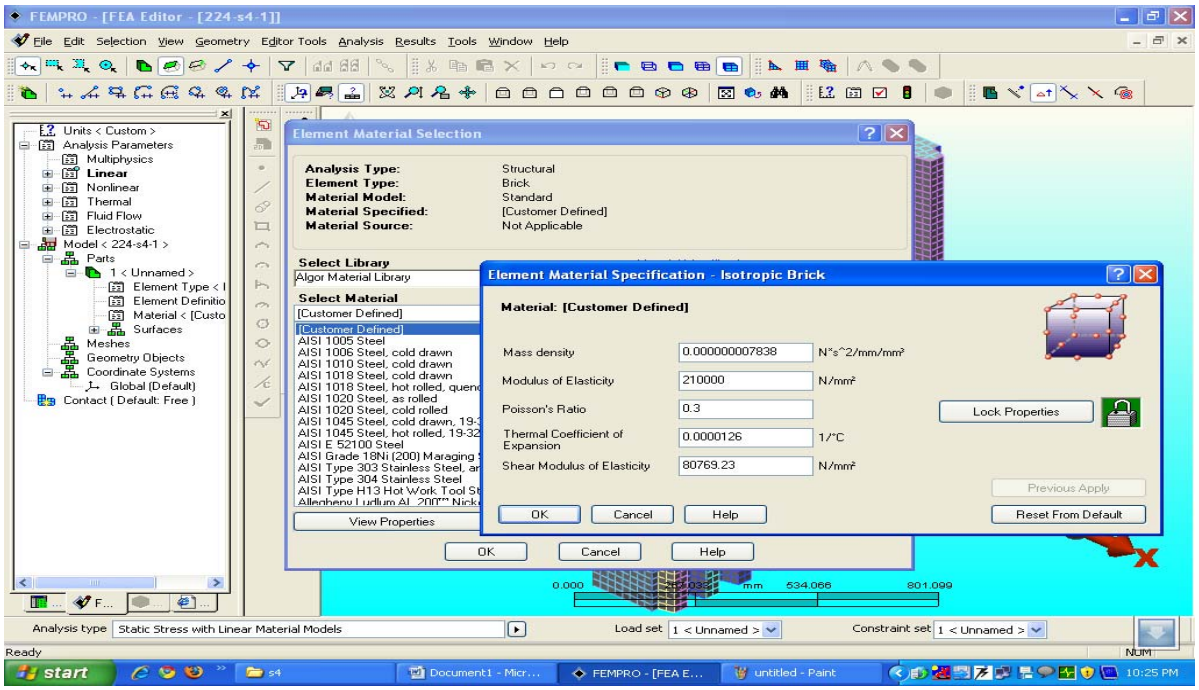

Fig.4.31Showing Stiffened Swing Jaw Plate Model for Material Selection

4.6.3Apply Boundary Conditions

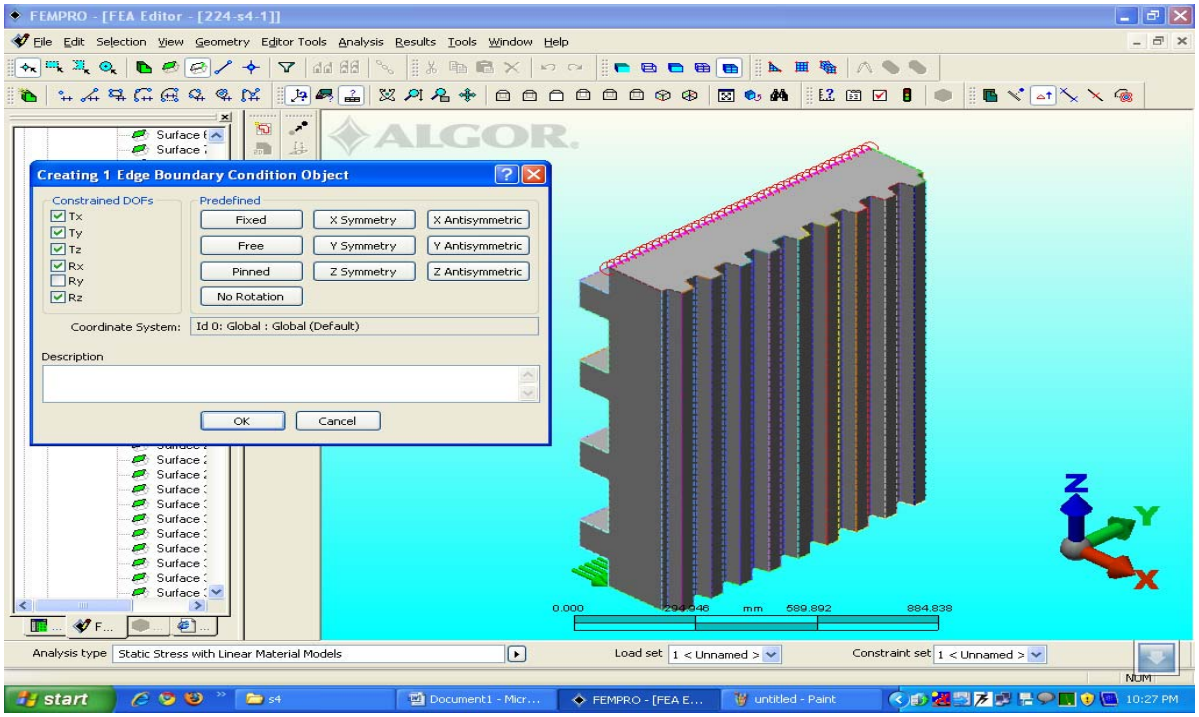

Fig.4.32 Showing Stiffened Swing Jaw Plate Boundary Condition (Toggle Force)

4.6.4Applying Loads

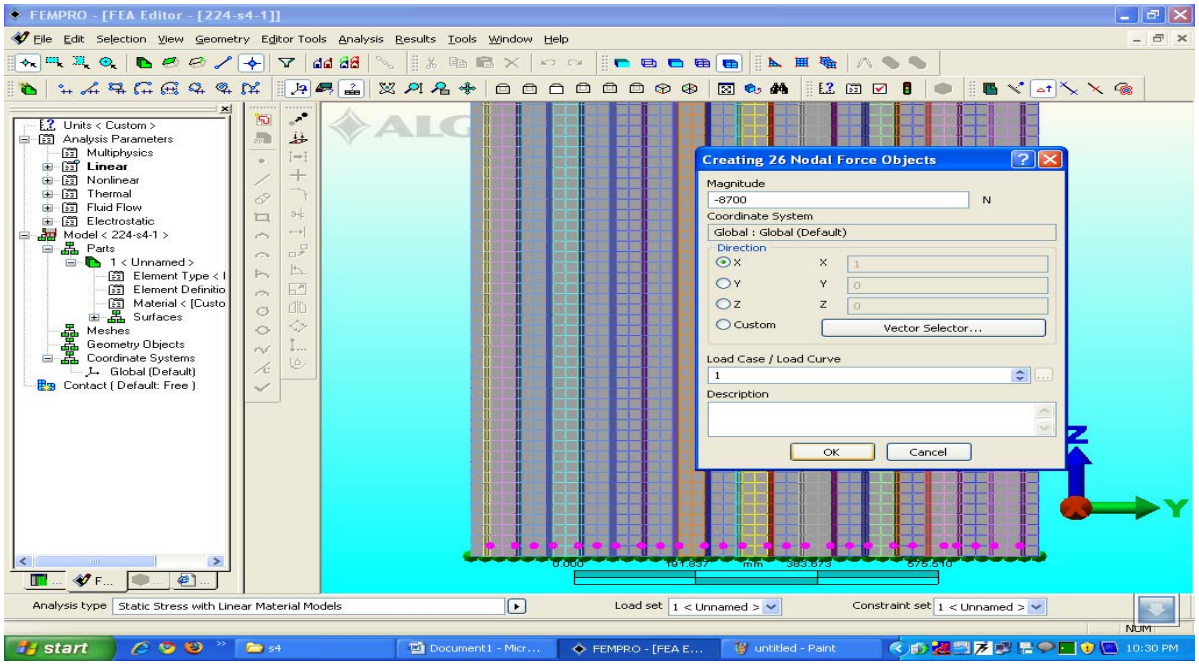

Fig.4.33 Showing Stiffened Swing Jaw Plate Model Applying Point Loads

4.6.5 Linear Static Stress Analysis Results

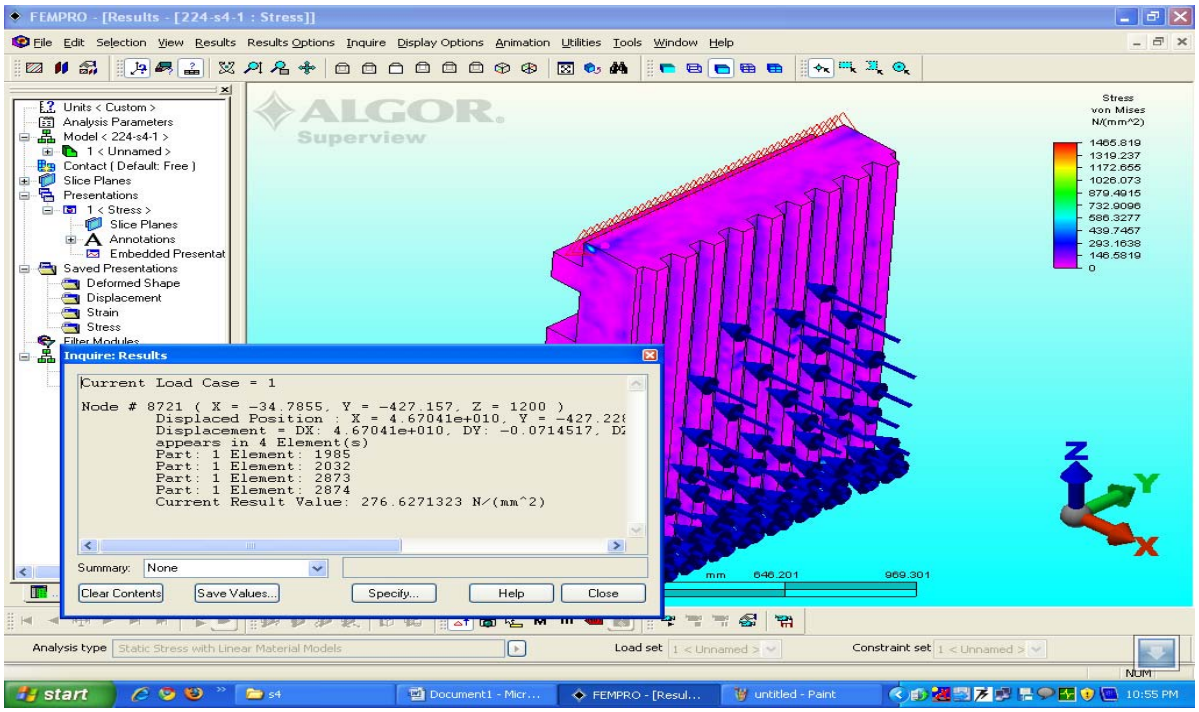

Fig.4.34 Showing Stiffened Swing Jaw Plate Stress Analysis

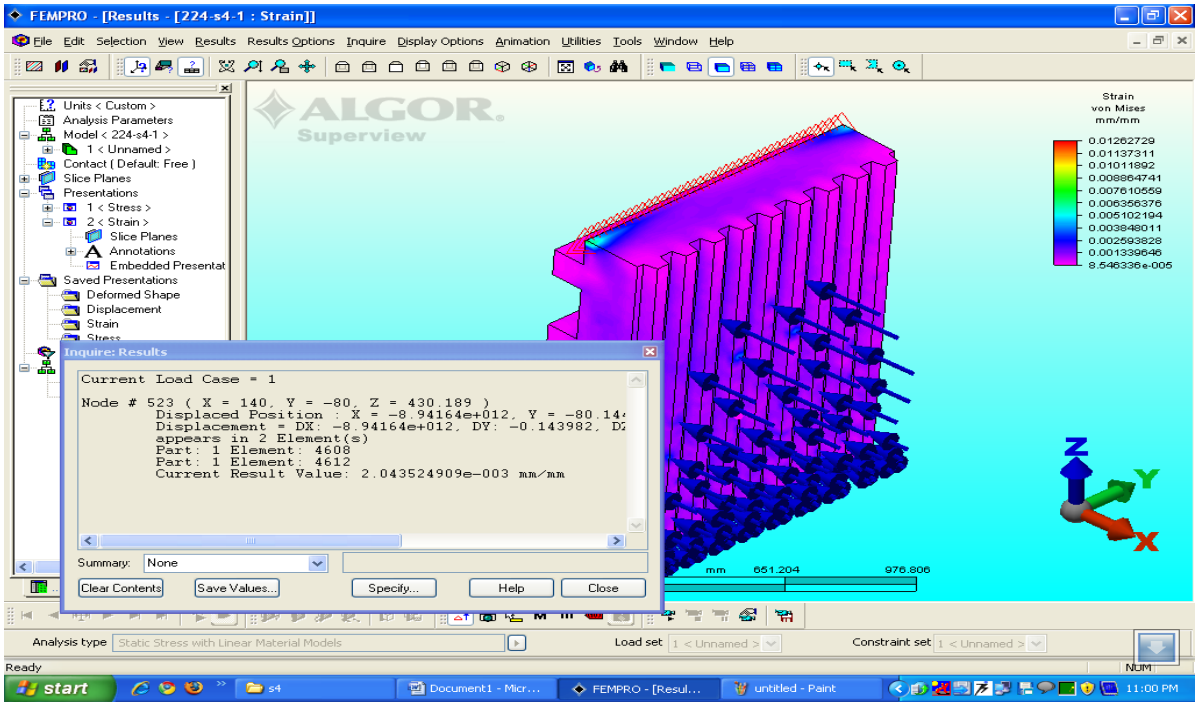

Fig.4.35 Showing Stiffened Swing Jaw Plate Strain Analysis

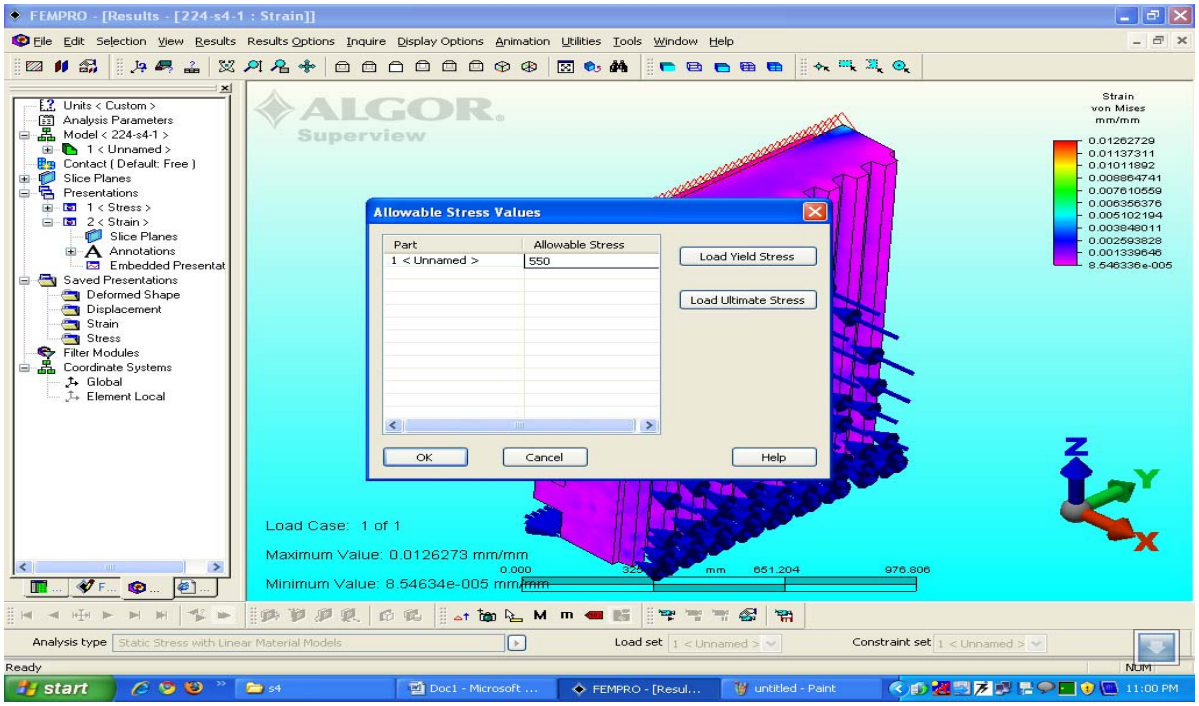

Fig.4.36 Showing Stiffened Swing Jaw Plate Allowable Stress Value

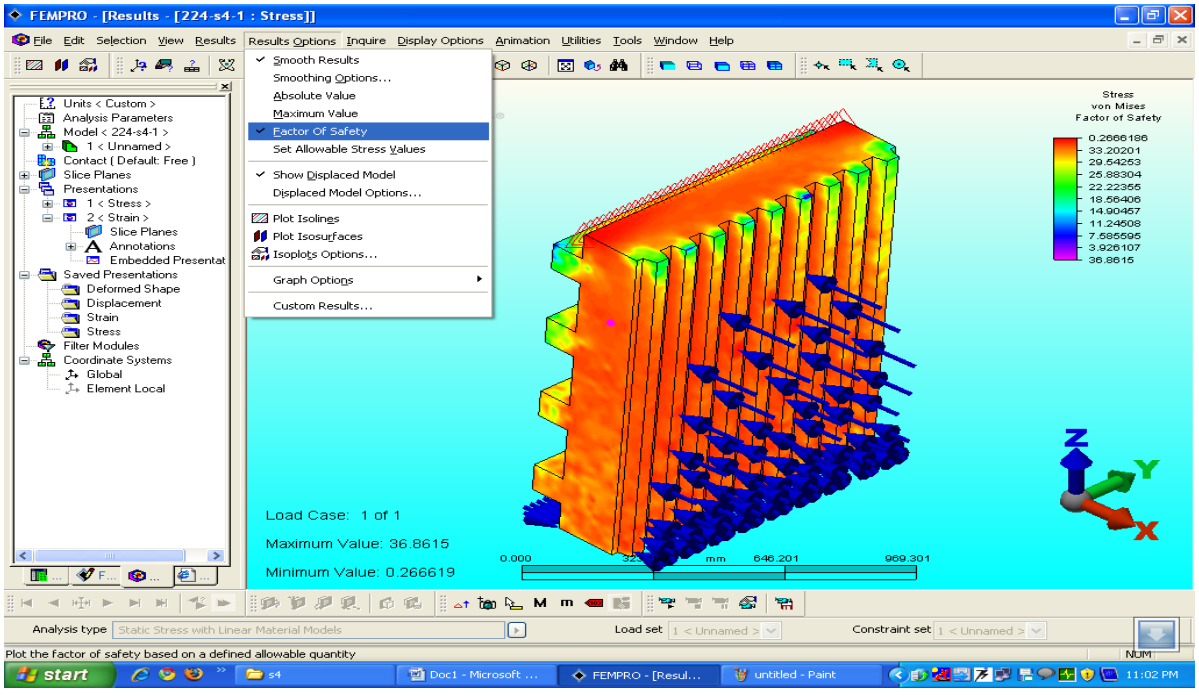

Fig.4.37 Showing Stiffened Swing Jaw Plate Factor of Safety Tool

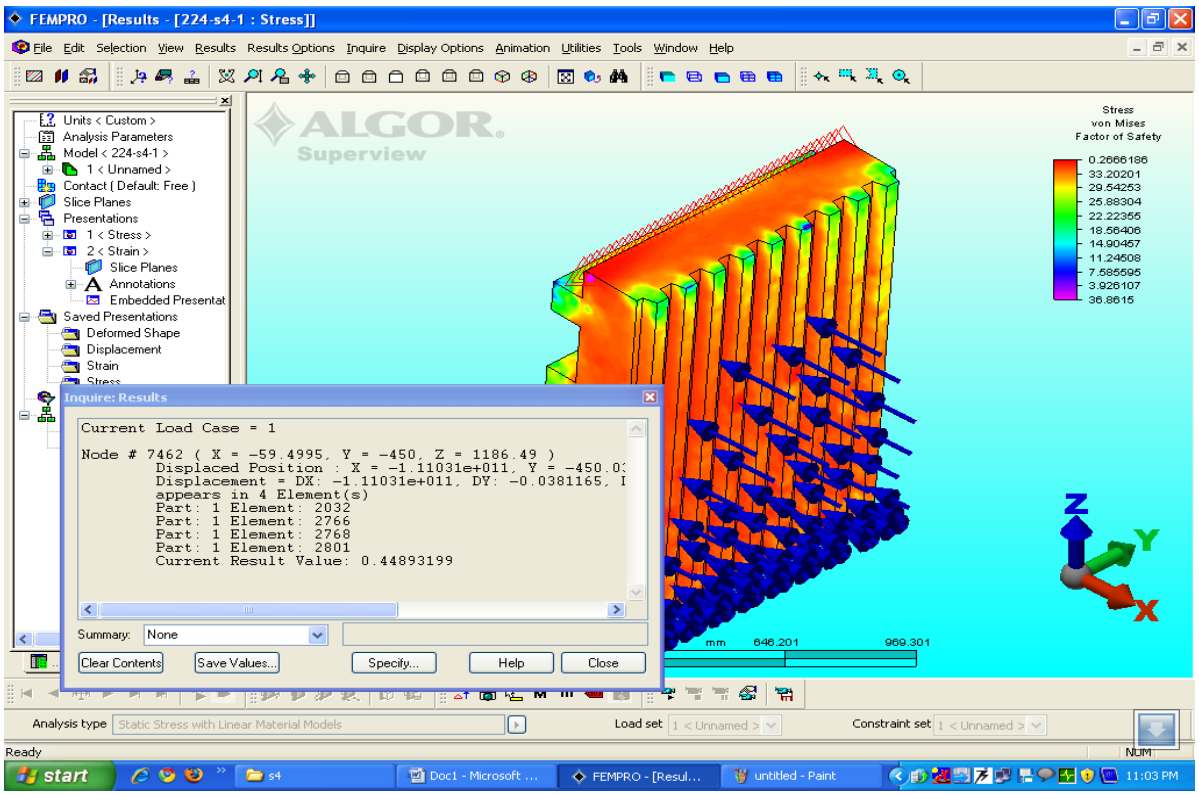

Fig.4.38 Showing Stiffened Swing Jaw Plate Factor of Safety Values

CHAPTER- 5

RESULTS, DISCUSSION AND CONCLUSION

5. RESULTS, DISCUSSION AND CONCLUSION

5.1 Static Stress Analysis Results

Since the PDF data were most complete for the amphibolites, these load-deformation relations were employed in the model. Laboratory data were extrapolated for the larger sizes according to the dotted line in the strength-deformation size relationships in Figs. 3.7 and 3.9. To obtain a comparison for the interactive model, the same beam model (same EI) was loaded with the same sized particles which were all assumed to fail simultaneously.

The load distribution found with simultaneous failure as shown and compared with the load distribution curve assumed by Molling [6]. The stepwise pressure distribution was found by distributing the ultimate point load for that size particle over the distance midway between each of the two adjacent loads. The similarity of the two distributions further substantiates the size-strength relations and particle size distribution employed in this study.

The numerical and FEA models using ALGOR are employed to calculate maximum tensile stresses and maximum toggle forces (T) for a variety of model plate thicknesses, using the rock properties of the amphibolites. The comparisons are presented in Table 5.1.

Table 5.1 Effect of thickness on maximum response when loaded with amphibolites

Jaw Plate Thickness		Stiffness (kN m^2)	Max. Tensile Stress (MPa)		Max Deflection (mm)		Max Driving
(in)	(mm)	($\times 10^5$)	Numerical Analysis	ALGOR Analysis	Numerical Analysis	ALGOR Analysis	Force (T) (MN)
8.8	224	1.74	226.42	228.36	0.071	0.104	1.17
8.5	216	1.60	242.34	245.51	0.079	0.114	1.17
8.0	203	1.33	261.91	262.48	0.094	0.137	1.17
7.5	191	1.10	269.55	273.56	0.112	0.168	1.17
7.0	178	0.90	278.30	281.65	0.137	0.206	1.17
6.5	165	0.73	286.15	289.26	0.178	0.257	1.17
6.0	152	0.55	291.84	293.19	0.226	0.325	1.17
5.5	140	0.44	308.90	309.99	0.292	0.424	1.17

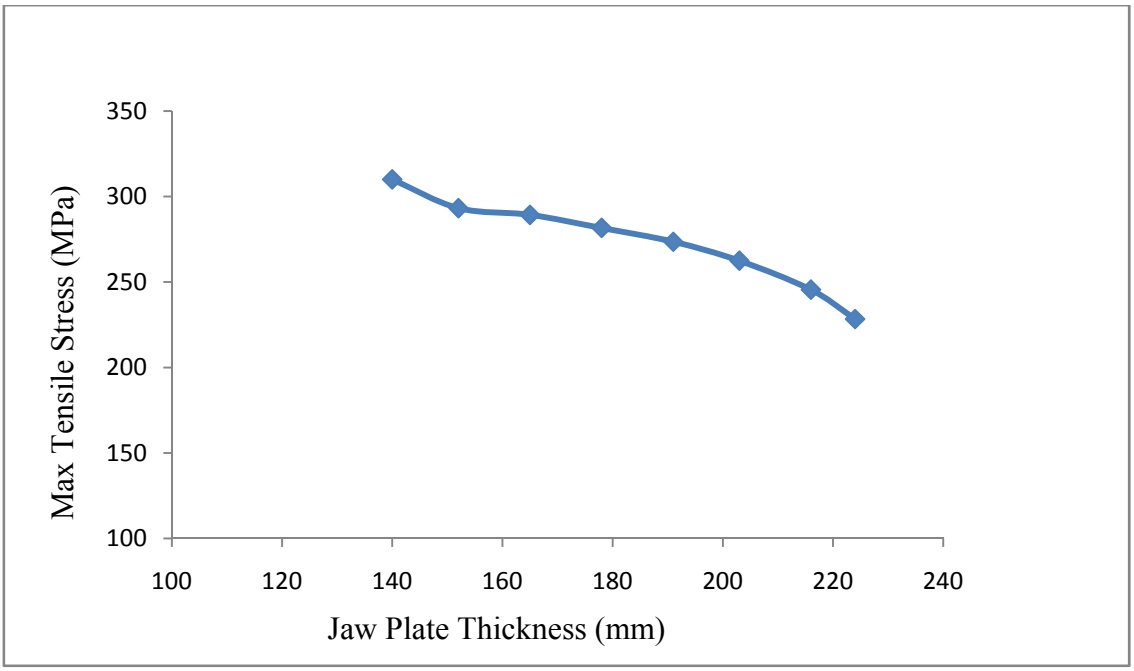

Fig.5.1 Maximum Tensile Stress Response for Various Jaw Plate Thicknesses

5.2 Effect of Stiffeners on Swing Jaw Plates

Table 5.2 Effect of stiffeners on maximum response for various jaw plate thicknesses

Thickness		Stiffness(EI) (kN m^2) ($\times 10^5$)	Number of Stiffeners				Max Driving Force (MN)
(in)	(mm)		NOS=4	NOS=3	NOS=2	NOS=1	
8.8	224	1.74	176.87	178.71	183.19	210.23	1.17
8.5	216	1.60	193.24	209.51	217.41	225.45	1.17
8.0	203	1.33	212.25	218.75	235.89	248.74	1.17
7.5	191	1.10	223.98	239.52	252.78	265.23	1.17
7.0	178	0.90	239.87	246.37	258.60	274.68	1.17
6.5	165	0.73	245.36	257.45	269.63	284.66	1.17
6.0	152	0.55	259.58	267.13	276.53	289.56	1.17
5.5	140	0.44	280.92	283.15	289.91	296.71	1.17

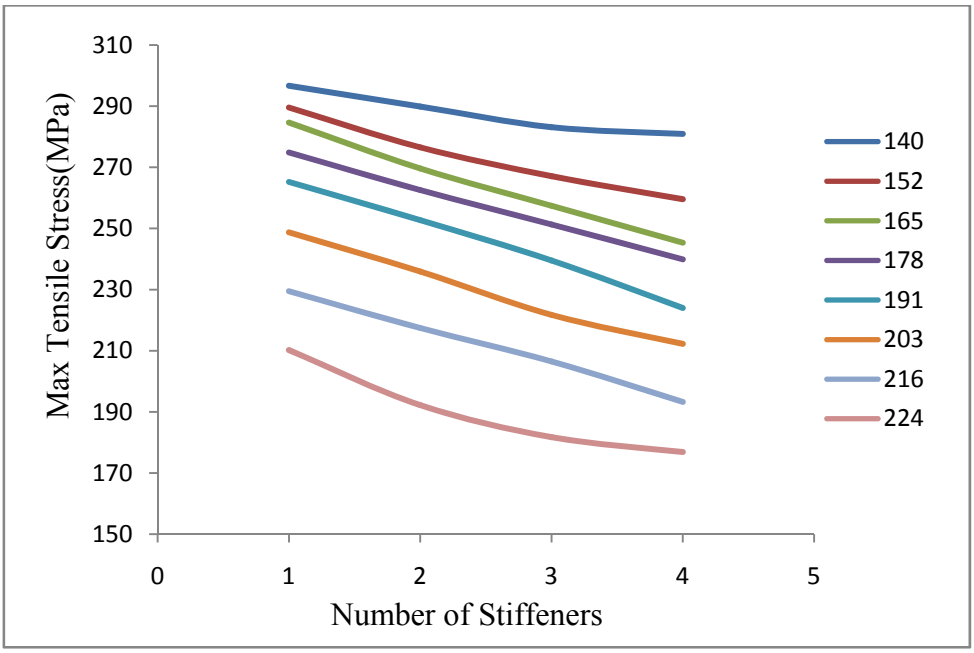

Fig.5.2 Effect of Stiffeners on Swing Jaw Plates Maximum Stress Response

5.3 Approximate Savings in Energy Using Stiffeners

If fatigue of the plate is of concern, then the maximum tensile stress is important. A comparison of data in Table 5.3 shows that the maximum induced tensile stress for the 203 mm (8.0 in) thick model plate equals that induced for the 152 mm (6.0 in) plate. This difference is found because the particles do not fail simultaneously but fail at different stages, U, of a single crushing cycle. Thus the assumption of simultaneous failure will result in design of a stiffer and heavier beam for the same maximum stress level.

The reduction in the toggle force necessary to push the lighter, stiffened plates can be translated into an approximate savings in energy. If the peak acceleration (a) of the 203mm and 152 mm plates is assumed to be equal, then the force reduction resulting from a smaller plate is proportional to the acceleration times the change in plate mass. It also follows that the change in energy per cycle (ΔW), could be approximated as the distance traveled (U), times the percent change in the average force, or

$$\Delta W = \frac{U\Delta F}{UF_1} = \frac{\Delta Ma}{M_1 a} = \frac{\Delta M}{M_1} \text{----------(12)}$$

Since the mass is somewhat proportional to the thickness of the 203 and 152 mm models, the crushing energy absorbed by plate movement is reduced by approximately [(203 – 152)/203] = 25%. Of course this 25% is an estimate, as the model plates which are stiffened and leads to reductions in plate weight and indicates that design of new energy-efficient systems should include deformation (PDF) properties of the crushed material. [5]

Table 5.3Comparison of Various Jaw Plates with and without stiffeners

Jaw Plate Thickness (in)	(mm)	Max Tensile Stresses (MPa) Number of Stiffeners NOS=0	NOS=4	NOS=3	NOS=2	NOS=1	Approximate Savings in Energy Number of Stiffeners NOS=4	NOS=3	NOS=2	NOS=1
8.8	**224**	**228.36**	176.87	178.71	183.19	210.23				
8.5	**216**	**245.51**	193.24	209.51	217.41	225.45				
8.0	**203**	**262.48**	212.25	218.75	**229.89**	248.74			**10%**	
7.5	**191**	**273.56**	223.98	239.52	252.78	265.23				
7.0	**178**	**281.65**	239.87	**246.37**	258.60	**274.68**		**17%**		**7%**
6.5	**165**	**289.26**	**245.36**	**261.45**	269.63	284.66	**23%**	**19%**		
6.0	**152**	293.19	**261.58**	272.13	276.53	**289.56**	**25%**			**8%**
5.5	**140**	309.99	**280.92**	283.15	**289.91**	296.71	**21%**		**15%**	

5.4 Conclusion

(1) Finite element analysis of swing jaw plates is carried out, using eight- noded brick element to predict the behavior when it is subjected to point loading under simply supported boundary conditions.

(2) The accuracy of results obtained using the present formulation is demonstrated by comparing the results with theoretical analysis solution. Moreover, the results of stresses are calculated at points and they are expected to differ from the analytical solutions.

(3) The present jaw plate models accurately predict the various stresses for plates. As the present models are developed using a non-conforming element, the results can be further improved using a conforming element with improved mesh size thereby increased no of elements. Infact, FEM results approach the true solutions, with the increase in the number of elements.

(4) The stiffened plate models which leads to reductions in plate weight and indicates that design of new energy-efficient systems of the crushed material.

(5) In case stiffened jaw plates as the number of stiffener increases the strength/weight ratio of the jaw plate increases making it stronger than that of without stiffener.

(6) The stiffened plate models which leads to 25% saving in energy, of course this 25% is an estimate.

(7) The packing arrangement of particles used for the jaw plate analysis shows maximum particles which the plate can accommodate in one crushing cycle.

(8) Consideration of the two particles between the crusher plates reveals the importance of the point-load failure mechanism. Thus, any design based upon both deformation and strength must begin with a point-load idealization.

(9) Design of lighter weight jaw crushers will require a more precise accounting of the stresses and deflections in the crushing plates than is available with traditional techniques.

(10) Rock strength has only been of interest because of the need to know the maximum force exerted by the toggle for energy considerations. Thus a swing plate, stiff enough to crush taconite, may be overdesigned for crushing a softer fragmental limestone.

(11) Design of crushers for specific rock types must consider the variability of point load strength and deformability implicit in any rock type name and quarry sized sampling region.

5.5 Further Scope for Study

Further work is needed to apply the basic, non-simultaneous failure and rock-machine interaction theory with the following modifications and extensions.

(1) Varying packing arrangements from the simplified row assumption to random distributions found in actual operation can be applied to get more accurate results.

(2) Extend the size-peak crushing force and stiffness relationships to account for larger sized feed stock and the effects of jointing and blast-induced micro fissures.

(3) All the Rock names are given on the basis of composition and texture, not strength or deformability. Thus limestone, as shown by the comparison of fragmental and dolomitic limestone, can have widely varying strengths. Therefore crushers cannot be selectively designed with low factors of safety without testing the exact rock to be crushed.

(4) Rock strength will vary even within a specific quarry. Other work has shown that coefficients of variation of rock strength can be as much as 20 - 50% of the mean for are stricted sampling region.

(5) Line loading also produces deformation hardening behavior. Such loading conditions may be applicable for modeling the behavior of slabby material when loaded with ridged plates.

REFERENCES

REFERENCES

1. Anon “Design of Jaw Crusher Avoids Toggles*”, Minerals Engineering, Volume3, Issue 6, March 1999 Pages571-580.*
2. Taggart, Arthur F “Hand Book of Ore Dressing”, *John Willey & Sons Inc, 1998, Pages 255-280.*
3. Lindqvist M., Evertsson C. M. “Liner wear in jaw crushers”, *Minerals Engineering, Volume 16, Issue 1, January 2003, Pages 1-12.*
4. DeDiemar R.B. “New concepts in Jaw Crusher technology”, *Minerals Engineering, Volume 3, Issues 1-2, 1990, Pages 67-74.*
5. Russell A.R., Wood D. M. “Point load tests and strength measurements for brittle Spheres”, *International Journal of Rock Mechanics and Mining Sciences, Volume 46, Issue 2, February 2009, Pages 272-280.*
6. Gupta Ashok, Yan D.S. “Mineral Processing Design and Operation-An introduction”, *Published by Elsevier, 2006, Pages 99-127.*
7. Dowding Charles H, Molling R, Ruhl C," Application of point load-deformation relationships and design of jaw crusher plates”, *International Journal of Rock Mechanics and Mining Sciences & Geomechanics, Volume 20, Issue 2, April 1983,Pages 277-286.*
8. Whittles D.N., Hiramatsu S., Oka I., “Laboratory and Numerical Investigation into the Characteristics of Rock Fragmentation”, *Minerals Engineering, Volume 19, Issue 14, November 2006, Pages 1418-1429.*
9. King R.P.,“Modeling and Simulation of Mineral Processing Systems”, *Butterworth-Heinemann, Boston, April 2001, Pages 588-593.*
10. Briggs, C.A. and Bearman, R.A. “An Investigation of Rock Breakage and Damage in Comminution Equipment”, *Minerals Engineering, Volume 9, Issue 5, November 1996, Pages 489-497.*
11. Berry P, Dantini E.M. and Masacci, P. “Influences of Mechanical Characteristics of Rock on Size Reduction Processing”, *Proceedings of Mineral Processing and Extractive Metallurgy, Beijing, January 1984, Pages 15-26.*
12. Guangjun FAN, Fusheng MU, “The Study of Breaking Force of Jaw Crusher”, *Hunan Metallurgy, Volume 14, Issue 6 July, 2001, Pages 115-123.*

13. Weiss N.L., "Jaw Crusher", *SME Mineral Processing Handbook, New York, 1985, Chapter 3B-1, Pages 245-261.*

14. Niles I. L., "MS Thesis -Point Load Strength: Jaw Crusher Design", *August, 1978.*

15. Georget Jean-Pirrre, Lambrecht Roger "Jaw Crusher" *United States Patent, Patent Number 4, 361, 289, Issued on November, 1988.*

16. Georg Muir, "The Principles of Single-Particle Crushing", *Handbook of Powder Technology, Volume 12, 2007, Pages 117-225.*

17. Pollitz H C, "Crusher Jaw Plates" *United States Patent, Patent Number 3,140,057, Issued on July, 1982.*

18. Zhiyu Qin, Ximin Xu, "A Method of Optimization of the Mechanism of Compound Swing Jaw Crusher", *Journal of Taiyuan Heavy Machinery Institute, July1992. Pages 255-263.*

19. FishmanYu. A.,"Features of compressive failure of brittle materials", *International Journal of Rock Mechanics and Mining Sciences, Volume 45, Issue 6, Sep 2008, Pages 993-998.*

20. Cao Jinxi, Qin Zhiyu, Wang Guopeng, "Investigation on Kinetic Features of Multi-Liners in Coupler Plane of Single Toggle Jaw Crusher*", Journal of Taiyuan Heavy Machinery Institute, July200.Pages 210-219.*

21. Yashima Schimum, "Analysis and Optimization of Crushing Energy of a Compound Swing Jaw Crusher", *Journal of Taiyuan Heavy Machinery Institute, March 1995, Pages 188-192.*

22. Lytwynyshyn G. R., "MS Thesis-Jaw Crusher Design", *Northwestern University, Evanston, August1990.*

23. Gabor M. Voros "Finite element analysis of stiffened plates" *Mechanical Engineering Volume51Issue2, 2007, Pages 105-112.*

24. Kadid Abdelkrim "Stiffened Plates Subjected to Uniform Blast Loading" *Journal of Civil Engineering and Management, Volume14, Issue3, July 2008, Pages155–161.*

25. Hansen L. Scott "Applied CATIA V5R15" *Industrial Press, New York, USA, 2006, Pages 1-475.*

26. Joseph R.P."Austenitic Manganese Steel" *ASM Handbook of Properties and Selection; Iron, Steel and High Performance alloys, Volume 1, Edition10, 1990, Pages 822-840.*

27. Harter James A. "ALGOR Users Guide and Technical Manual" *Wright-Patterson , June 2003, Pages 1-211.*
28. Mukhopdhyay M, Sheikh A. B, "Matrix and Finite Element Analyses of Structures" *Ane Books, New Delhi, 2004, Pages 408-413.*
29. Yamaguchi E. "Basic Theory of Plates and Elastic Stability", *Structural Engineering Handbook Ed. Chen Wai-Fah Boca Raton: CRC Press LLC, 1999.*
30. Liu G. R., Quek S. S., "Finite Element Method: A Practical Course", *Butterworth-Heinemann, Edition 1, March 2003.*
31. Rao S. S., "The Finite Element Method in Engineering", *Butterworth-Heinemann, Edition 4, Dec 2004.*
32. Timoshenko S. and Goodier J. N, "Theory of Elasticity", *Tata McGraw-Hill, New York, 2001.*
33. Tickoo Sham "Catia for Engineers and Designers V5R15", *DreamTech Press, Germany, 2000.*
34. Dukkipati Rao V, Rao M.Ananda, Bhat Rama, "Computer Aided Analysis and Design of Machines Elements", *New Age International (P)Ltd, New Delhi,2000.*
35. Krishnamurthy C S, Rajeev S , Rajaraman A, "Computer Aided Design (Software and Analytical Tools)",*Narosa Publishing House, New Delhi, Edition 2,2005.*
36) http://www.mistryjawcrusher.com/full-images/681579.jpg
37) http://www.miningbasics.com/html/crushing practices and theorie
38) http://www.agregatepros.com/jaw crusher/technical data and description
39) http://nucat.library.northwestern.edu/cgi-bin/Pwebrecon.cgi784772
40) http://www.kolbergpioneer.com/jaw crusher data/specifications
41) http://www.westpromachinery.com/jaw crusher/components/jaw plates
42) http://www.sbmchina.com/jaw crusher/working principle/structure characteristics
43) http://www.harisonjawcrusher.com/crusher-model.htm
44) http://www.cadcim.com
45) http://www.algor.com